Deanship of Graduate Studies

Al- Quds University

P3HT: PCBM Organic Photovoltaic Devices Fabrication and Testing

Alaa A. T. Abu Arquob

M. Sc. Thesis

Jerusalem – Palestine

1436/ 2014

P3HT: PCBM Organic Photovoltaic Devices Fabrication and Testing

Prepared by:

Alaa A. T. Abu Arquob

A Thesis Submitted in Partial Fulfillment of Requirement
for the Degree of Master of Science in Physics

Supervisor

Salman M. Salman

Physics Department, Al- Quds University, Palestine

M.Sc. Thesis

Jerusalem – Palestine

1436/ 2014

P3HT: PCBM Organic Photovoltaic Devices Fabrication and Testing

Alaa A. T. Abu Arquob

B. Sc. of Physics, Al-Quds University, Palestine

Supervisor

Salman M. Salman

A Thesis Submitted in Partial Fulfillment of Requirement
for the Degree of Master of Science in Physics

Physics Department, Al-Quds University, Palestine

Jerusalem – Palestine

1436/ 2014

Deanship of Graduate Studies

Al- Quds University

Physics Department

Thesis Approval

P3HT: PCBM Organic Photovoltaic Devices Fabrication and Testing

Prepared by: Alaa Azmi Taha Abu Arquob

Registration No: 21112014

Supervisor
Dr. Salman M Salman
Physics Department , Al-Quds University, Palestine

Master thesis submitted and accepted, Date 13/12/2014

Names and Signatures of the Examining Committee Members

1. Chairman of the Committee: Dr. Salman M Salman Signature: ……..
2. Internal Examiner: Dr. Husain Alsmamra Signature: ……..
3. External Examiner: Dr. Mustafa Abu Alsafa Signature: ……..

Jerusalem, Palestine

1436/2014

Dedication

I dedicate this thesis to my family, especially, to my father, to my mother's soul, to my brothers, and to my sisters for opening my eyes to the world.

To the soul that hugs my soul, to the heart that pours secrets in my heart, to the hand that lit my emotions, to the faith that is considered the frame of my love I present this Work.

Alaa A. T. Abu Arquob

Declaration

I hereby declare that this thesis is based on the results found by myself. Materials and work conducted at Al-Quds University and Bethlehem University. This thesis, neither in whole or in part, has been previously submitted for any degree.

The work was done under the supervision of Professor Salman M. Salman from the Physics Department, Al-Quds University, Palestine.

Signature: …….

Alaa A. T. Abu Arquob

Date:13/12/2014

Acknowledgements

First I wish to express my gratitude to the Almighty Allah for providing the grant to make this thesis possible.

Thanks and appreciation to my supervisor Dr. Salman M Salman who helped me through all stages of my studies and research.

Special thanks are extended to Dr. Jamal Ghaboun, for giving me the chance for working in his Project "AL-Maqdisi", and the facility to using the equipment in the Physics Laboratory at Bethlehem University.

I would deeply thank Dr. Marc Chaigneau from the E-Cole Polytechnique - Paris, for his continuous supporting and helping in technical training and scientific issues.

I wish to express my thanks to the employees at Nano Research Laboratory at Al-Quds University, for their helping and their training to use their instruments and equipment.

Many thanks to my family and friends, who stood beside me and encouraged me constantly.

Alaa A. T. Abu Arquob

Abstract

Renewable energy is becoming one of the highly active research fields. Polymer-based organic photovoltaic systems hold the promise for a cost-effective, lightweight solar energy conversion platform, which could benefit from simple processing of the active layer.

Among the organic materials used, fullerene derivatives show great potential being electron acceptors. A combination of narrow band donor and fullerene derivatives provide a possible solution for the production of efficient organic cells, including the best organic layer P3HT:PCBM. Fullerene polymers are effective acceptors because of their high electron affinity and ability to transport charge effectively.

The best organic solar cell efficiency is about 5%, thus significant advances in the fundamental understanding of the interplay between the active layer morphology and electronic properties are needed to make this technology a viable option.

This project was conducted mainly at Alquds University nanotechnology laboratory for spin coating and testing; and Bethlehem University for Au and Al evaporation. We fabricated 12 organic cells using P3HT:PCBM compound as an active layer with different ratios between the components and different thicknesses, in addition to using two speeds for spin coating.

The optimum thickness was about 100 nm and the best mixing ratio between the components was 1:1. The coating procedure did not show a significant impact on the overall efficiency of the cells. We measured the IV curves for the cells and even though we used illumination input power only 10% of the standard power of 100mw the efficiency did not degrade as was expected. We have achieved 4.5% efficiency compared to 5% reported using the standard illumination.

Our success in fabricating the cells under restricted conditions encourages the proposal to try improving the efficiency through using active layer materials with high absorption coefficients; high solubility in organic solvents; and smaller band gap through adding gold Nano particles (Au NPs).

P3HT: PCBM Organic Photovoltaic Devices Fabrication and Testing of Structure and Functions

Table of Contents

List of Tables

List of Figures

List of Appendices

Abbreviations

Abbreviation	Description
AFM	Atomic Force Microscopy
AM	Air Mass
BHJ	Bulk Hetero Junction
BIPV	Building Integrated Photovoltaics.
D/A	Donor/Acceptor Interface
DSSC	Dye Sensitized Solar Cell
EQE	External Quantum Efficiency
eV	Electron Volt
FF	Fill Factor
FTIR	Fourier Transform Infrared
H-H	Head to Head
HOMO	Highest Occupied Molecular Orbital
H-T	Head to Tail
Imax	maximum current
IPCE	Incident Photon to Current Efficiency
IPV	Inorganic Photovoltaic
IQE	Internal Quantum Efficiency
IR	Infrared
I_{SC}	Short Circuit Current
J_{SC}	Short Circuit Current Density
LUMO	Lowest Unoccupied Molecular Orbital
MIS	Metal-insulator-semiconductor.
Nm	Nano meter (10-9m)
NPs	Nano Particles.
OPV	Organic Photovoltaic
P3HT	Poly 3-HexylThiophene
PCBM	Phenyl-C61-Butyricacid Methylester
PEDOT:PSS	Poly-3,4-EthyleneDiOxyThiophene : PolyStyreneSulfonate
Pin	Input Power
Pmax	Maximum Power
Pout	Output Power
PV	Photovoltaic
Q	Quantum Efficiency
RPM	Round Per Minute
SC	Solar Cell
TFPV	Thin Film Photovoltaic

TFSC	Thin Film Solar Cell
TFT	Thin Film Transistor
T_g	Glass Temperature
UV	Ultraviolet
V_{max}	Maximum Voltage
V_{OC}	Open Circuit Voltage
VTE	Vacuum Thermal Evaporation
H	Power Conversion Efficiency
Mm	Micro meter (10^{-6}m)

Chapter 1

Introduction and Review of Solar Cells

The fossil fuels or renewable energy sources are distributed all over the earth, and they are used in different percentages as shown in **figure 1.0**.

Solar energy is the most important renewable energy source and represents mankind with the main inexhaustible energy source. The annual energy input of solar irradiation on Earth (5% UV, 43% visible, 52% IR) exceeds the world's yearly energy consumption by several thousand times.

Solar energy usage can reduce toxic carbon emissions by 23 million metric tons per year by 2030, i.e. it is clean energy source. Reducing fossil consumption improves air quality by producing clean electricity. Solar energy saves $100 billion per year for manufacturing industries and businesses by averting power outages. Solar generated power correlates well with daily load patterns for utilities as power is available when needed most—during daylight.

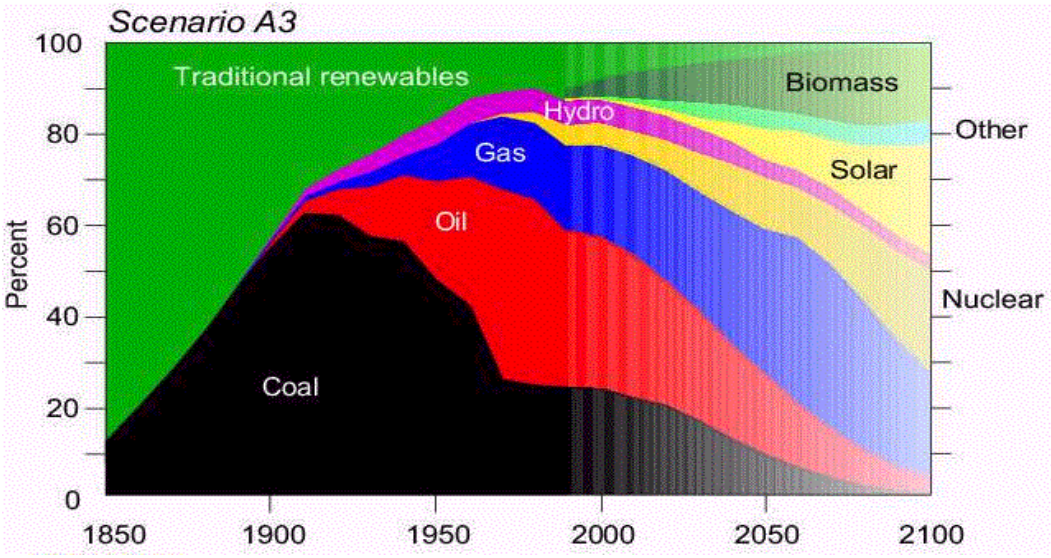

Figure 1.0: Global energy sources (source: world energy council)

For steady growth in the solar energy contribution to the total power consumption, new and continuous improvements in photovoltaic cells structure, efficiency and cost are needed.

1.1 Definition

Photovoltaic research is related to the use of photovoltaic cells in producing electricity from light.Although it is often used to refer to the generation of electricity from sunlight, cells are described as photovoltaic when the light source is not necessarily sunlight. In such cases the cell is used as a photo detector, detecting light or measuring light intensity.

A photovoltaic cell is a specialized diode that converts visible light into direct current (DC).Some photovoltaic cells can convert infrared (IR) or ultraviolet (UV) radiation.

Leaves of green plants do something similar when they convert sunlight to chemical energy, and organic solar cells started like that. There are many types of solar cells based on the active material used.

1.2 History

In 1887, Heinrich Hertz discovered that electrodes illuminated with ultraviolet light create electric sparks more easily. In 1905Albert Einstein published a paper that explained experimental data from the photoelectric effect as a result of light energy being carried in discrete quantized packets. (http://en.wikipedia.org/wiki/Photoelectric_effect).

The first practical photovoltaic cell was developed in 1954 at Bell Laboratories by Daryl Chapin, Calvin Fuller and Gerald Pearson. They used a diffused silicon p–n junction that reached 6% efficiency. From 1954 to 1960 Hoffman improved the efficiency of Solar Cells from 2% to 14%. At first, cells were developed for toys and other minor uses, as the cost of the electricity they produced was very high. Many attempts have been done looking for high-efficiency low-cost solar cells, leaving several significant milestones.

In 1970, the first high effective hetero-structure cell was developed in the USSR. In 1980, the first thin-film cell using Cu_2S/CdS was developed at the University of Delaware with efficiency of 10%. In 1991, the first dye-sensitized cell was invented and in 1994, the first cell using GaInP/GaAs exceeded 30% conversion efficiency. Finally in 2006, the "40% efficient barrier" was broken.

Besides material research, a considerable work was done for increasing sunlight concentration, carrier collection, and cell stability. Despite their low efficiency, the organic polymers have attracted strong interest**(Weihao G., 2009).** A chronology of the solar cells development from the date of discovering the photovoltaic effect is outlined in appendix A.

1.3 Solar Cells Types

There are many types of solar cells depending on the active material used. Some are silicon based semiconductors (crystalline and amorphous). Others are germanium based (GaAs, GaInP, Cu (InGa) Se and CdTe). **Figure 1.1** shows the best cell efficiencies produced at prominent world laboratories and based on various manufacturing technologies.

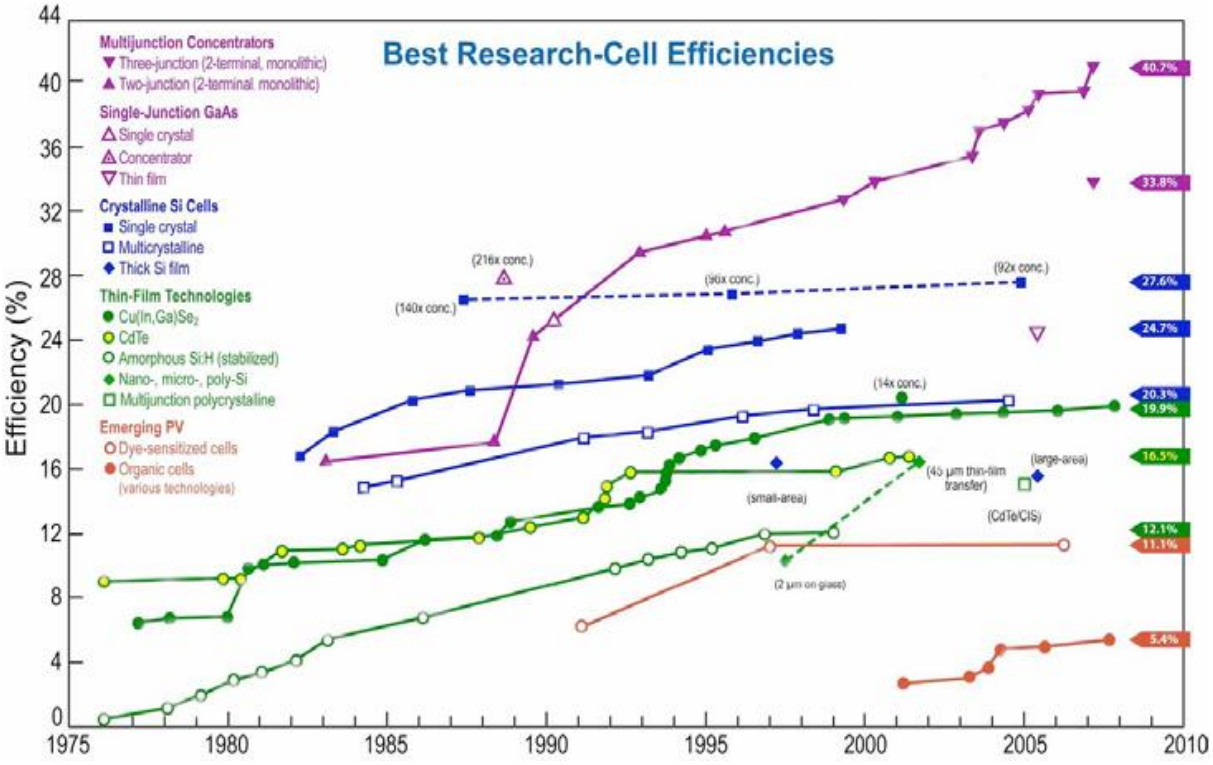

Figure 1.1: Best cell efficiencies (NREL)

Solar cells materials are chosen largely on the basis of how well their absorption characteristics match with the solar spectrum and upon their cost of fabrication. Silicon is a common choice because its absorption characteristics match fairly well with the solar spectrum. Accordingly silicon based fabrication flourished (**Luque A. and Hegedus S., 2011).**

Another important factor for choosing semiconductors for cell fabrication is the crystal structure that makes four bonds, e.g. tetrahedral lattice in silicon and the Zincblends (For example, in GaAs III-V compound one interpenetrating FCC unit cell is composed entirely of Gallium atom and the other entirely of Arsenide atom) that occur in the binary III-V and II-VI semiconductors. **Figure 1.2** shows the general types of solar cells.

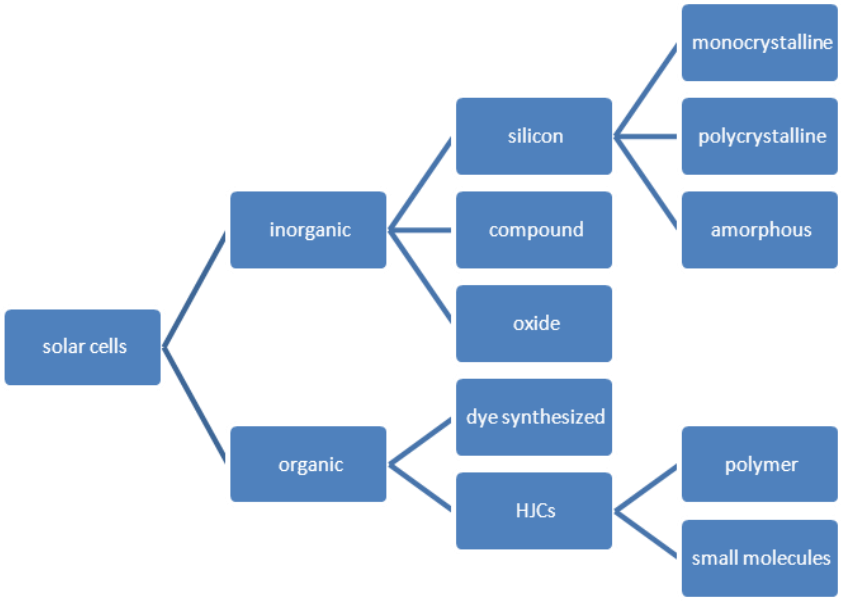

Figure 1.2: Types of solar cells

1.4 Inorganic Photovoltaic (IPV) Cells

A-1 Crystalline Silicon

This was the first generation of PVs. Traditionally single crystalline (mono silicon) is used to produce silicon based microelectronic devices while the pure polycrystalline (poly silicon) is used for macro-scale production. By 2006, over half of the world's supply of poly silicon was used for the production of solar panels. Mono silicon has higher efficiency andcost. Commercial mono silicon efficiency reached 22% as produced by US and Japanese solar manufacturers.

Monocrystalline cells are effectively a slice from a crystal. In appearance, it has a smooth texture. They are the most efficient but they are expensive to produce. They are rigid and must be mounted on rigid frames to protect them.

Polycrystalline (or Multi crystalline) cells are effectively a slice cut from a block of silicon, consisting of a large number of crystals. They have a speckled reflective appearance and they are slightly less efficient and cheaper compared to monocrystalline cells. They too need to be mounted on a rigid frames.

Crystalline silicon devices have theoretical limiting efficiency of 29% and can achieve an energy payback period of 1-2 years. Most of the low end manufacturing use poly silicon PV cells with efficiency of 7-8%. (http://www.solartech-usa.com/types-of-solar-cells).

A-2 Amorphous Silicon

Amorphous cells are made by placing a thin film of amorphous silicon onto a wide surface. These are the least efficient and least expensive to produce. Due to the amorphous nature of the thin layer, it is flexible, and if mounted on a flexible surface, the whole solar panel can be flexible. One problem with amorphous solar cells is that their power output degrades in the first few months, and then they stabilize. The quoted output of an amorphous panel is what it produces after stabilization.

A Thin-Film Solar Cell (TFSC) or Photovoltaic Cell (TFPV) is made by depositing few layers of the photovoltaic material on a substrate. The layer thickness varies from few nanometers (thin-film TF-Si) to tens of micrometers (Amorphous A-Si)

Thin film cells have an efficiency of 12-20%, prototype modules 7-13% and production module 9%. State-of-the-art thin film cells efficiency can reach 10-18%.Thin film technology is used for Building Integrated Photovoltaics (BIPV). These are semitransparent solar cells that can be used as window glazing while generating electricity.(http://www.solartech-usa.com/types-of-solar-cells).

B- Compound Cells

Compound semiconductors made from II–VI or III–V elements are key materials in the plans to harvest energy from photovoltaic devices. In the search for low-cost efficient alternatives to crystalline silicon, thin film compound semiconductor materials are commonly used. It is

more efficient to create an electric field at an interface between two different semiconductor materials (hetero-junctions).

A typical polycrystalline thin film has a thin layer on top known as a "window" material. It lets most of the light through the interface to the absorbing layer. The absorbing layer has to have a high absorption in the generation of current and a suitable band gap to provide good voltage. **(Srivani A., et al,2013).**

These cells are classified into two main types:

Type III-V: GaAs or InP

The main characteristics include high absorption length, conversion efficiency and irradiation impedance; broad spectral response; and a concentrator system where a wide area of sunlight is focused onto the solar cell with the help of an optical device **(Lee C., 2010).**The most efficient compound cells are GaInP/GaAs/Gewith great success for use in satellites.

Type II-VI: CdTe/CdSor Cu_2S/CdS

They are used as photo resistors and the first efficient solar cells used CdTe as quantum dots. Crystals can act as solid state lasers. Its energy gap is about 2.42eV **(Kasap S., 2006).**

C - Oxides Cells

Optically transparent oxides tend to be electrical insulators, by virtue of their large electronic band gap ($\geq$3.1 eV). The most notable exceptions are doped versions of the oxides In_2O_3, SnO_2 andZnO; all are n-type conductors that are widely used as the transparent electrodes in flat-panel displays. On the other hand, no transparent oxide exhibiting high p-type conductivity are known to exist, whereas such materials could open the way to a range of novel applications. For example, $CuAlO_2$ cells a combination of the two types forming apn junction can produce a 'functional' window that transmits visible light yet generates electricity in response to the absorption of ultraviolet photons **(Kawazoe H., 1997).**

ZnO is a wide-band gap semiconductor of type II-VI semiconductor while Zinc, is a transition metal member of the IIB group. The native doping of the semiconductor (due to oxygen

vacancies or zinc interstitials) is n-type. It has several favorable properties, including good transparency, high electron mobility, wide band gap, and strong room-temperature luminescence. These properties are used in emerging applications for transparent electrodes in liquid crystal displays, energy-saving or heat-protecting windows, thin-film transistors and light-emitting diodes **(Özgür Ü., et al, 2005).**

1.5 Organic Photovoltaic (OPV) Cells

An organic solar cell is a type of polymer cell that uses organic electronics, a branch of electronics that deals with conductive organic polymers or small organic molecules, for light absorption and charge transport to produce electricity from sunlight.

OPV cells are potentially cost-effective for photovoltaic applications. Molecular engineering (e.g. changing the length and functional group of polymers) can change theenergy gap that allows chemical change in these materials.**(Swarup A. ,Khare P. S., 2009).**

OPV cells gained significant interest as a potential economic source of renewable energy. In particular blends of conjugated polymers with functionalized fullerene have shown good certified power conversion efficiencies of about 6%. **(Kosyachenko L.A., 2011).**

Shortcomings associated with OPV cells compared to inorganic cells include low efficiency, low stability, and fragility. This situation however is changing and OPVs may become a competitive option. The optical absorption coefficient of organic molecules is high, so a large amount of light can be absorbed by a small amount of material. They are lightweight, flexible shape, versatile synthesis and device fabrication, for large scale industrial production. They are low cost with continuous tenability of materials energy and gaps via molecular design synthesis. In addition they can be integrated to other products such as textile (solar cell tents), flexible packaging systems, lightweight consumer goods, and optoelectronics devices that are compatible with biological tissues. **(Luque A., Hegedus S., 2011).**

1.5.1 Organic Photovoltaic Materials

The materials used in OPV cells are classified as organic semiconductors due to their capability to absorb light and conduct electricity either within molecules such as conjugated

polymers or through molecular networks. Conjugated polymers that were studied for photovoltaic applications include polythiophenes, poly-phelene-vinlene (PPVs), poly-fluorenes and polycarbazoles, whereas simple organic semiconductors include functionalized fullerene, phthalocyanines, perylene derivatives and pentacene as shown in **figure 1.3**.

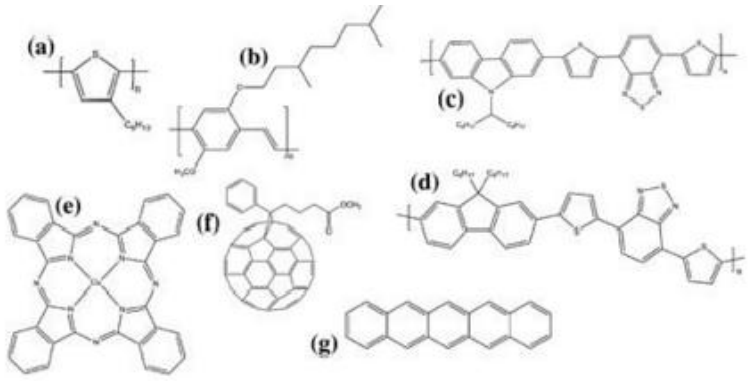

Figure 1.3: Examples of organic semiconductor materials: (a) P3HT, (b) MDMO-PPV, (c) PCDTBT, (d) F8DTBT, (e) PCBM, (g) Pentacene

The desirable properties of the visible spectrum absorption and charge transport in organic molecules arise from the network of π bonds between unsaturated carbon atoms. The Carbon atoms in the conjugated section of the molecule form strong **π bonds** using sp^2 orbitals, whereas the p orbitals lying perpendicular to the plane of the molecule form **σ bonds**, that are less tightly localized than the strong orbitals in conjugated polymers. This typically extend over 2-10 repeat units.

A conjugated system is formed when carbon atoms covalently bond with alternating single and double bonds. Their electrons orbitals form delocalized bond π orbitals with a π* anti-bond orbital. The delocalized π orbital is the highest occupied molecular orbital (HOMO), and the π* orbital is the lowest unoccupied molecular orbital (LUMO). The separation between HOMO and LUMO is considered the band gap of organic materials and it is typically in the range of 1–4 eV.

The most studied fullerene polymer is based on PCBM (Phenyl-C61-Butyricacid Methylester) and the conversion efficiencyis around 4.5 – 5%. The P3HT: PCBM performance is close to the maximum efficiencyof 5%**(Kingsley J. W., et al, 2009)**.We investigated this type of material.

1.5.2 Types of Organic Photovoltaic Cells (OPVs)

Typical organic cell devices have a layered structure and an organic active absorbing layer. For other layers (e.g. electrods) metals and in organic materials can be used. **Figure 1.4** shows a typical OPV cell structure.

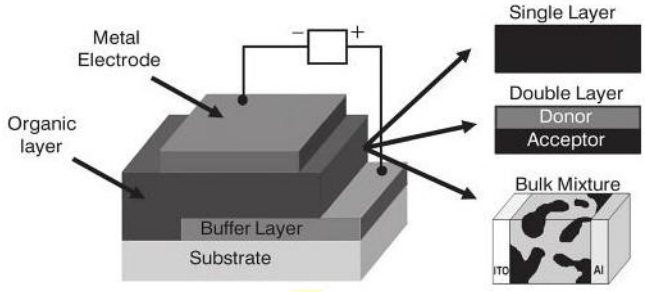

Figure 1.4: Geometry of OPV (KrebsF. G.,2012, p. 5)

A- Single Layer OPV

Single layer OPV cells are the simplest of the OPVs. They are made by sandwiching an organic layer between two metallic conductors. A typical layer of indium tin oxide (ITO) with high work function and a metal layer of low work function such as Al, Mg or Ca, is shown in the **figure 1.5**.

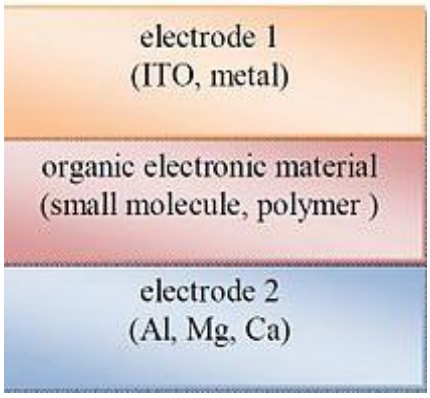

Figure 1.5: Single layer OPV structure.

The difference of the work functions between the two conductors sets up an electric field in the organic layer. When it absorbs light, electrons will be excited to the LUMO and leave holes in the HOMO, thereby forming excitons. The potential created by the different work functions helps to separate the exciton pairs, pulling electrons to the positive electrode and holes to the negative electrode. Using an external electric field is not the best way to break

upexcitons: hetero-junction based cells could be more effective. But they have problems: (**Magic Materials Chemistry, 2010**)

1. Low quantum efficiencies (<1%) and low power conversion efficiencies (<0.1%).
2. The field between the two electrodes is seldom sufficient to break up the excitons. The electrons recombine with the holes before reaching the electrodes.

B- Bi-layer OPV

This type is built from two layers of materials different with electron affinity deposited between the electrodes as shown in figure 1.6. The electron affinity is defined as the energy change when an electron is added to a neutral atom or molecule to form a negative ion. $X + e^{-} \rightarrow X^{=} +$ energy.

The ionization energy of an atom or molecule describes the amount of energy required to remove an electron from the atom or molecule in the gaseous state. $X +$ energy $\rightarrow X^{+} + e^{-}$. The different affinities between the two layersgenerate a potential that can break up the excitons. The layer with higher electron affinity and ionization potential is called the acceptor, and the other layer is called the donor. This structure is also called a planar donor-acceptor hetero-junction.

The main problem with this type is that the diffusion length of the excitons in the organic materials (order of 10 nm) is small compared to the practical thickness to absorb enough photons for power conversion (100 nm). At such a large thickness, only a small fraction of the excitons can reach the heterojunction interface.

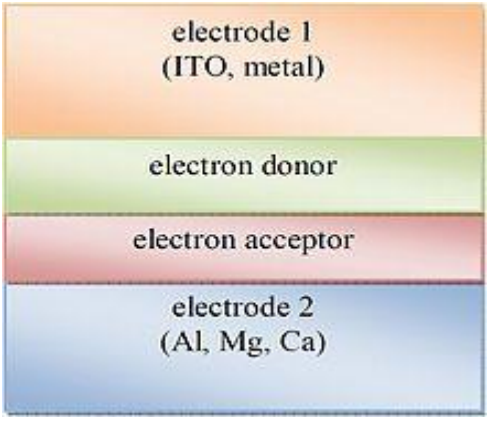

Figure 1.6: Bilayer OPV structure

C- Bulk Heterojunction (BHJ) OPV

These cells are similar to the bi-layer cells but the acceptor and the donor layers are mixed to form a blend layer sandwiched between the electrodes as shown in **figure 1.7**.This form was invented in the mid-1990s. The junction is formed by mixing donor and acceptor materials in a solution then forming the active layer by spin coating of the mixture on the substrate. The resulting film represents a nanoscale network of donors and acceptors. The phase separation within the film is about 10-20 nm which is comparable to the exciton diffusion length **(Choy W., 2013).**

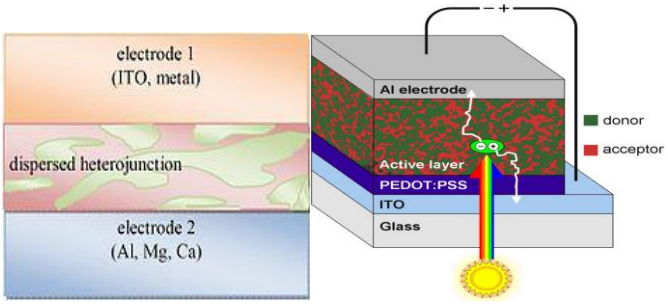

Figure 1.7: BHJ cell structure.

In this configuration most of the excitons generated may reach the interface, where they break efficiently. While most bulk hetero-junction cells are of the two component variety, three component cells have also been explored. The third component, a secondary donor polymer, absorbs light in a region of the solar spectrum different from the other donor.

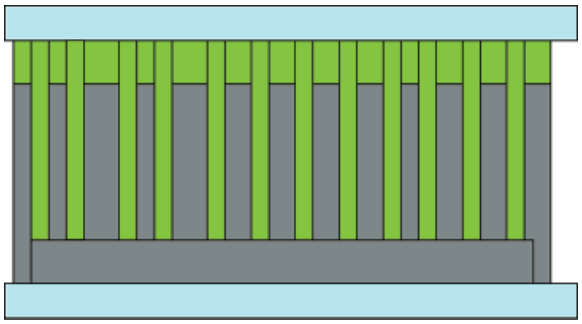

Figure 1.8: Ideal structure of BHJ cells. (Sariciftci N. S., et al, 2007)

The ternary cells can operate through one of three mechanisms: charge transfer, energy transfer and parallel-linkage. In **charge transfer**, both donors contribute directly to the generation of free charge carriers. Holes pass through only one donor domain before collection at the anode. In **energy transfer**, only one donor contributes to the production of

holes. The second donor acts solely to absorb light, transferring extra photon energy to the first donor material. In **parallel linkage**, both donors produce excitons independently that migrate to their respective D/A interfaces and dissociate.

Due to the small phase separation in the BHJs, a thicker active layer can be used. The efficiency of the BHJ cells depends on the morphology of the layer. The BHJ cells performance is susceptible to parameters variations. Various fabrication parameters like thermal annealing, modifying polymer functional groups and the donor-acceptor compound ratio have been studied to optimize performance. **Our work here will test the various parameters for optimum manufacturing. BHJ cells can be classified based on the donor-acceptor layers material.**

C-1 Polymer-Polymer

An *n*-type polymer is used as the electron acceptor instead of a fullerene or another small molecule, as shown in **figure 1.9**.

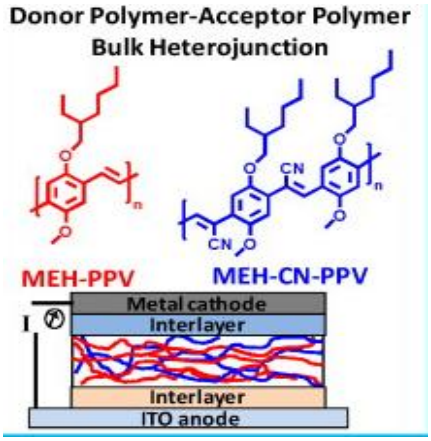

Figure 1.9 Polymer -polymer cell

Figure 1.10shows some examples of donor and acceptor polymers **(Facchetti A., 2013).**

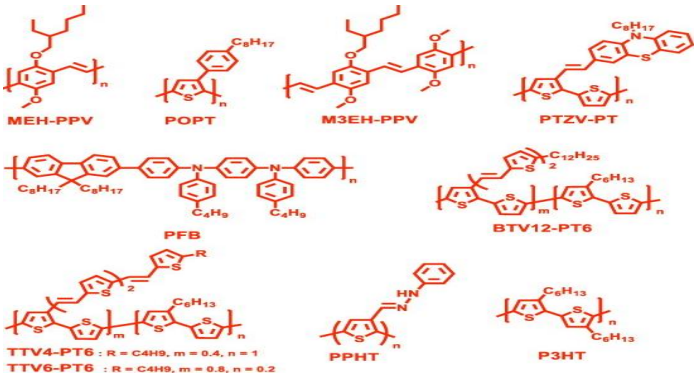

a) donnors

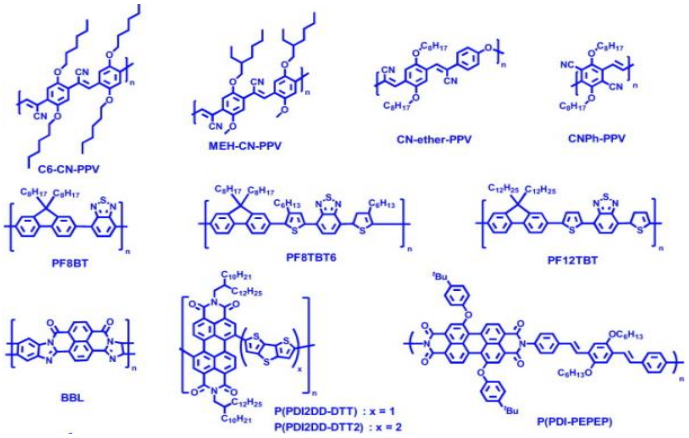

b) acceptors

Figure 1.10: Chemical structure for a) Donor polymers, b) Acceptor polymers

These cells have some unique advantages:

1. Semi-conducting polymers have high absorption coefficients in the visible spectral region, while fullerenes are limited. Although C_{70} derivatives are better than C_{60}s, it is quite difficult to extend their absorption to the red and near-infrared regions.
2. Polymer energy levels can be tuned more efficiently. A low-lying acceptor LUMO can result in more efficient photo-induced charge separation at the donor/acceptor interfaces, but it may reduce V_{oc}.
3. Polymer-Polymer blends offer superior flexibility in controlling solution viscosity, an important factor for large scale OPV module production by solution processes.

C-2 Polymer-Fullerene

In Polymer-Fullerene cells**figure 1.11** the electron affinity of the fullerene is reduced.

Figure 1.11: Polymer- Fullerene cell

The use of multiply substituted fullerenes leads to an increase in V_{oc} with no loss of charge generation in P3HT blend, but may adversely affect the blend morphology and reduce the carriers' mobility.

C-3 PolyFullerene Blends

In some **Poly-Fullerene blends** increasing the frontier orbital offset between the donor HOMO and acceptor LUMO may also lead to the formation of triplet states that are detrimental to performance and long-term stability **(McEvoy A., et al, 2012).**

C-4 Block Co-Polymer

Block copolymer-based devices demonstrate efficient photo conversion well beyond devices composed of homo polymer blends. 3% efficiencies were achieved without the use of a fullerene acceptor. X-ray scattering results reveal that the good performance of block copolymer cells is due to self-assembly into meso scale lamellar morphologies with primarily face-on crystallite orientations. Conjugated block copolymers thus may enhance performance through control of donor–acceptor interfaces **(GuoJ. et al, 2010).**

Figure 1.12.b shows a fully functionalized block copolymer that consists of a donor and an acceptor block. The block copolymers phase separates into highly ordered nanostructures. The immiscibility of both blocks and their molecular interconnectivity lead to a micro phase separation, resulting in a highly ordered self-assembled morphologies such as spheres, cylinders, gyroids or lamella that depend on the volume ratio of the two blocks, as shown in **figure 1.12.a** Cylindrical or gyroidal nanostructures are ideal morphologies for organic cells, since they have domain sizes in the range of the exciton diffusion length.

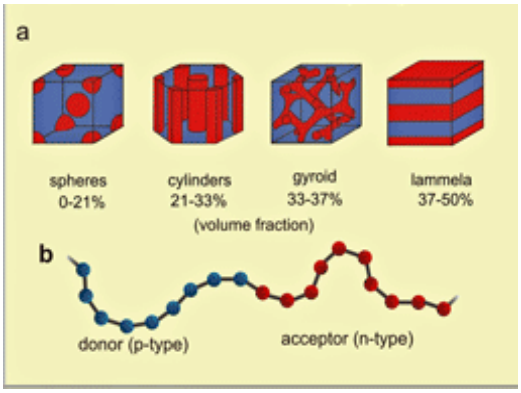

Figure 1.12: Block copolymers (a: block copolymer, b: phase separation copolymers)

Figure 1.13 shows one of the functionalized block copolymers as it was synthesized for this purpose. Donor -Acceptor block copolymer consisting of polyhexylthiophene(P3HT) (donor) and a perylenebisimide derivative (acceptor).**(Hüttner S., 2010)**

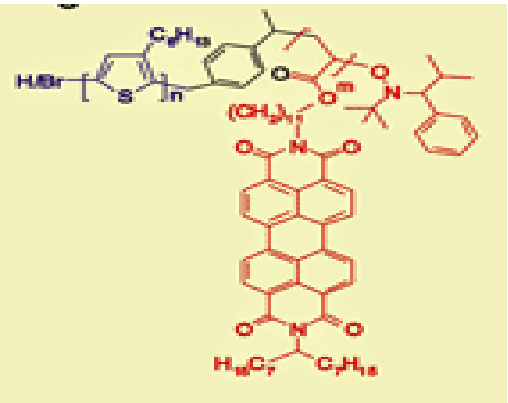

Figure 1.13: P3HT-PeryleneBisimide block co-polymer

A comparison between the interfaces of the three types of the organic cells is shown in the **figure 1.14**.

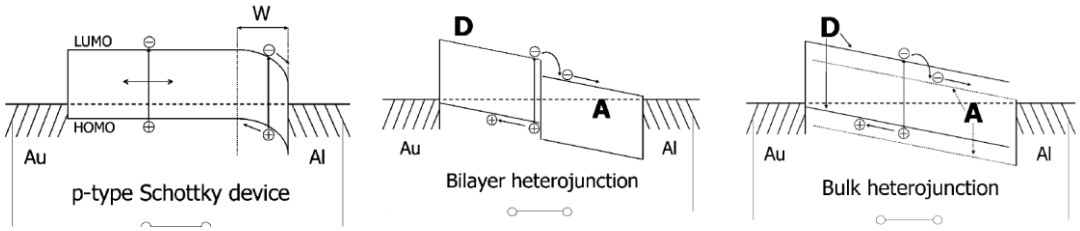

Figure1.14: Junction structure for the organic cells (WeihaoGe, 2009).

D- Inorganic- Organic Hybrid: Can come in different materials content:

D-1 Metal Oxide- Polymer

Titanium Dioxide Based Hybrid (TiO_2- polymer). Nano structured TiO_2 has been studied since the 1980s. The solid (TiO_2-polymer) cell has the advantage of utilizing the complete hetero structure for exciton dissociation, potentially leading to thinner devices, since the entire polymer-filled pore volume is available for exciton generation, rather than only a dye monolayer at the TiO_2 surface. Further, the rigid structure of TiO2 offers better mechanical stability compared to pure OPVs. The efficiency is about 6.1% for PCDTBT:$PC_{70}BM/TiO_x$. **(Adikaari A. A. T. et al, 2009).**

D-2 Zinc Oxide Based Hybrid

ZnO is a direct wide band gap (3.3 eV at 300 K) II-VI compound semiconductor. It can be grown with simple crystal-growth technologies. High-quality ZnO films can be grown at temperatures less than 700°C. An additional property makes ZnO preferable over other wide-band-gap materials include: it can be doped substitutionally and by controlling the doping level, electrical properties can be changed from insulator through n-type semiconductor to metal while maintaining optical transparency. The major obstacle against wide use of ZnO is the difficulty of reaching a p-type material. The highest efficiency achieved using ZnO-polymer is P3HT: PCBM/ZnOis about 4.6%.

D-3 Carbon Nanotube-Organic

Single wall carbon nanotubes (SWCNTs) are comprised of a single graphene cylinder, with diameters in the range 0.4-3.0 nm. Multi-wall carbon nanotubes (MWCNTs) are comprised of several co-axially fixed tubes of different radii with an inter-tube separation close to the inter-plane separation in graphite (0.34-0.35 nm). MWCNTs have diameters as large as 100 nm.

However, PV device applications, diameters less than 20 nm are preferred due to the ~100 nm organic layer thickness limit for structures. The cylindrical, covalently bonded structure of carbon nanotubes are extremely strong with a tensile strength comparable to steel, at only a fraction of the density of Al. They are efficient charge conductors with high heat transmission capacity that is useful for thermal management of hybrid PV devices. CNTs can be used in three applications: as an active layer; as a charge collection interface at the electrode and as the transparent conductive oxide. For the Glass/ITO/MWCNT/P3HT: PCBM /LiF/Al the highest efficiency reached was 2.70%**(Adikaari A. A. T. et al, 2009).**

D-4 Semiconductor Nanowire Organic

This involves the use of nanowires as electron acceptors. Silicon nanowires grown on a silicon substrate has been transferred in to a P3HT: PCBM bulk heterojunction active layer, before deposition of an Al electrode. These devices have 1.9% efficiency, and that is low compared to the typical 4% efficiency for such systems.

P3HT: MWCNT blend with Si nanowires grown on a Si wafer gave efficiency of 0.6%. Si nanowires directly grown on ITO coated glass substrates for while P3HT:PCBM with Si nanowire yielded 0.43% efficiency. CdS nanowire /MEH:PPV on FTO coated glass substrates yielded an efficiency 1.62%.**(Adikaari A. A. T. et al, 2009).**

D-5 Semiconductor Quantum Dot Organic

Semiconductor Nanocrystals (NCs) with dimensions comparable to the Bohr radius of the material show vastly different properties. This results from the change of the electronic configuration due to quantum confinement. Most notably,the energy of the lowest exciton state changes inversely with size. Furthermore, the energy levels change configuration in a molecular like absorption spectrum. Such optical tuning can be utilized to realize novel developments foroptoelectronic devices such as light emitting diodes, lasers and PVs.

Photoactive organic materials posse's high optical band gaps and that limits light absorption capability. It is believed that the use of NCs could potentially address this critical limitation by increasing the spectral sensitivity of hybrid devices to match the solar spectrum, and increase the power conversion efficiency. **(Sariciftci N. S., Sun S., 2005)**

D-6 Dye-Sensitized Solar Cell (DSSC)

First developed by Gratzel`s group in 1991, it is a hybrid cell that uses inorganic semiconductor and organic dye. All three primary functions are allocated separately allowing for independent optimizing. A dye is chosen for light absorption, a semiconductor is used to transport electrons, and a third component is used to transport holes. Currently the most popular electron transport medium in DSSC is Titanium dioxide (TiO_2 wide band 3.2 eV). TiO_2 absorbs ultraviolet which is only 5% of sunlight. Nevertheless, if a dye can be tightly adsorbed on the surface of TiO_2 and the energy of the dye excited state is suitable to move an electron into the conduction band of TiO_2, then a photovoltaic effect can be initiated by all the photons absorbed.

The hole transport medium must replenish electrons to the oxidized dye. The energy levels must be appropriate for efficient charge transfer. The dye often sets between a donor and

acceptor. After a photon creates an exciton state, electrons are pushed toward the acceptor or the transport medium **(Zang L., 2011).**

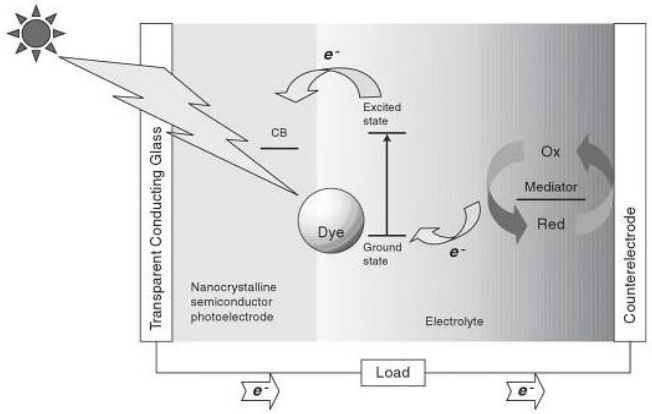

Figure 1.15: The operating principle of DSSC (Abd-El-Aziz A. et al, 2010).

A strong point against DSSC lies in the manufacturing geometric arrangements. TiO_2 is formed as a thin film of nanoparticles, with 15-30 nm particle size and a layer thickness of 5-15μm. This layer is screen painted and then annealed between 450°-550° to remove the organic additive such as binders and dispersants.

1.5.3 The Working Principle of Organic Electronics and Cells

A successful OPV manufacturing needs an optimization of the following processes to obtain high conversion efficiency. Absorption of light and excitons generation; diffusion of excitons to an active interface; and charge separation, transport and collection. **Figure 1.16** and what follows summarizes the working principles of OPV cells.

1. Incident photons are absorbed in organic layers and excitations are formed. These excitations are closely linked (usually in the same molecule) electron-hole pairs by columbic interaction, which promotes the electrons to the LUMO level while leaving the positive charge carrier "holes" to the HOMO.

2. These excitations have binding energy of few hundreds of MeV and they have to diffuse without recombination to the junction of two different materials. **Molecule with lower ionization potential is called donor and the other (high electron affinity) is called acceptor**.

3. When excitations successfully reached donor-acceptor junction, electron and hole are forced to be separated by the difference of energy level or electric field at the junction.

4. Generated free carriers are now collected by respective electrodes. Electrons transport occurs via LUMO level of acceptor molecule and holes move through HOMO level of donor molecule. **(Kim C. H. and Jeon T.,2012).**

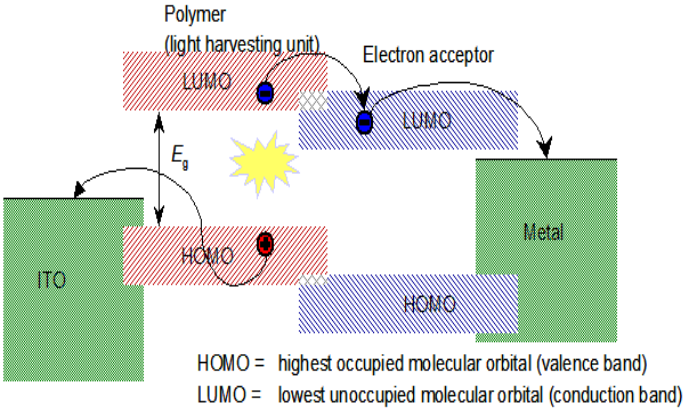

Figure 1.16: Working principle of solar cell

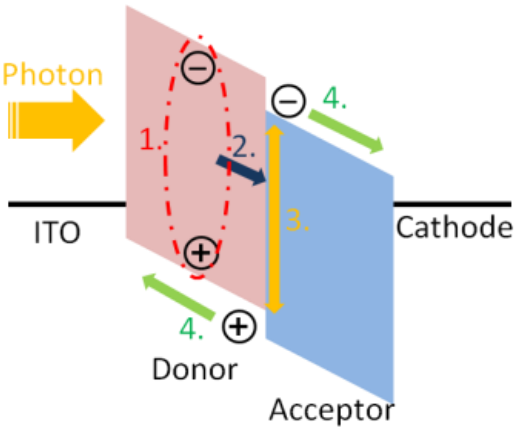

Figure 1.17: Working principle of Solar Cells (Kim Ch. H., and Jeon T., 2012).

The main difference between inorganic and organic processes is that in inorganic cells free charge carriers are generated when absorbing a photon, while in organic cells excitons are created. The excitons are bound states of excited electrons and holes. **(Krebs F. C.,2012).**

Each step is crucial for efficient power generation and there are many loss mechanisms involved in the sequence. An important parameter for the absorbing material is its optical band gap between the HOMO and LUMO energies. The donor and acceptor materials having different ionization energy and electron affinity force excitons to split into free charge

carriers. The charge collection at opposite electrodes is ensured by the symmetric ionization energy (or work function of the electrodes).

One of the reasons the efficiency of the OPVs is lower than the inorganic is because the charge carriers lose a certain amount of energy during the separation of the excited pairs.

The active layer donor-acceptor composite governs most aspects of the working principle, except the charge collection, which is based in the electronic interface between the active layer and the electrodes. This is shown in **figure 2.6**.

Besides the fundamental steps, the open circuit voltage (V_{OC}) is governed by the energetic relationship between the donor and acceptor materials. Specifically, the HOMO and LUMO difference is to correlate with the V_{oc} value. **(Thompson B. C. and Frechet J. M., 2008).**

The solar cell in the dark acts as a simple diode, and the equivalent electric circuit that approximates is shown in **figure 1.18** which comprises:

1. A diode with ideality factor n and saturation I_0 (current in the dark reverse bias)
2. A current source that corresponds to photocurrent I_L generated during illumination.
3. R_s series resistance, for current leakage through shunts as a result of defects in the films.

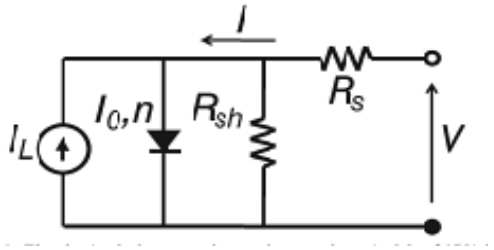

Figure 1.18: Circuit that approximates the working principle of OPV cell.

The low performance of organic cells is attributed to the following two factors:

1. Inefficient photo-induced charge generation due to low exciton diffusion length compared to the optical absorption length.
2. Poor collection efficiency due to low carrier mobilities ($10^{-3}cm^2/Vs$). However, carrier mobilities approaching those of amorphous Silicon have been achieved in certain organic

semiconductors. The progress in this field will depend on materials improvements and innovative engineering **(Satyen K. D., 2004).**

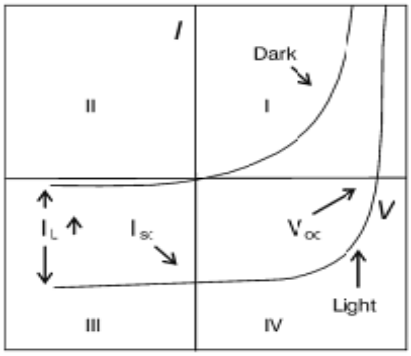

Figure1.19: Dark and light IV curves for an OPV (Krebs, F. C., 2012).

For good performance R_s should be low and R_{sh} high. When light shines the cell the current-voltage (IV) curve becomes a superposition of the dark IV with the light generated current, and the curve is shifted down to the fourth quadrant, as shown in **figure 1.19**.

1.5.4 Cell Characterizations

To understand the dark and light IV curve of the organic cell, we need to familiarize with some parameters related to the electrical characteristics of the cell, namely the: Short-Circuit current density (J_{sc}), Open Circuit Voltage (V_{oc}), Fill Factor (FF) and efficiency (η).

Short-circuit current(I_{sc} or J_{sc})

It is the current through the cell when the voltage across it is zero (short circuited V = 0). The short-circuit current is due to the generation and collection of light-generated carriers. For an ideal solar cell, the $\mathbf{I_{sc}}$ and the light-generated current should be identical, i.e. the $\mathbf{I_{SC}}$is the largest current that can be drawn from the cell.$\mathbf{I_{SC}}$ depends on the following factors:

1. **The active material area:** to normalize one can use current density (J_{SC} in mA/cm^2).
2. **Light or photons intensity**. J_{sc} is directly proportional on the light intensity.
3. **The spectrum of the incident light**: and the active cell excitation region
4. **The optical properties** (absorption and reflection).
5. **The collection probability** which depends on the surface passivity and the minority carrier lifetime in the base.

When comparing cells of the same material type, the most critical material parameters are the diffusion length and surface passivation. In a cell with perfectly passivated surface and uniform generation, the equation for the $\mathbf{I_{SC}}$ can be approximated as:

$$I_{SC} = qG(L_n + L_p)$$

Where G is the generation rate, L_n and L_p are the electron and hole diffusion lengths respectively. Although this equation makes several assumptions which are not true for the conditions encountered in most solar cells, it nevertheless underscores the strong dependence of the$\mathbf{I_{SC}}$ on the generation rate and diffusion length.

Open Circuit Voltage (Voc)

It is the electrical potential difference between the two terminals when there is no external load current flow between the terminals (when I_{ext}=0). The voltage is given the symbol Voc. The Voc of batteries and cells are often quoted under particular conditions (state-of-charge, illumination, temperature, etc.). Voc can be increased as shown in **figure 1.20** through increasing the polymer ionization potential; the band gap and decreasing the driving force for hole transfer and decreasing the driving force for the electron transfer.

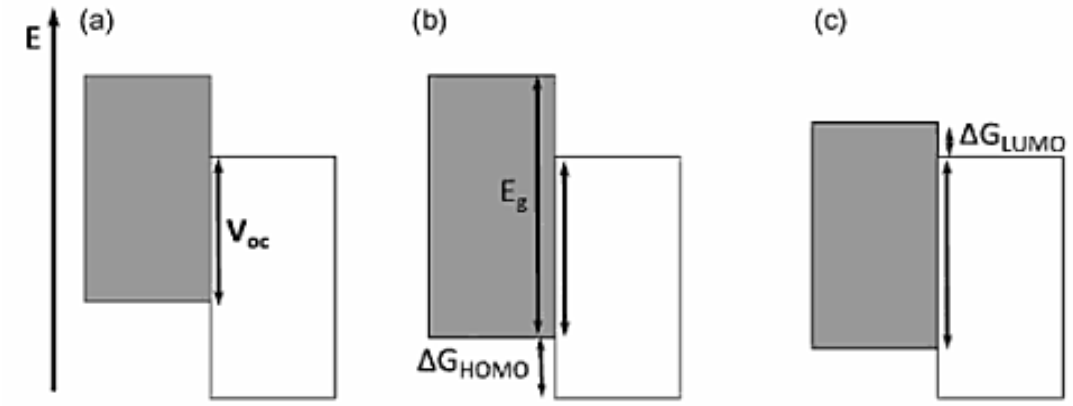

Figure 1.20 Methods for increasing the open circuit voltage (Voc) for solar cell (McEvoy A., et al, 2012).

Illuminated Current (I_L)

It is the light generated current inside the cell. At short circuit conditions the externally measured current is I_{SC} is equal to I_L and can be used interchangeably. However for high

series resistance (> 10 Ωcm^2) I_{SC} becomes less than I_L and using it in the cell equation is incorrect.

Another assumption is that the illumination current I_L solely depends on the light intensity does not depend on the voltage across the cell. In reality however, I_L varies with voltage in the case of drift-field cells and when carrier lifetime is a function of injection level like the case of defected multi-crystalline materials.

Fill Factor (FF)

It is a parameter that determines the maximum power from a cell in conjunction with V_{oc} and I_{sc}. It is defined as the ratio of the maximum power from the cell over the product of V_{oc} and I_{sc}. Graphically, the FF is a measure of the "squareness" of the cell and it is represented as the area of the largest rectangle that fit in the IV curve. **Figure 1.21** illustrates the concept.

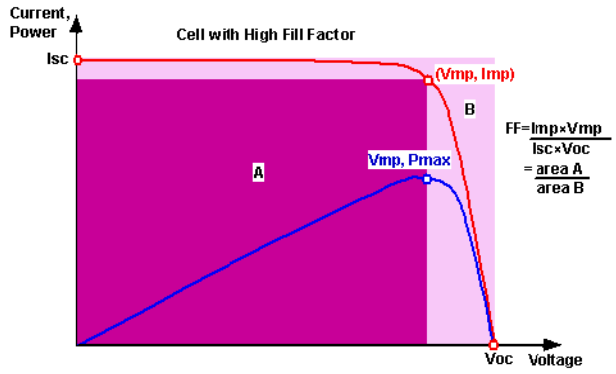

Figure 1.21: Graph of cell output current (upper line- red) and power (lower- blue) as a function of voltage. (http://pveducation.org/pvcdrom/solar-cell-operation/fill-factor).

A cell with a higher voltage has a larger FF value because the "rounded" portion of the IV curve takes up less area. The maximum FF can be determined from setting the firstderivative with respect to voltage equal to zero.

Power (P) =IV and dP/dV = d (IV)/dV = 0. **1.1a**

Gives FF = P_{max} /V_{oc}. I_{sc} = $V_{max.}$ I_{max}/$V_{oc.}$ $I_{sc.}$ **1.1b**

Or in terms of current density FF =V_{max}. J_{max}/V_{oc}. $J_{sc.}$ **1.1c**

The fill factor of PV devices depends strongly on the charge transport characteristics of the photoconductive blend and the charge transfer through the systems where electrons and holes mobilities are balanced.

The energy levels of buffer layers and work functions of the electrode materials should be synchronized to facilitate maximum collection of the charge carriers. FF values of 65-75% are reached for OPV **(Bottari G. et al, 2013).**

Efficiency η

Efficiency is the most commonly used parameter to compare the performance of cells. It is defined as the ratio of energy output from the cell to the input energy from the sun.

$$\eta = P_{out}/P_{in} = (FF)\,(J_{sc}.V_{oc})/P_{in} = J_{max}.V_{max}/P_{in} \qquad 1.2$$

In addition to reflecting the performance of the cell itself, the efficiency depends on the spectrum and intensity of the incident sunlight and the temperature of the cell. Therefore, conditions under which efficiency is measured must be carefully controlled in order to when comparing different cells.

Two solar cells have the same V_{OC} and J_{SC} but different efficiency. The one which has a higher FF will have higher efficiency as shown in **figure 1.22**

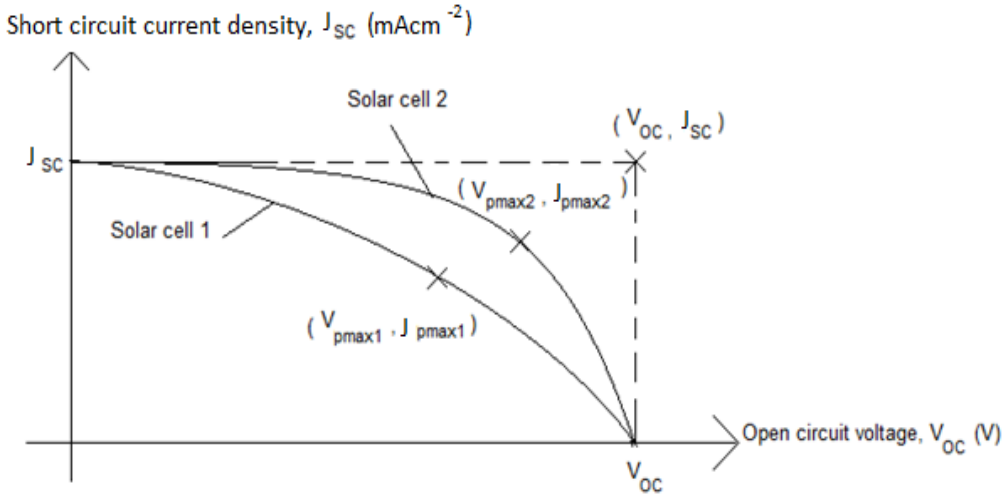

Figure (1.22): Two cells have the same V_{OC} and J_{SC}, but solar cell 2 has higher FF than solar cell (Marcus T. Ch., 2012)

The efficiency of the cell depends on the following parameters:

1. Dimensions, internal construction and active area.

2. Material properties (optical, electrical and energy levels).
3. Junction characteristics.
4. Anti-reflective coating, and surface texture.
5. Contact and grid configuration.
6. Irradiation damage.
7. Environmental exposure history. **(Chandra B. P. and Nath R., 1989).**

Quantum Efficiency (QE)

It is the efficiency as a function of the energy or wavelength of incident radiation. For a particular wavelength, it specifically relates the number of charge carriers collected to the number of photons shining on the device. It can be reported in two ways:

External Quantum Efficiency (EQE)

This type includes losses by reflection and transmission. External quantum efficiency is also called Incident Photon to Current Efficiency (IPCE).

Internal Quantum Efficiency (IQE)

It factors out losses due to reflection and transmission of photons like processes involving absorbed photons. By accounting for transmission and reflection processes, EQE can be transformed into IQE. **(Benanti T. L. and Venkataraman D., 2006).**

1.5.5 Comparison with Inorganic Cells

Light absorption results in photo excitation of electrons (excitons). In order to achieve charge separation an electrical field is necessary. This is provided by the contact junction to another material exhibiting a different work function (ionization energy).

In the case of crystalline inorganic semiconductors these processes are described by energy-band models. The situation in polymeric organic semiconductors is more complex due to the lack of a three-dimensional crystal lattice, different intermolecular interactions, local structural disorders, amorphous and crystalline regions, and chemical impurities.

For example the energy-band structure of organic conductors, calculated using the extended Hiickel method (or Hückel molecular orbital method (HMO), proposed by in 1930, for the determination of energies of molecular orbitals of pi electrons in conjugated hydrocarbon systems, such as ethene, benzene and butadiene) is more complex than inorganic crystalline or amorphous semiconductors figure 1.23. As a consequence light absorption often results in excitons formations. Excited electron and generated hole interact strongly and diffuse as uncharged particles until they dissociate.

The charge-carrier mobilities are several orders of magnitude lower than inorganic semiconductors. Still classical band model theories can provide qualitative understanding of the phenomena in molecular organic materials.

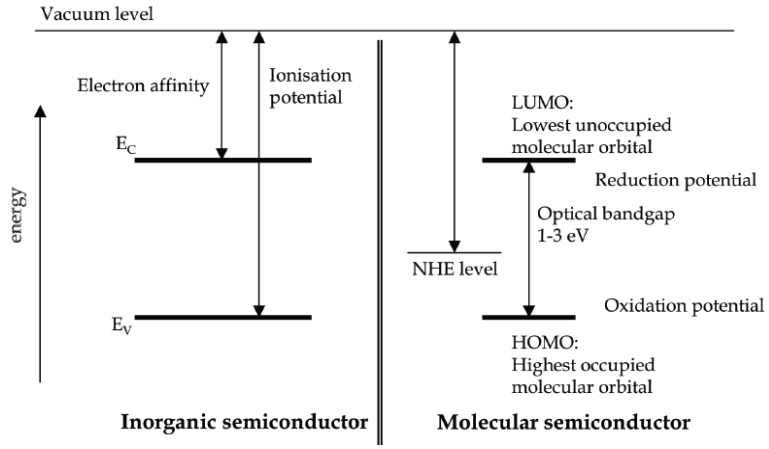

Figure 1.23: Energy levels in inorganic semiconductor and molecular semiconductor.

One then can utilize Schottky and pn-junction models, to understand a rough- behaviors of the organic materials. **Figure 1.24** shows the charge separation distance differences between inorganic and organic cells.

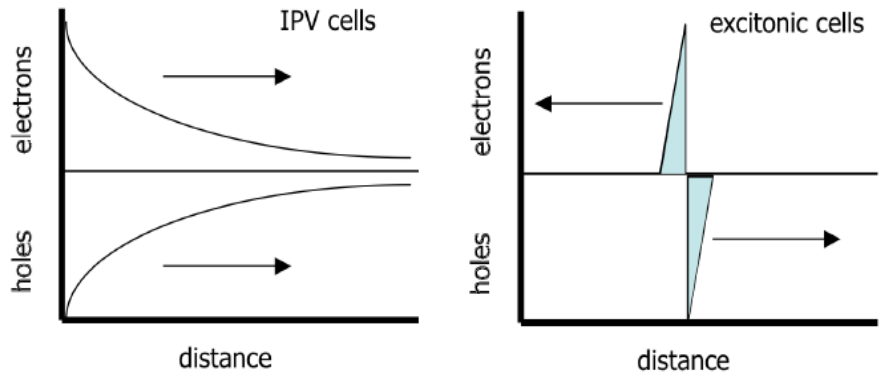

Figure 1.24: Charge seperation distance in inorganic and organic solar cells.

According to classical theories, p-type and n-type doping of intrinsic material creates new energy levels in the band gap close to the band edges. This changes the chemical potential of electrons in the material (Fermi levels).

If a semiconductor is brought into contact with another material having a different work function the Fermi levels equilibrate by building up space-charge layers at the interface. Due to its low charge-carrier density, this space-charge region is formed almost completely within the semiconductor in contact to a metal electrode.

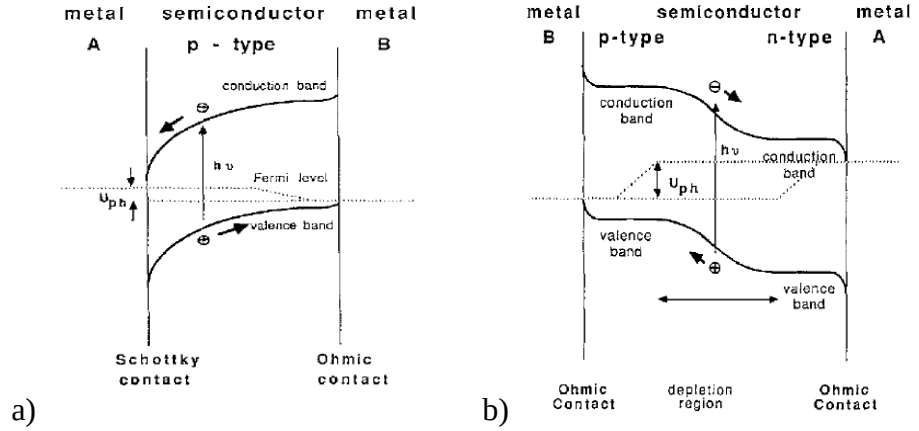

Figure 1.25:Schottky contact as formed between a metal A of low work function and a p-type semiconductor. The metal B here forms an ohmic contact. b) Classical pn junction. Both metals are chosen to form ohmic contacts. Up, = photo voltage.

Figure 1.25 shows a p-type semiconductor with a high work function and a metal with a low work function (A1 4.2 eV, In 4.1 eV), under illumination. The majority carriers (holes)

produced by light excitations move into the semiconductor and the electrons towards the metal. **(Wohrle D.,Meissner D., 1991).**

The Fermi levels shift due to this charging effect and a photo voltage is produced. However, the situation, even in mono-crystalline semiconductors, is usually complicated due to interface layers formed by chemical reactions at the interface. **(Wohrle D.,Meissner D., 1991).**

At the contact of a p-type and n-type material, space-charge layers are formed at both sides of the interface as shown in **Figure 1.26**. On illumination, charge carriers flow in both directions (electrons to the n-side, holes to the p-side) and establish a photo voltage **(Savenije T. J., 2012)**

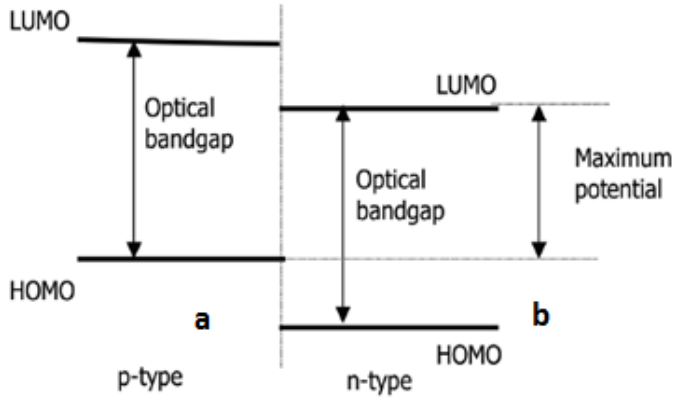

Figure 1.26: Energy level difference between p-type and n- types semiconductors

For IPV cells the Voc is limited by the electrostatic potential at the junction. For OPV cells based on two materials, optical excitation leads to the formation of an exciton in one of the layers. For the charge separation process part of the original photon energy is lost, causing an electron in the n-type and a positive charge in the p-type as shown above in **figure (1.17)**. In case there is no potential loss at the electrodes (Voc= Ionization potential of the p-type material – electron affinity of the n-type layer). In practice, the potential loss in the electrodes is about 0.2eV. **(Savenije T. J., 2012).**

1.5.6 Organic Solar Cells Applications and Challenges

Inorganic PVs are used to feed the main grid and to provide power for systems that cannot be connected to the grid like remote systems, orbiting satellites, consumer systems, handheld calculators or wrist watches, remote radio-telephones and water pumping applications.

OPVs cells are not intended to compete with IPVs, but rather to be used for specific applications, such as packaging, clothing, flexible screens, and recharging cell phones and laptops. However, in the longer term, they could make a significant contribution.

Improvements in efficiencies by about a factor of ten must be obtained to generate commercial interest. Very low production costs for organic solar cells might then favor their application. Today's research is mainly focused on obtaining a greater understanding of the mechanism of operation of these devices in order to find a ways to improve the performance. Solar cells with nano-porous Titania with 45nm diameter pores and filling the pores with polymer have been built, but the excitons could not reach the organic-interface to split. This could be overcome by making smaller pores and increasing the diffusion length of excitons.

The introduction of organic-inorganic interface with small band gap materials has several advantages. The most notable is that excitons can be transferred to the interface from relatively large distances by Förster energy transfer, but then need to adjust the material energy levels to split excitons at the interface.

Polymer chains can be aligned in 75 nm diameter pores and that can increase the charge carrier mobility by a factor of 25**.(McGehee M. D., 2005).**

Many attempts are made to tailor the organic molecules for specific purposes. Widely separated Fermi levels of the two materials forming the active contact are necessary for high Voc. Using organic molecules containing strong donating groups on one side of the contact and strong withdrawing groups on the other side, may shift the Fermi levels in the appropriate directions. For the p-type material, adding acceptor-like compounds ("doping") can shift the Fermi level closer to the valence band. For the n-type material, "doping" with strong electron

donors leads to a shift towards the conduction band. The problem, however, is that I_{SC} becomes too small due to the high series resistance established in the organic materials.**(Thompson B. C. and Frechet J. M., 2008).**

Perhaps different absorbers in combination should be tailored to have higher absorption coefficients over the entire visible spectrum up to about 1000 nm. The optical filtering effect in the first layer of p-n devices needs to be lowered in order to improve charge-carrier generation close to the interface. Band- and energy levels must match at the interface of p-n type cells.**(Wohrle D., Meissner D., 1991).**

Finally, losses due to reflection, current collection and resistance must be minimized. Organic layers offer other possibilities. Only very recently, a photosynthesis-type of charge generation and separation was implemented using the Longmuir-Blodgett technique, based on the molecular arrangement: electron donor/ sensitizer/ electron acceptor. In this device, unidirectional photocurrent was observed. After excitation, the electron is transferred from the sensitizer to the acceptor and at the same then replaced from the donor molecule on the opposite side. (**SalleoA. et. al, 2008**).

Chapter 2

Experimental Procedure and Techniques

P3HT: PCBM Cell Architecture and Fabrication

We focused our study to the P3HT:PCBM organic solar cell {P3HT: poly3-hexylthiophene; PCBM: Phenyl-C61-butyric acid Methylester}. It is of the type BHJ Polymer-Fullerene (section 1.5.2-C2). In this chapter the method of fabrication with acceptable efficiency and the procedure to study the cell properties is reviewed.

2.1 BHJ Cell Architecture

The BHJ cells consist of layers as shown in **figure 2.1**. These are mainly; an ITO (Indium Tin Oxide) coatedglass substrate, with gold electrodes directly deposited on it, followed by a PEDOT:PSS layer, covered by the organic active layer, over which lies an aluminum cathode.

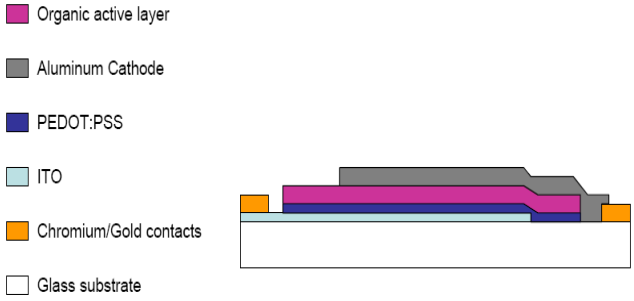

Figure 2.1: BHJ cell architecture.

2.1.1 The substrate comes coated with ITO layer.A section is itched using HCl with Zn powder to deposit the electrodesand other layers as shown in **figure 2.1**.

2.1.2 Au Electrodes

They are deposited directly on the substrate and their function is that to collect the excitons within their lifetimes.A high work function anode and low work function cathode are used and this difference creates a built-in electric field within the solar cell that determines the V_{OC} of the cell. **(Choy W., Fung D., 2013).**

2.1.3 PEDOT: PSS [Poly 3, 4-EthyleneDiOxyThiophene: Poly-Styrene Sulfonate] as shown in figure 2.2 is a mixture of two ionomers. The PSS component is made up of sodium polystyrene sulfonate and carries negative charge. The PEDOT is a conjugated polymer and carries positive charges. Together they form a macromolecular salt. That is used as a transparent, conductive polymer with high ductility.The compound improves the surface quality of the ITO layer, i.e. reducing the probability of shorts, and facilitates the hole injection/ extraction.

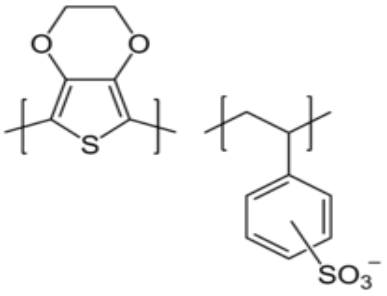

Figure 2.2: PEDOT:PSS structure.

2.1.4 The active layer (P3HT: PCBM)

A-P3HT: PCBM Chemical Structure

One of the most efficient materials used in the cells active layers are P3HT and PCBM. It has a reported efficiency about 5% and this high for organic materials. The structure is shown in **figure 2.3**.

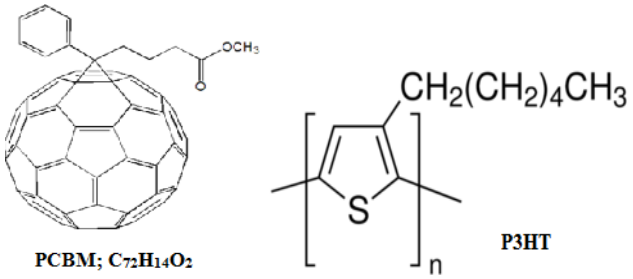

Figure 2.3: The structure of P3HT, PCBM.

PCBM is a fullerene derivative, because of the high hole mobility it plays the role as an ideal electron acceptor for many reasons. First, is the spherical shape and the favorable electron affinity with good electron mobility of 10^{-3} $cm^2V^{-1}s^{-1}$. Second, it has an energetically deep-lying LUMO, which endows the molecule with high electron affinity relative to many

potential organic donors. Third, the triply degenerate LUMO using PCBM: $C_{60}H_{24}O_2$ allows a reversible reduction with up to six, illustrating its ability to stabilize negative charge. The problem is that this molecule has a low solubility, to solve the problem this molecule has in organic solvents. Fullerenes are typically substituted with soluble side chains. We used the PCBM: $C_{60}H_{24}O_2$for its high crystallization and charge mobility.**Figure 2.4** shows the band structure diagram for different donors relative to the fullerene acceptor PCBM.

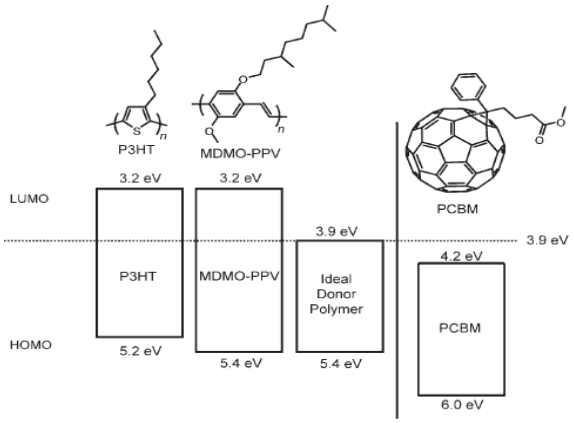

Figure 2.4: Band structure diagram illustrating the HOMO and LUMO energy of MDMO-PPV, P3HT and Ideal donor relative to PCBM (Thompson B. C.,and Frechet J. M., 2008)

P3HT is a member of the Polythiophene conducting polymer family. The excitation of the π-orbital electron gives the photovoltaic effect in the blend.Polythiophenes represent an important class of conjugated polymers, because they meet the essential requirements of process ability, adequate charge transport properties, and the possibility of structural modifications. Due to the poor solubility of un-substituted polythiophene in organic solvents, a hexyl-chain is added in the 3 position, rendering it asymmetrical.

The 3-hexylthiophene monomers can be coupled with different orientations with respect to the side chain. Polymerization leads to regiorandom (RRa) and regioregular (RR-P3HT), as shown in **Figure 2.5**. RRa-P3HT has no practical use low crystallinity. On the other hand RR-P3HT features a high crystallinity because of the π-π stacking of thiophene rings resulting in agood hole mobility up to 10^{-2} $cm^2V^{-1}s^{-1}$. **(Pani R. C. et al, 2013).**

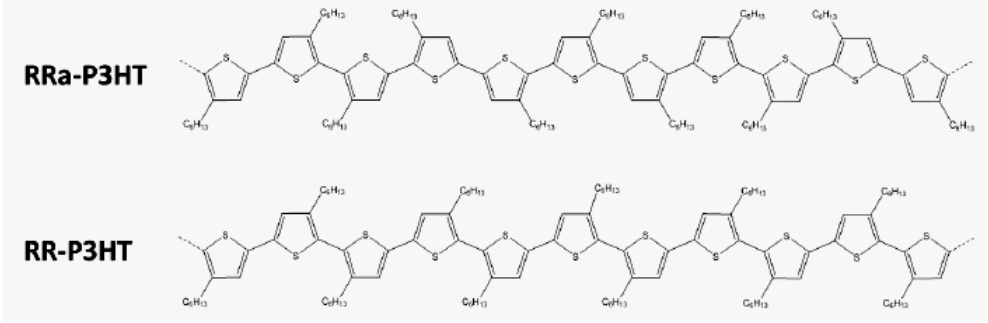

Figure 2.5: Sections from regiorandom (top) and regioregular (bottom) P3HT chains (BrigerFreisinger, 2013).

We used these polymers in our work because of their relatively short excitation diffusion length (10~20 nm). This type of active layer has shown impressive progress in terms of power conversion efficiency. **(Sariciftci N. S., Scharber M. C., 2013).**

B- P3HT: PCBM Blend Characteristics

Donor- Acceptor Interaction: the mechanism is described in **figure 2.6**

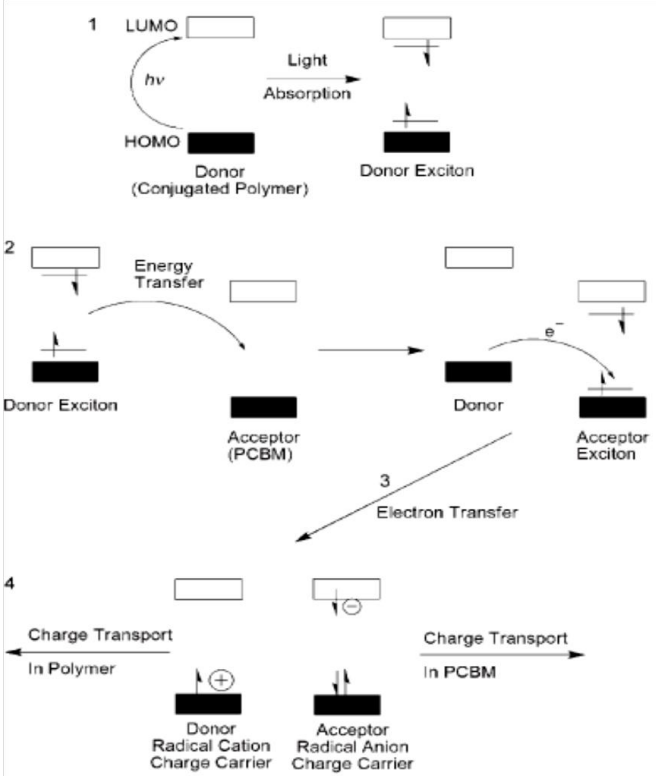

Figure 2.6 Conversion mechanism of the P3HT:PCBM BHJ Polymer-Fullerene cells

Absorption Spectrum

The organic polymers have wide band gaps, and thus they have efficient absorption near UV spectrum. The blend of the two materials changes the effective gap to 1.8eV corresponding to a maximum efficiency around 650nm as shown in **figure 2.7**.

One interesting characteristic of this compound is that, the band gap can be altered by changing the alignment of P3HT chains, i.e. head-tail alignment has narrower gap than head-head alignment. It was found also that in several materials, different arrangements in lateral chains can result in different band gap structures. **(Weihao G., 2009**). In addition, changing the ratio of P3HT:PCBM can change the gap **(Al-Ibrahim M., Ambacher O., 2005).**

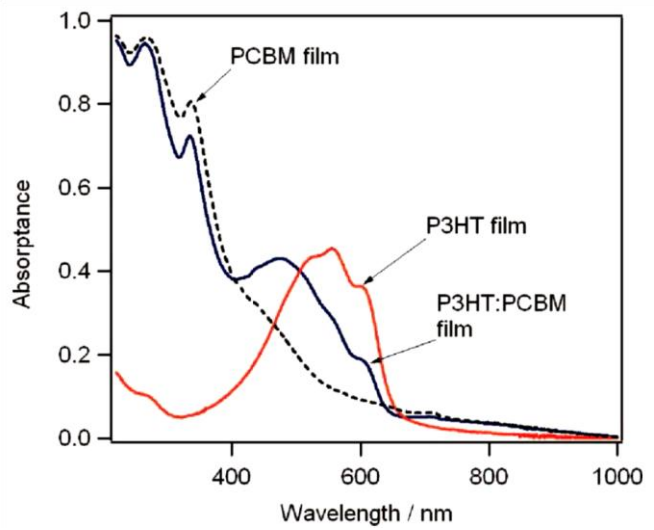

Figure 2.7 Absorption spectrum P3HT: PCBM film and its components (WeihaoGe., 2009).

Charge Generation

In the presence of P3HT, the PCBM excitons can effectively split quiet fast ($P3HT^{+}$, $PCBM^{-}$). The charge transfer is faster than the decay time of the PCBM excited states, i.e. the excitons separate before the recombination of electrons and holes. The Gibbs free energy(Gibbs free energy: Free enthalpy , thermodynamic potential that measures the "usefulness" or process-initiating work obtainable from a thermodynamic system at a constant temperature and pressure) during splitting can be calculated using the Marcus-Hush theory (Explains the rates of electron transfer reaction, the rate which an electron can move or jump from donor to

acceptor.). It is approximately 1eV and that is over half of the absorbed photon energy of 1.8eV. It is also larger than the binding energy of the excitons (0.3 - 0.5eV) indicating that a large portion of photon energy is wasted into heat.

Efficiency

Nanoscale morphology is important for improving the cell efficiency. When P3HT: PCBM, blends adopt an organized morphology the P3HT molecules align and the PCBM takes a nano-crystal structure, the cell's performance is improved **(Weihao G., 2009)**. It is found that the absorption spectrum widens, I_{SC} increases V_{OC} slightly decreases and the surface resistivity decreases. The Voc change is likely a result of the change in donor -acceptor band structures.

This is supported by the observation that when applying electric field in synthesizing the organized structure, an increase in V_{OC} is achieved, indicating the occurrence of certain polarized structure in the material. With a widened absorption spectrum, more excitons can be produced. Moreover, this morphology gives a large interface, increasing separate percentage. **(WeihaoG., 2009)**.

An experiment has also shown that there's a preferred orientation, which provides charge carrier channel, enhancing charge mobility, and decreases surface resistivity. These factors combined increase I_{SC}. The power conversion can reach 5% **(Reyes- Reyes M., et al., 2005).**

2.1.5 Al Electrodes

These electrodes are built as the Au electrodes to collect the excitons generating in the cell, and to applyit's built – in electric field that determines the V_{OC} of the cell.

2.2 Cell Fabrication Procedure

The experiment was conducted at the Nanotechnology Research Laboratory (NRL), Al-Quds University, where we used the AFM microscope, the spin coater and the Cryogenic Four-Probe Station. The thermal vacuum evaporator we used is at the Physics Laboratory, Bethlehem University. See section 2.3 for details about the instruments.

2.2.1 ITO Substrate Preparation:

The ITO substrate was masked with scotch except for the last 5 mm as shown in **figure 2.8**. Then the Zn powder was spread over the unmasked part and rubbed with a cotton swab dipped in HCl. Then the cell was washed with water and the mask was rapidly removed.

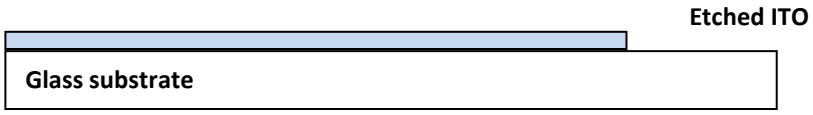

Figure 2.8: Etched ITO substrate.

Washing

The etched ITO glass substrate was cleaned by sonification: first in microelectronic detergent for 15 minutes then in de-ionized water 3 times 15 min each. Then it was rinsed under an acetone bath for 15 min, and in isopropyl bath for 15 min. Finally, the sample was dried by blowing nitrogen gas.

Figure 2.9: Washing ITO substrate.

Electrodes Deposition

Depositing the Au and Al electrodes with certain thickness was done using Vacuum Thermal Evaporation **(VTE)**. The technique involves heating the electrodes materials in vacuum. The substrate was placed several centimeters away from the source so that the evaporated material can directly deposit onto the substrate, as shown in **figure 2.10**.

The method is useful for depositing many layers of different materials without chemical interaction between the layers. However, there are sometimes problems with making uniform thickness over large-area substrates. In addition, the materials that deposit on the chamber wall can contaminate later depositions. This method can create holes in the film due to shadowing, which can increase the series-resistance and may create short circuits.When evaporation is performed in poor vacuum or close to atmospheric pressure, the resulting deposition is generally non-uniform and tends not to be a continuous or smooth film. Rather, the deposition will appear fuzzy.

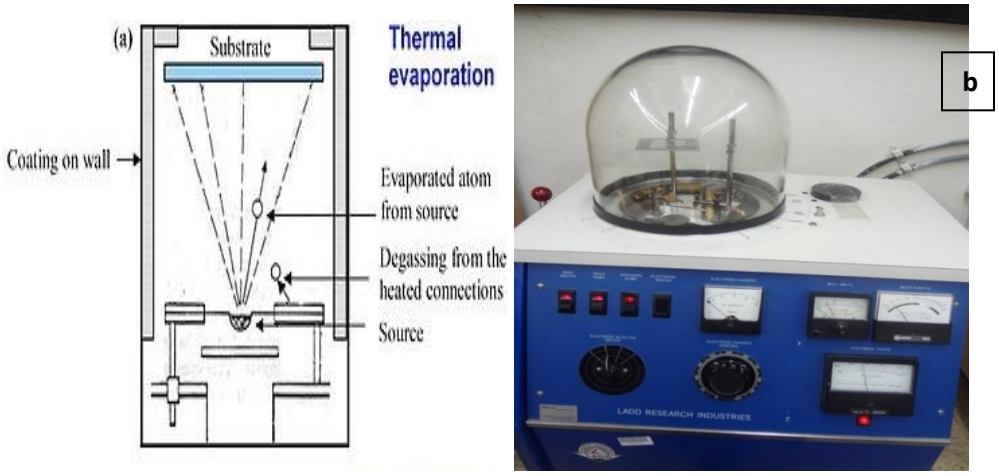

Figure 2.10: a) Thermal evaporator process, b) Thermal Vacuum evaporator

2.2.2 Au Electrodes Deposition

To deposit the electrodes by thermal evaporation, the substrate was covered by a scotch except for few millimeters from both sides as shown in **figure 2.11**.We deposited the electrodes with 100 nm thickness.

Au started melting at the current value of 9A and evaporation at 11A. The pressure before the melting was 9.10^{-6}torr, but during evaporation it was $1.5.10^{-5}$torr.

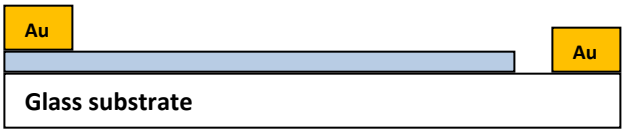

Figure 2.11: Gold electrodes deposited substrate.

The typical pressures for the VTE are 10^{-6} to 10^{-8} torr. **(Kymissis L., 2008).**

Figure 2.12: Photo of the evaporator during gold deposition.

Washing

The deposited gold was washed for 15 min in iso-propanol path, then dried with N_2 gas and finally put in UV-ozone for 15 min.

PEDOT:PSS and P3HT: PCBM Deposition

Many methods can be used to deposit the active layer in the cell. That includes spraying; spin coating; vaporization; (screen, stamping, gravure and ink-jet) printing; roll to roll and slot-die coating **(Augustin T. J. et al, 2012).** We used spin coating to deposit the PEDOT:PSS and the active layer.

Spin coating is the method applied to standard flat wafers. It involves the acceleration of a liquid puddle on a rotating substrate. The coating material is deposited at the center of the substrate either manually or by a robotic arm.

The coating involves a balance between the rotational centrifugal forces controlled by the spin speed and forces determined by solvent viscosity. Some parameters involved in spin coating are solution viscosity, solid content, angular speed, and spin time.

Thermal Annealing It is better to anneal the sample after the deposition of PEDOT:PSS layer and before depositing the active layer which is should be annealed too. Thermal annealing is used to optimize the material morphology. Annealing helps the polymer chains to reorganize, and the fullerene molecules to diffuse freely into the composite and reorder

(Thompson B. C. and Frecher J. M. J. 2008). It helps the blend to get a better organized structure, with the P3HT forming long thin fibers while PCBM becomes more homogeneous.

Annealing heats the active layer to a temperature greater than the T_g of the material. For P3HT T_g reported value is 110°C, **(Kim Ch. H., et al, 2005).**

At room temperature the crystallization of the two components is inhibited by their presence together. Thermal annealing helps the creation of crystalline structure. When P3HT chains are crystallized, nucleation sites are provided for PCBM. The growth of ordered conformation on large areas is possible. **(Weihao G., 2009).**

Figure 2.13: Spin Coater

2.2.3 PEDOT:PSS

This mixture was filtered using a 0.45 μm filter before deposition on the substrate by spin coating at 3000 rpm for 30 sec then 3500 rpm for another 30 sec.

Figure 2.14: 0.45μm filter.

The thickness of this layer is around 40 μm. We rapidly cleaned the electrodes using a cotton swab. This layer was dried (annealed) at 110° for 2 min.

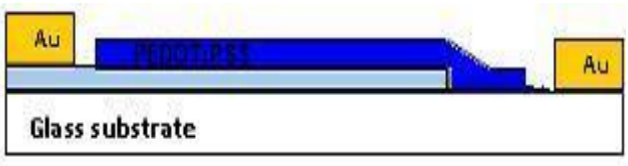

Figure 2.15: PEDOT:PSS deposited layer.

2.2.4Preparing the Active Layer Blends and Depositions

We prepared different concentrations of the active layer components using spin coating under different spin speeds and duration, to optimize the best possible blend that may affect the cells efficiency. The active material was solved in an organic solvent (dichlorobenzene). **Table 2.1** and **figure 2.16** show the different ratios of the active layer components.

Table 2.1 Mixtures with different P3HT: PCBM Ratio

P3HT PCBM Ratio	P3HT (mg)	PCBM (mg)	Dichlorobenzene(ml)
1:1	15	15	2
2:1	30	15	3
1:2	15	30	3
1:3	15	45	4
3:1	45	15	4

Figure 2.16: Active layer preparation

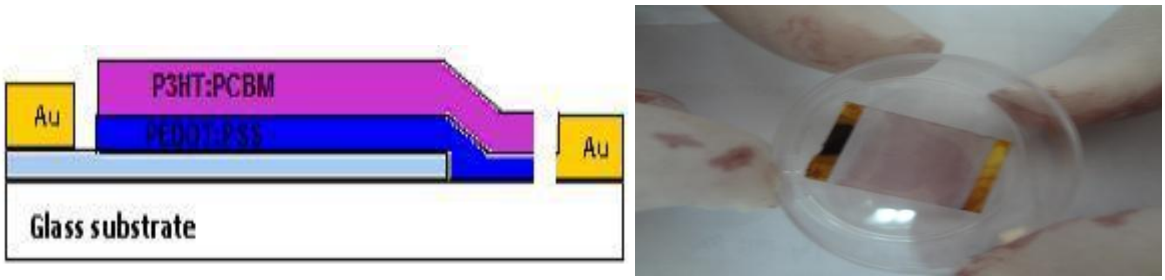

Figure 2.17: Active layer deposition

2.2.5 Al Electrode Deposition

The cell was completed by evaporating the Al material thermally using a mask. For Al the melting current was about 12A, and for evaporation was 15A. The pressure before melting was about $9*10^{-6}$torr. The thickness of the electrode is about 100nm. The cell active area was 0.28 cm^2. **Figure 2.18** shows the schematic of the cell and **figure 2.19** shows one of the prepared the cells.

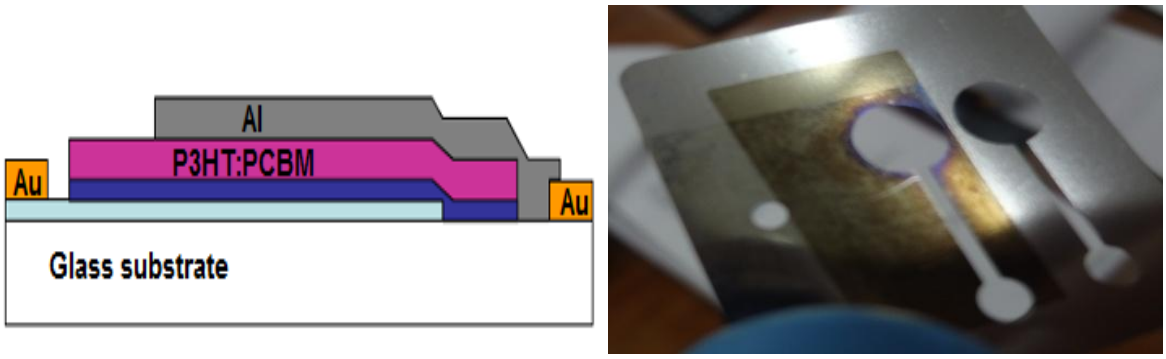

a) **b)**

Figure 2.18: a) AL electrode deposition. b) The Mask.

2.2.6 Manufactured Cells and Their Specifications

A total of 12 cells were made using different active layer components mixing ratios, spin speeds and spinning duration. 10 cells were standardized to 100nm thickness and 2 cells with active layer thickness of 50nm and 150nm, to compare the efficiency dependence on thickness and other parameters. **Table 2.2** shows the active layers parameters for the 12 cells.

The blend material was filtered using 0.45µm filter before spin coating. For single step coating (spin type: 1) the speed was 500 rpm for 60 sec. For 2 step coating (spin type: 2) the

spin speeds were successively 500 rpm for 18 sec and 1000 rpm for 50 sec. We rapidly water cleaned the electrodes cotton swab, then the film was annealed at T= 108° for 1 min.

Table 2.2 Active layer parameters for the 12 cells. Spin Type 1: 500 rpm for 60 seconds; 2: 500 rpm for 18 sec then 1000 rpm for 50 sec. Annealing time 1 min at T=108C. The active area 0.28cm^2.

Cell Number	Cell ID	Thickness (nm)	Spin Type	P3HT/PCBM
B1	C11-1-50	50	1	1/1
B2	C11-1-150	150	1	1/1
B3	C11-1-100	100	1	1/1
B4	C11-2-100	100	2	1/1
B5	C12-1-100	100	1	1/2
B6	C12-2-100	100	2	1/2
B7	C21-1-100	100	1	2/1
B8	C21-2-100	100	2	2/1
B9	C13-1-100	100	1	1/3
B10	C13-2-100	100	2	1/3
B11	C31-1-100	100	1	3/1
B12	C31-2-100	100	2	3/1

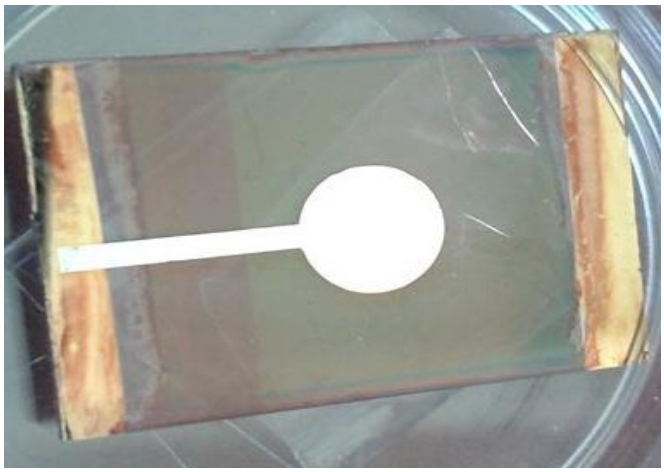

Figure 2.19: One of the prepared cells (B3, C11-1-100).

2.3 Testing and Measurements

We will give a review about the basic testing instruments used

Atomic Force Microscope (AFM): with a resolution of a nanometer, 1000 times better than the optical diffraction limit. The AFM consists of a cantilever with a sharp tip (probe) at its end that is used to scan the specimen surface. The cantilever is typically silicon or silicon nitride with a tip radius of curvature in the order of nanometers. When the tip is brought into proximity of a sample surface, forces between the tip and the sample lead to a deflection of the cantilever according to Hooke's law. Depending on the situation, forces that are measured by AFM include mechanical contact force, Vander Waals forces, capillary forces, chemical bonding, electrostatic forces, magnetic forces, Casimir forces, solvation forces, etc.

Additional quantities can be measured through the use of specialized types of probes. Typically, the deflection is measured using a laser spot reflected from the top surface of the cantilever into an array of photodiodes. Other methods used include optical interferometry, capacitive sensing or piezoresistive AFM cantilevers. These cantilevers are fabricated with piezoresistive elements that act as a strain gauge. Using a Wheatstone bridge, strain in the AFM cantilever due to deflection can be measured, but this method is not as sensitive as laser deflection or interferometry.

If the tip is scanned at a constant height, there is a risk it may collide with the surface, causing damage. Hence, in most cases, a feedback mechanism is employed to adjust the tip-to-sample distance to maintain a constant force between the tip and the sample. Traditionally the tip or sample is mounted on a 'tripod' of three piezo crystals, responsible for scanning in the three dimensions. Later tube scanners were incorporated into AFMs later where they can move the sample in 3D using a single tube piezo with a single interior contact and four external contacts. The tube scanner has a better vibrational isolation, On the other hand the x-y motion can cause unwanted z motion resulting in distortion.

The AFM can be operated in a number of modes, depending on the application including static modes and a variety of dynamic modes where the cantilever is vibrated.

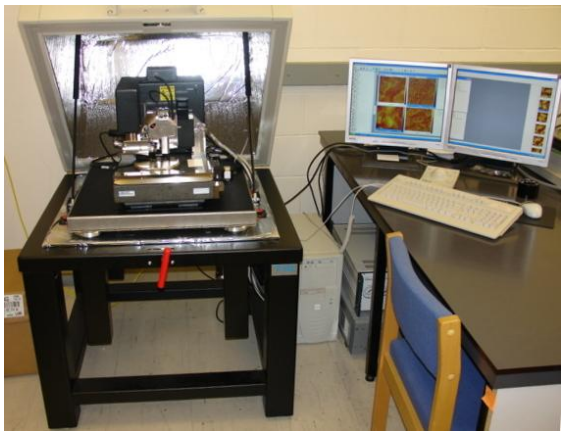

Figure 2.20: AFM microscope used in our work.

Cryogenic Four-Probe Station: it is a mechanical probe station, which is used to acquire signals from the internal nodes of a semiconductor device. The probe station utilizes manipulators which allow the precise positioning of thin needles on the surface of a semiconductor device. If the device is being electrically stimulated, the signal is acquired by the mechanical probe and is displayed on an oscilloscope. The mechanical probe station is often used in the failure analysis of semiconductor devices.

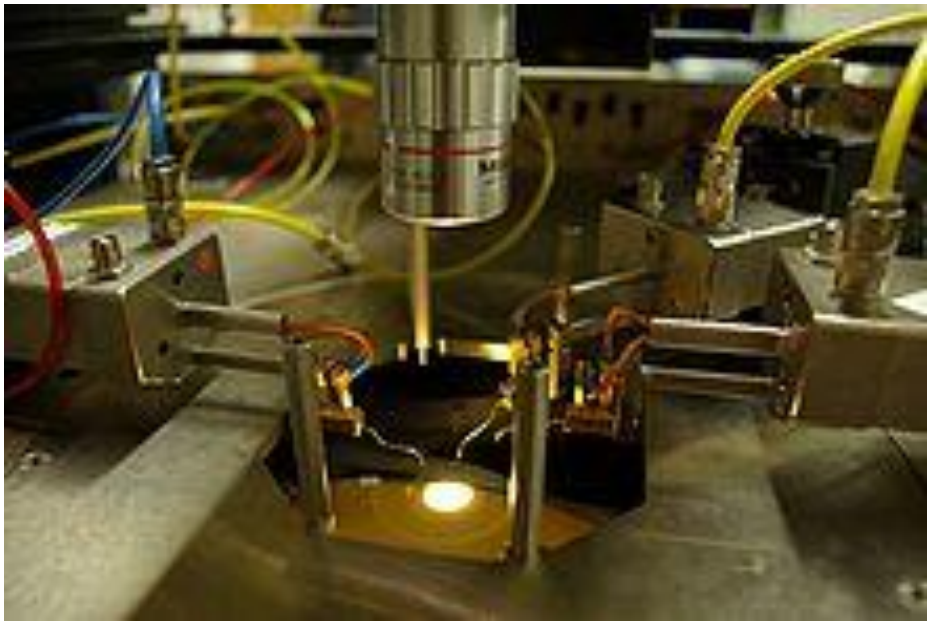

Figure 2.21: The Four Probe Station at NRL, Alquds University

There are two types of mechanical probes: active and passive. Passive probes usually consist of a thin tungsten needle. Active probes utilize a FET device on the probe tip in order to significantly reduce loading on the circuit.

Stage I: The current-voltage (IV) characteristics: We measured the open-circuit-voltage (V_{OC}) and the short current density (J_{SC}), to calculate the Fill Factor (FF) and efficiency (η)based on an input power of 30mW/cm^2. The IV characteristics were measured with a source meter under illumination (a lamp), in both light and dark modes for the same cell. In our case we used the Cryogenic Four-Probe Station Instrument which measured the IV characteristics in both light and dark conditions.

Stage II: We checked morphology and thickness of the layers: we used the AFM to determine the characteristics of bulk-heterojunction. The information about the surface was probed mechanically using piezoelectric elements that facilitate tiny but accurate and precise movements on electronic command that enabled the scanning. In some variations, electric potentials can also be scanned using conducting cantilevers. In more advanced versions, currents can be passed through the tip to probe the electrical conductivity or transport of the underlying surface.

2.4 Standard Testing Conditions

STC provides the same testing condition to all types of solar cells, modules and array so that manufactures and customers can make comparison.

The standard conditions are 100 mW/cm^2 of irradiance at a temperature 25ºC and Air Mass (AM) of 1.5 which is a measure of how much atmosphere sunlight must travel through to reach the earth`s surface. This is denoted as AM (x), where x is the inverse of the cosine of the zenith angle of the sun. AM describes the spectrum of radiation not the intensity. **(Bananti T. L. and Venkataraman D., 2006)**AM of 1.5 indicates 1.5 times the thickness of atmosphere. In other words, AM 1.5 indicates the sun shines about 30º from the horizon.The higher the air mass, the larger the radiation amount absorbed by the sky. **(Marcus T. Ch., 2012)**

We conducted our testing at room temperature with an estimatedinput power of 30 mW/cm^2, (effective power of the lamp is 1 watt, and after divergence the illuminated area is about 30cm^2). This should not make a major impact on the performance.

Chapter Three
Results and Analysis

3.1 Preview

In this chapter we present our results and the parameters that may affect the cell efficiency. That includes measuring the layers thickness using the AFM; and the IV measurements using the four probe station to conclude the effects of thickness, coating procedure and blend ratio on the efficiency.

3.2 The Cell Characteristics

3.2.1. AFM measurements

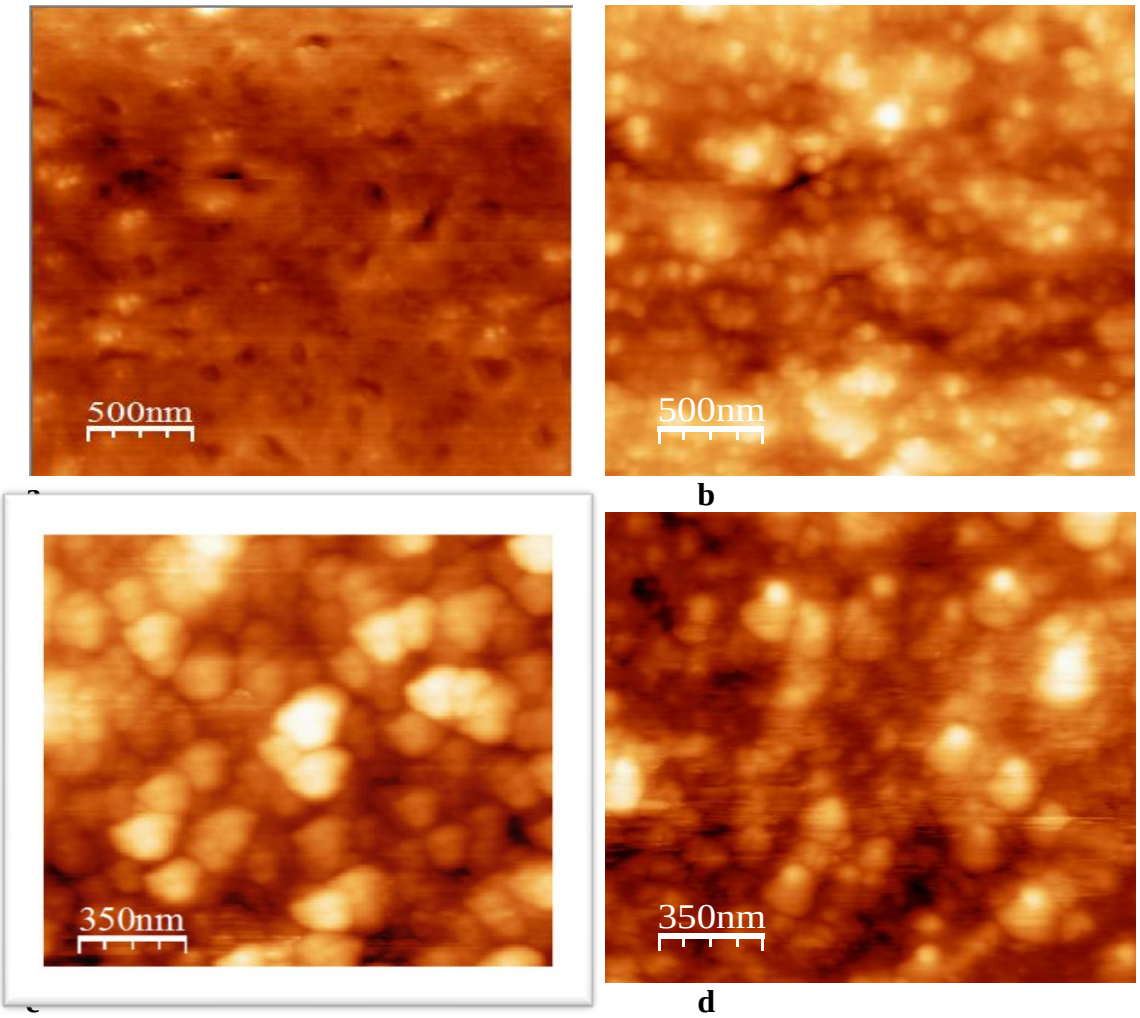

Figure 3.1: AFM morphology of the active layer blends (a) not annealed film, (b) 1:1 (c) 1:2, (d) 2:1 (b, c and d annealed at 108°C for 1 minute). Ratio: P3HT/PCBM

As shown in **figure 3.1** the annealing time plays a definingrole in crystallizing the molecules in the active layer which effects directly the exciton diffusion.

3.2.2. IV- Characteristics

Table 3.1 summarizes IV characteristics and efficiency dependence on active layer thickness. Tables 3.2 and table 3.3 show the performance dependence on the active layer blend ratio. The input power for all setups was 30 mW/cm^2 and the active area is 0.28 cm^2 for all cells. From the tables, we can see the following parameters that affect the efficiency of the cells

Table 3.1: IV characteristics and efficiency dependence on the thickness of the active layer Blend ratio 1/1; 1 step spin coating

Cell No. & ID	t (nm)	I_{SC} (mA)	J_{sc} (mA/cm^2)	V_{OC} (V)	I_{max} (mA)	J_{max} (mA/cm^2)	V_{max}(V)	FF	$\eta = \frac{Jmax.Vmax}{Pin}$
B1, C11-1-50	50	-0.477	1.7	0.62	- 0.0391	0.139	0.48	0.06	0.22 %
B3, C11-1-150	150	-0.085	0.30	0.61	- 0.0606	0.216	0.36	0.425	0.26 %
B3, C11-1-100	100	-1. 24	4.42	0.57	- 0.9767	3.488	0.40	0.554	4.65 %

Table 3.2: IV characteristics and efficiency dependence on the active layer blend ratio Thickness 100nm , 1 step spin coating

Cell No. & ID	Blend ratio	I_{SC} (mA)	J_{sc} (mA/cm^2)	V_{OC} (V)	I_{max} (mA)	J_{max} (mA/cm^2)	V_{max}(V)	FF	$\eta = \frac{Jmax.Vmax}{Pin}$
B3, C11-1-100	1/1	-1. 240	4.42	0.57	- 0.97676	3.488	0.40	0.554	4.65 %
B5, C12-1-100	1/2	-0. 884	3.157	0.6	- 0.73456	2.623	0.48	0.66	4.19 %
B7, C21-1-100	2/1	-1. 031	3.682	0. 6	- 0.83038	2.966	0.36	0.48	3.56 %
B9, C13-1-100	1/3	-0. 249	0.889	0.61	-0.1828	0. 65	0.40	0.48	0. 87 %
B11, C31-1-100	3/1	-0. 150	0.535	0.6	- 0.10592	0.378	0.28	0.33	0.35 %

Table 3.3: IV characteristics and efficiency dependence on the active layer blend ratio Thickness 100nm; 2 steps spin coating.

Cell No. & ID	Blend ratio	I_{SC} (mA)	Jsc (mA/cm^2)	V_{OC} (V)	I_{max} (mA)	J_{max} (mA/cm^2)	V_{max} (V)	FF	$\eta = \frac{Jmax.Vmax}{Pin}$
B4, C11-2-100	1/1	-1. 037	3.7	0.58	- 0.81397	2.907	0.40	0.54	3.87 %
B6, C12-2-100	1/2	-0. 731	2.61	0.58	- 0.61024	2.179	0.44	0.63	3.19 %
B8,C21-2-100	2/1	-0. 760	2.714	0.6	- 0.54831	1.958	0.36	0.43	2.35 %
B10, C13-2-100	1/3	-0. 242	0.864	0.6	- 0.17701	0.632	0.38	0.46	0.8 %
B12, C31-2-100	3/1	-0. 145	0.518	0.61	- 0.09072	0.324	0.32	0.33	0.35 %

1-The active layer thickness

The best efficient thickness of the active layer is about 100nm to absorb enough light. At larger thickness (150 nm), only a small fraction of the excitons can reach the hetero-junction interface. For less thickness (50nm) the recombination of the excitons will be more dominant which means less current is generated. The effect of the blend thickness on the efficiency is shown in **figure 3.2** in agreement with our analysis.

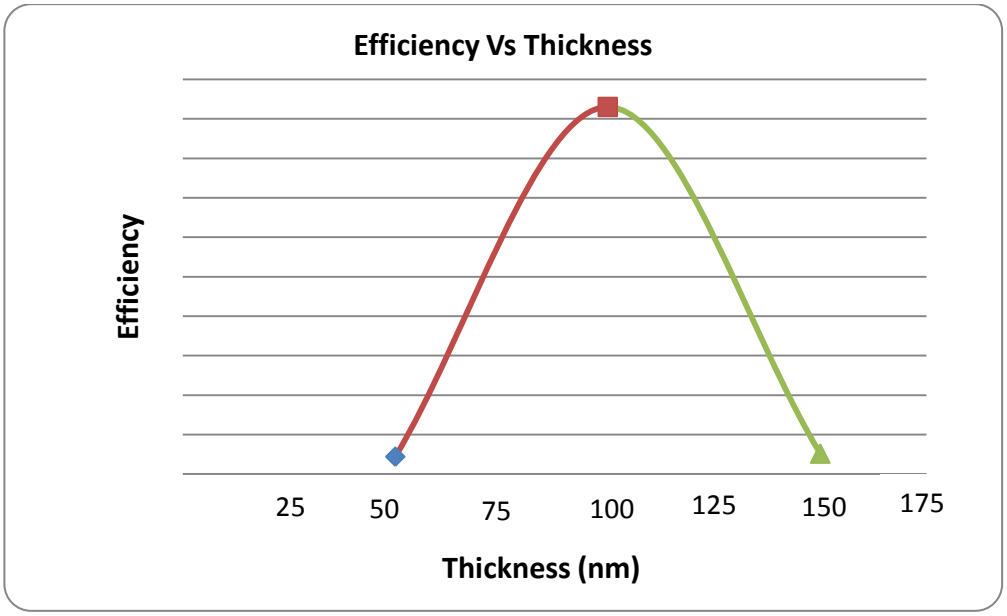

Figure 3.2: Efficiency vs. thickness of the active layer of the cells. 1:1 blend ratio

In general, the absorption coefficient depends on the photon wavelength and a thicker film can absorb photons with wider wavelength range. Exciton diffusion and charge collection process are more favorable in thinner films.All samples were annealed for the same time of 1 minute at 108°C (for better transport and decreased recombination) to standardize the effect of thickness with minimum variation of other factors.

2-Influence of the active layer mixture ratio

The highest efficiency η from our data was achieved at 1:1 ratio. From the fitting it could be about 1:1.3. The exciton diffusion length present in organic semiconductor, is about 10-20 nm. It seems such ratio provides the best nano-scale composition for charge separation and collection.

For the IV curves the 1:1 has the highest current most of the time but it falls earlier than the 1:2 case which is the second efficient. 2:1 has the same behavior but less efficient. The 1:3 and 3:1 cases are too weak to make any comparisons. The 1:1 and 1:2 similar IV behavior indicates the best ratio is between the two. The maximum power is achieved at around V=0.4 for 1:1 and 2:1 while it is delayed until V=0.5 for the 1:2 curve. This is consistent with the conclusion that the optimum efficiency is between 1:1 and 1:2. The efficiency curve fitting shows the best ratio is around 1: 1.3 or about 0.76.

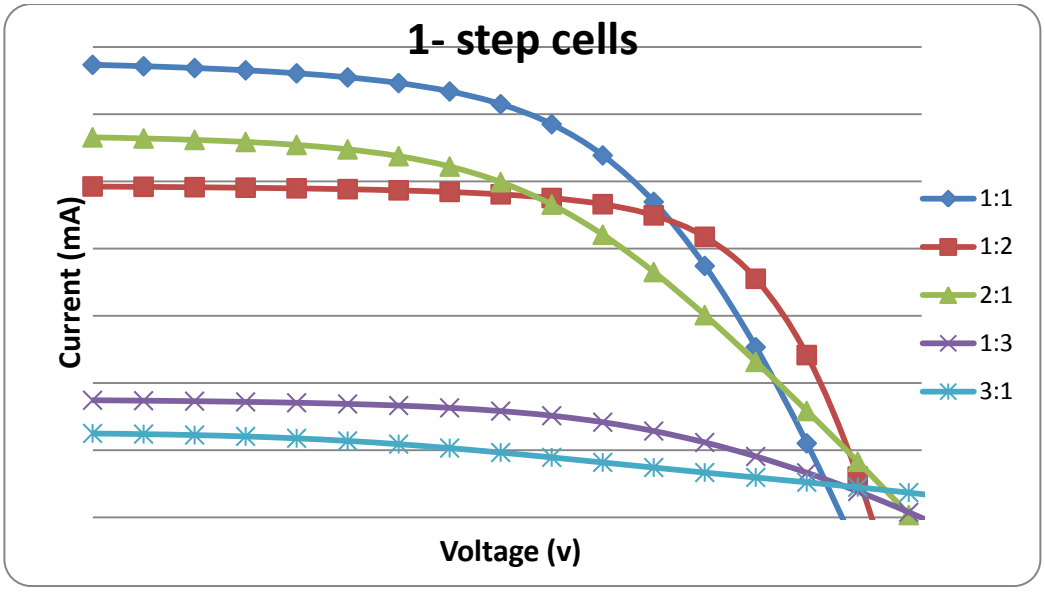

Figure 3.3a) IV curve for the various mixes using 1 step coating.

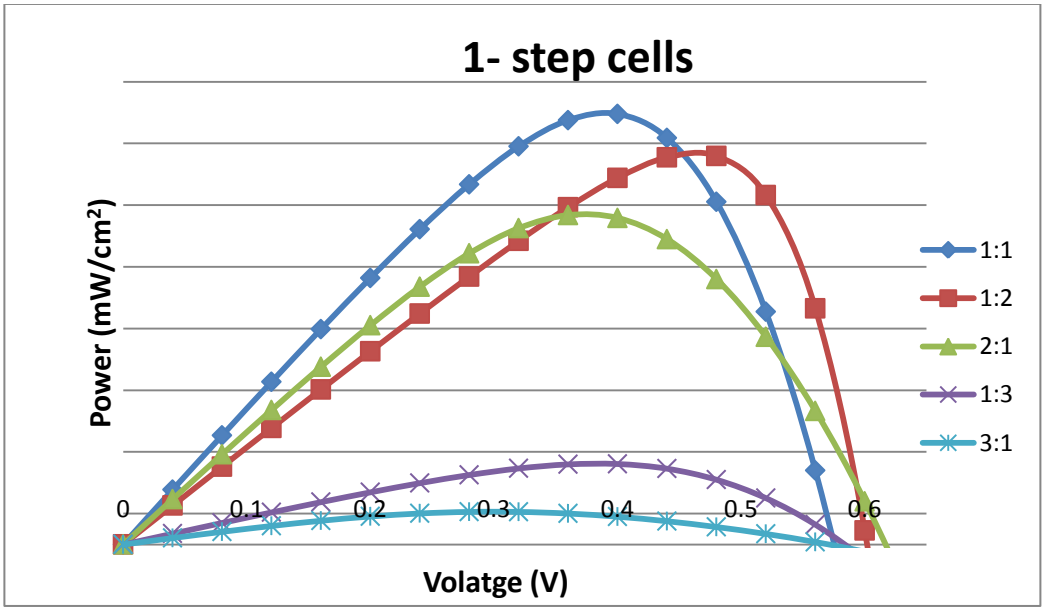

Figure 3.3b) Power- Voltage curve for the various mixes using 1 step coating.

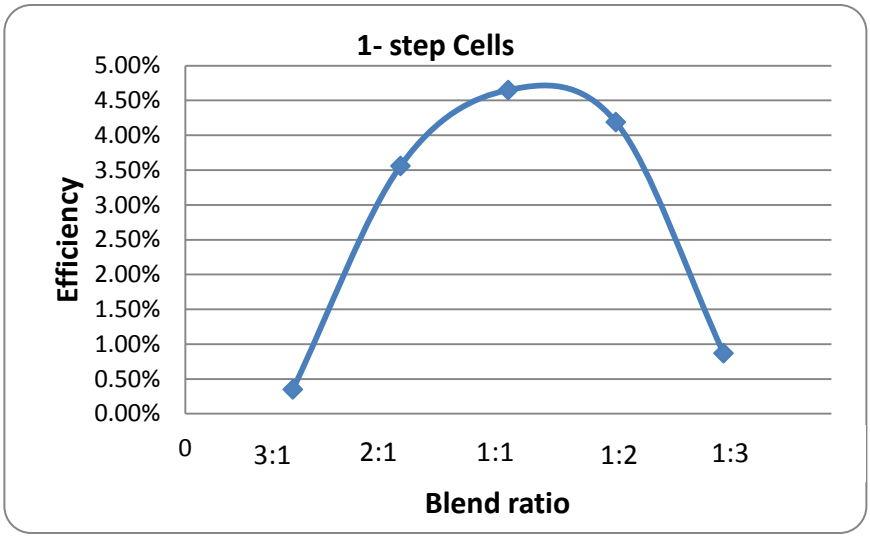

Figure 3.3: c) The efficiency vs. the mixing ratiofor the various mixes using 1 step coating.

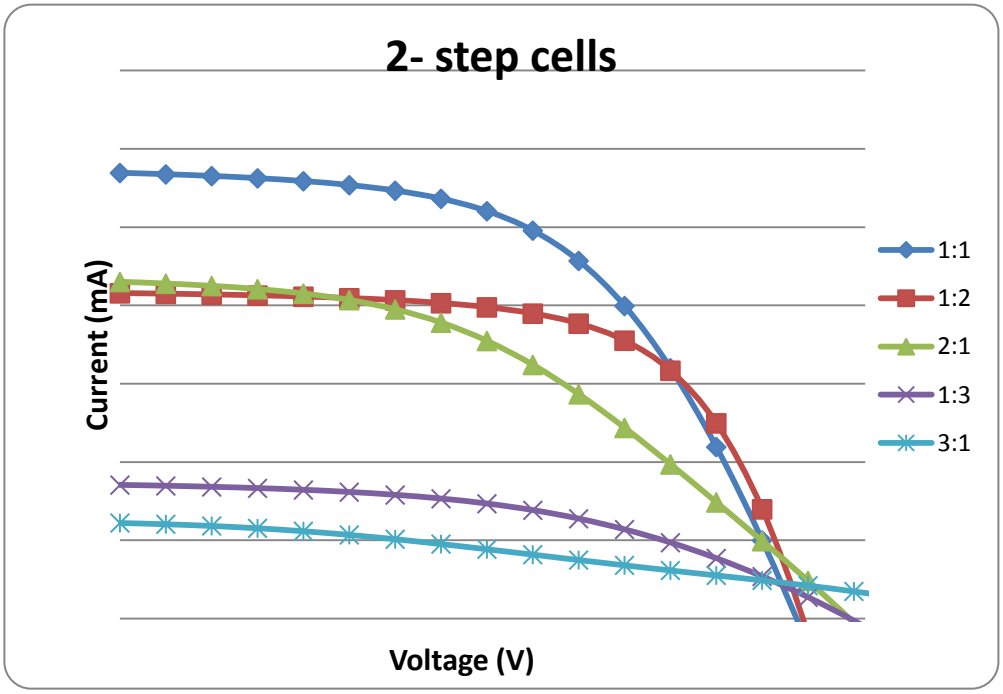

Figure 3.4: a) IV curve for the various mixes using 2 step coating.

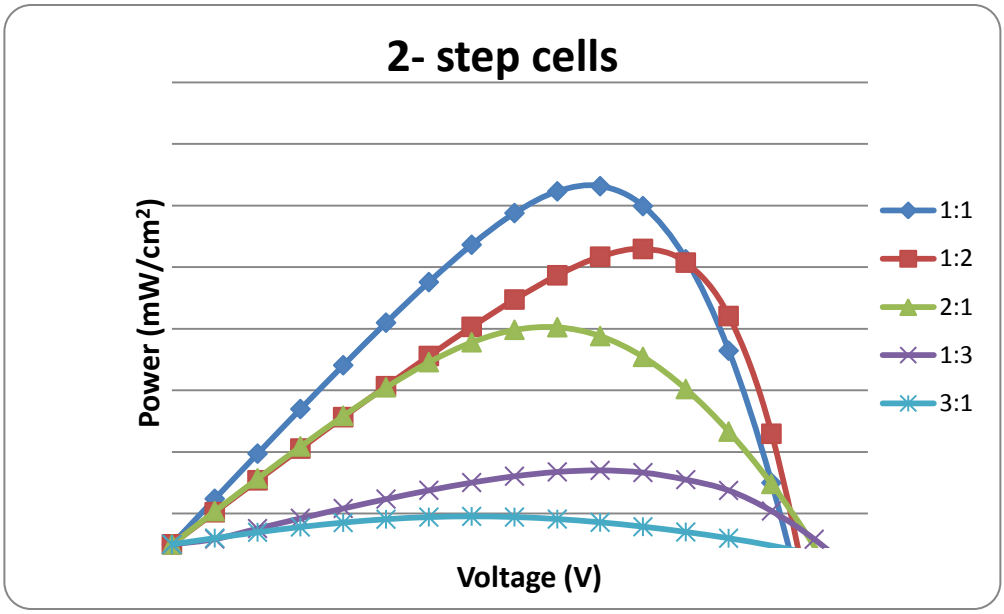

Figure 3.4: b) Power- Voltage curve for the various mixes using 2 step coating.

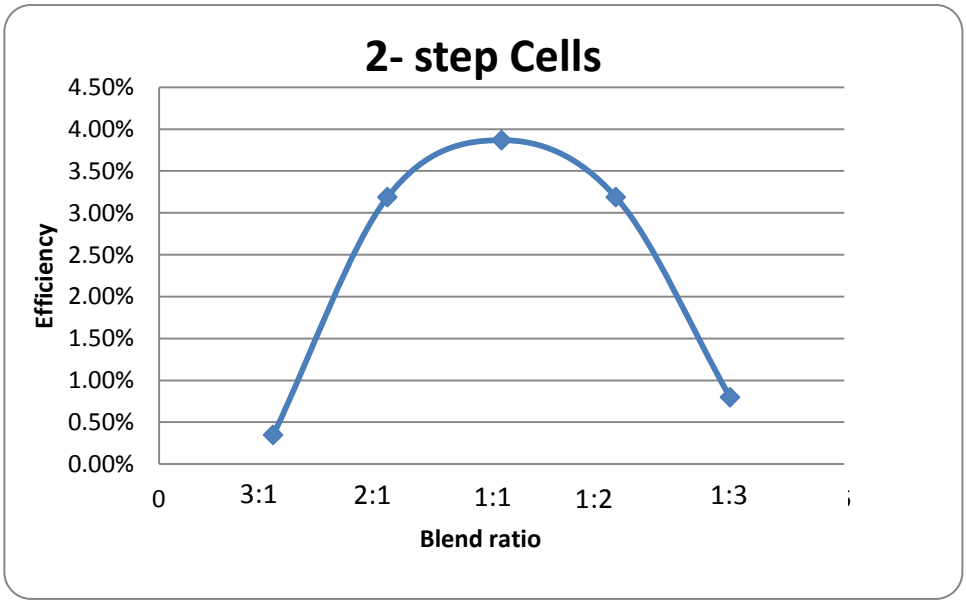

Figure 3.4: c)The efficiency vs. the mixing ratiofor the various mixes using 2 step coating.

3-The spin coating impact on the IV curves

Figures 3.5 and 3.6 show the impact on the IV and power curves. The overall observation is that single step coating cells have higher currents, powers and in turn efficiencies than the double step cells. Their overall behavior is the same: the IV shape, the power shape are the same. This means the overall spin coating is better achieved by a single step. The reason still

could be due to a non-uniform distribution through the two step compared to the one step which results in the same overall behavior but with a loss of efficiency for sections of the cell.

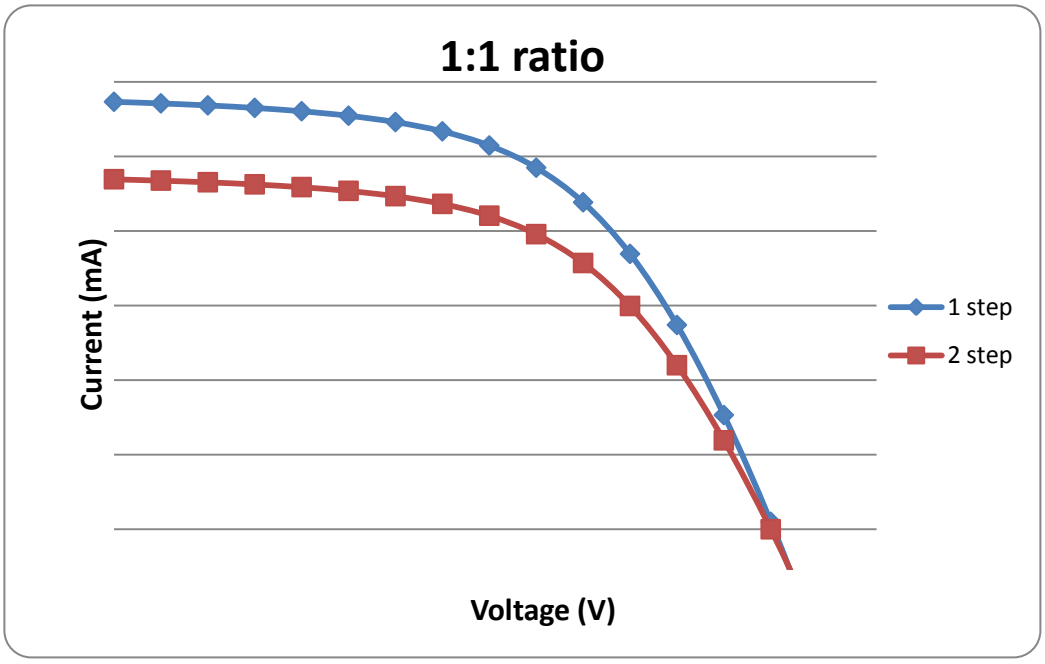

Figure 3.5: a)Spin coating effect on IV curve for various mixing ratios.

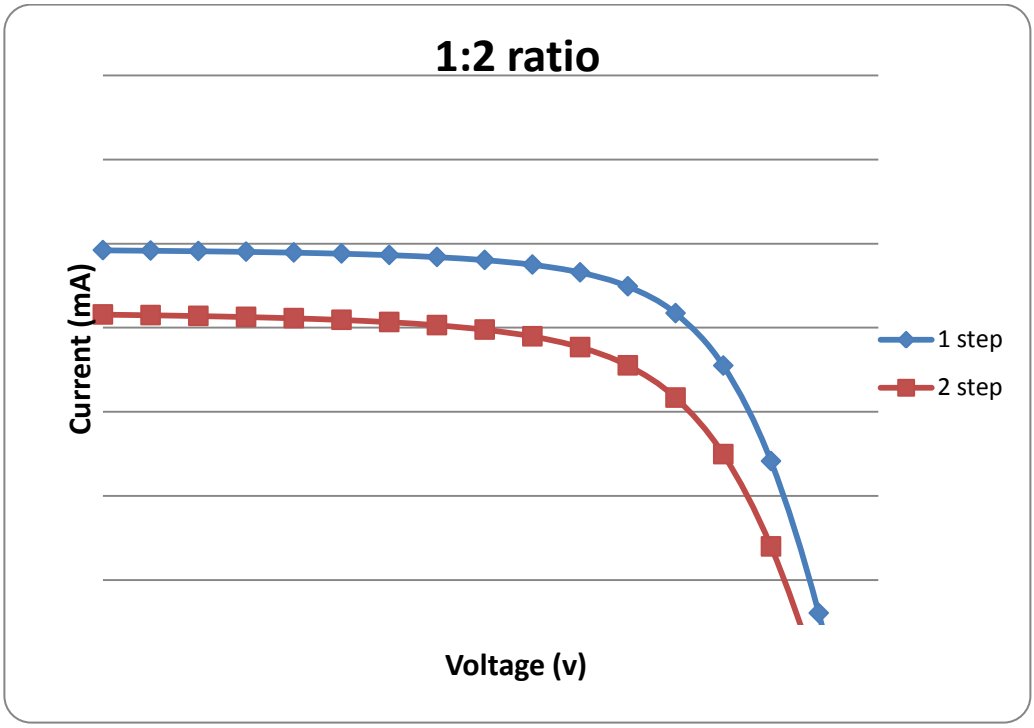

Figure 3.5: b)Spin coating effect on IV curve for various mixing ratios.

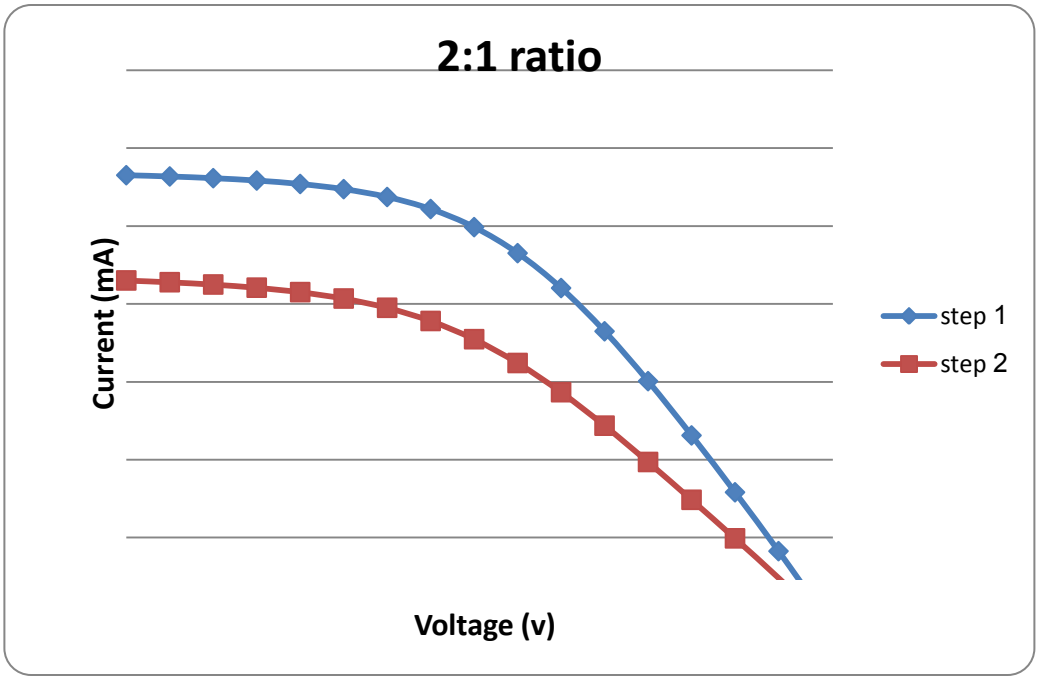

Figure 3.5: c)Spin coating effect on IV curve for various mixing ratios.

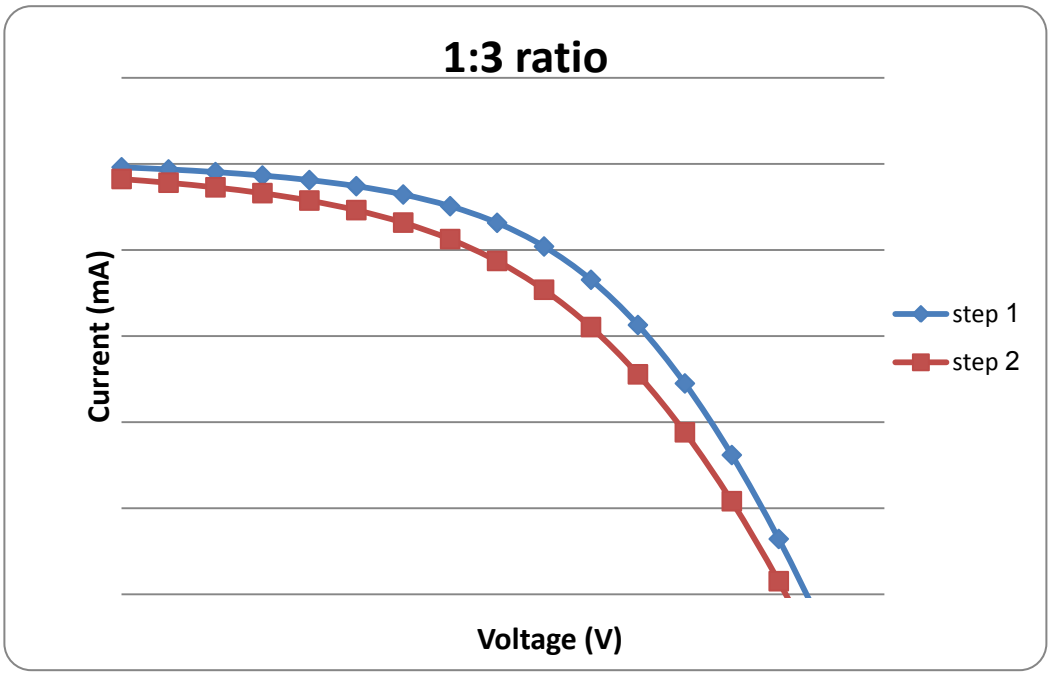

Figure 3.5: d)Spin coating effect on IV curve for various mixing ratios.

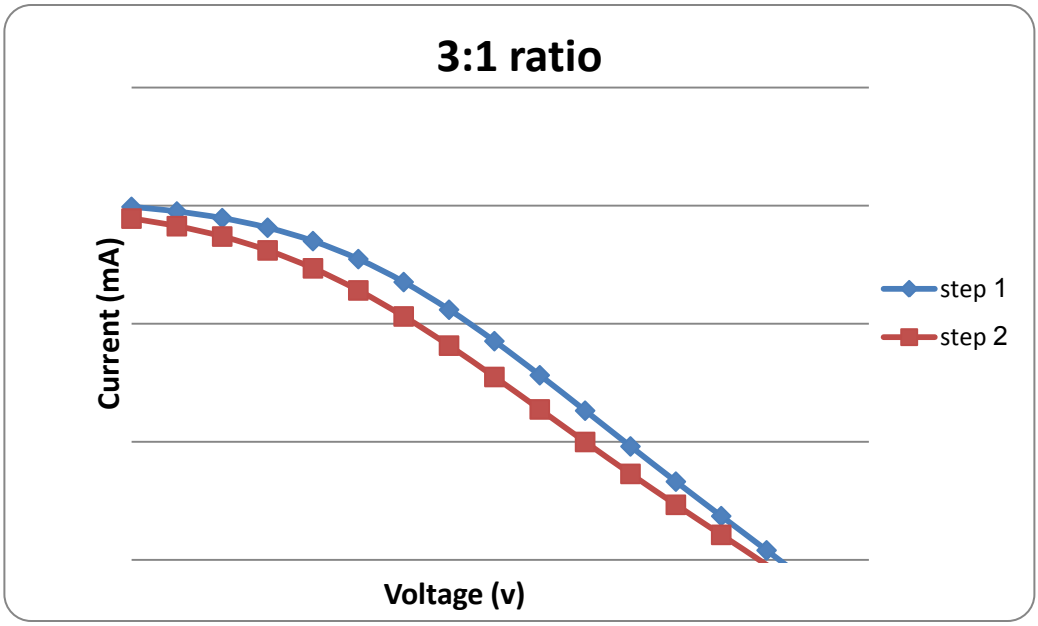

Figure 3.5: e)Spin coating effect on IV curve for various mixing ratios

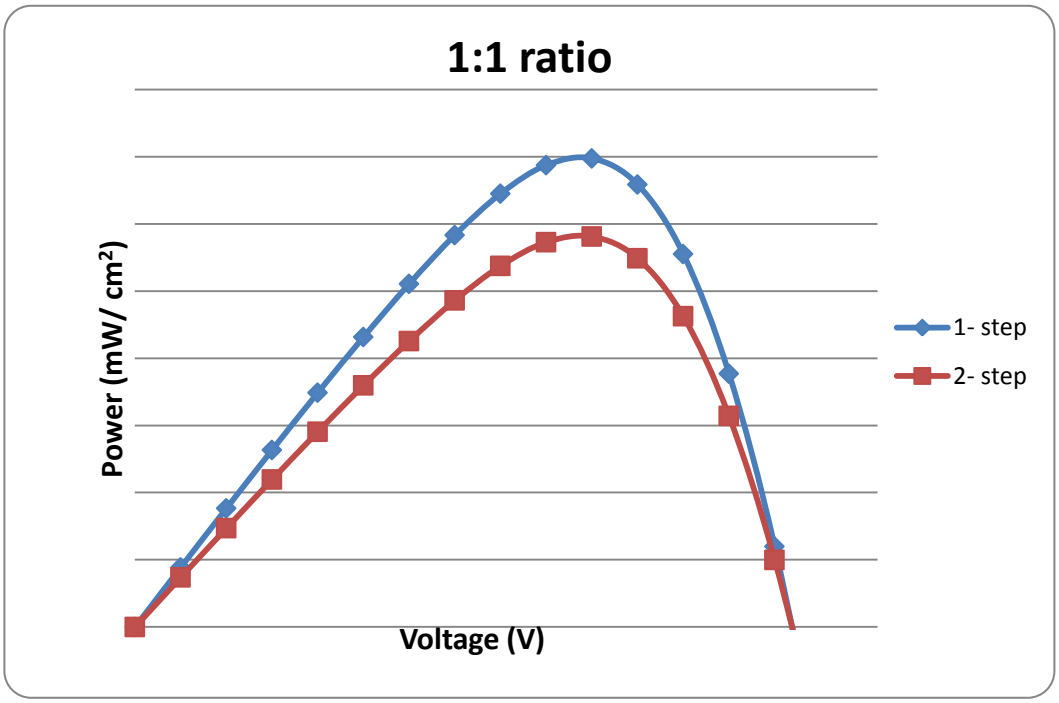

Figure 3.6: a)Spin coating effect on Power- Voltage curve for various mixing ratios

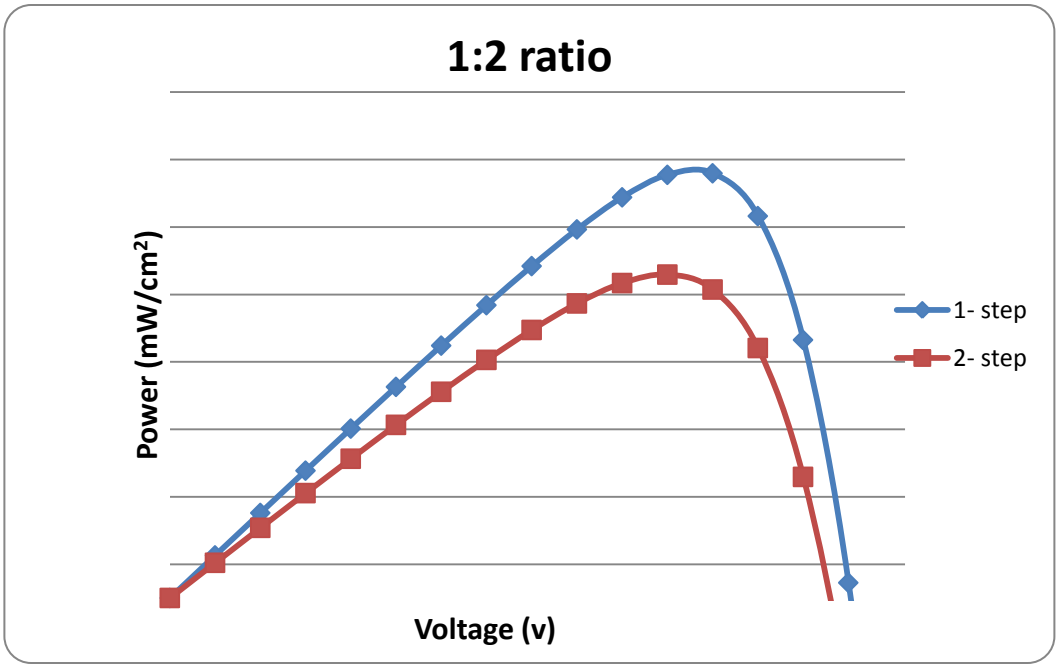

Figure 3.6: b)Spin coating effect on Power- Voltage curve for various mixing ratios

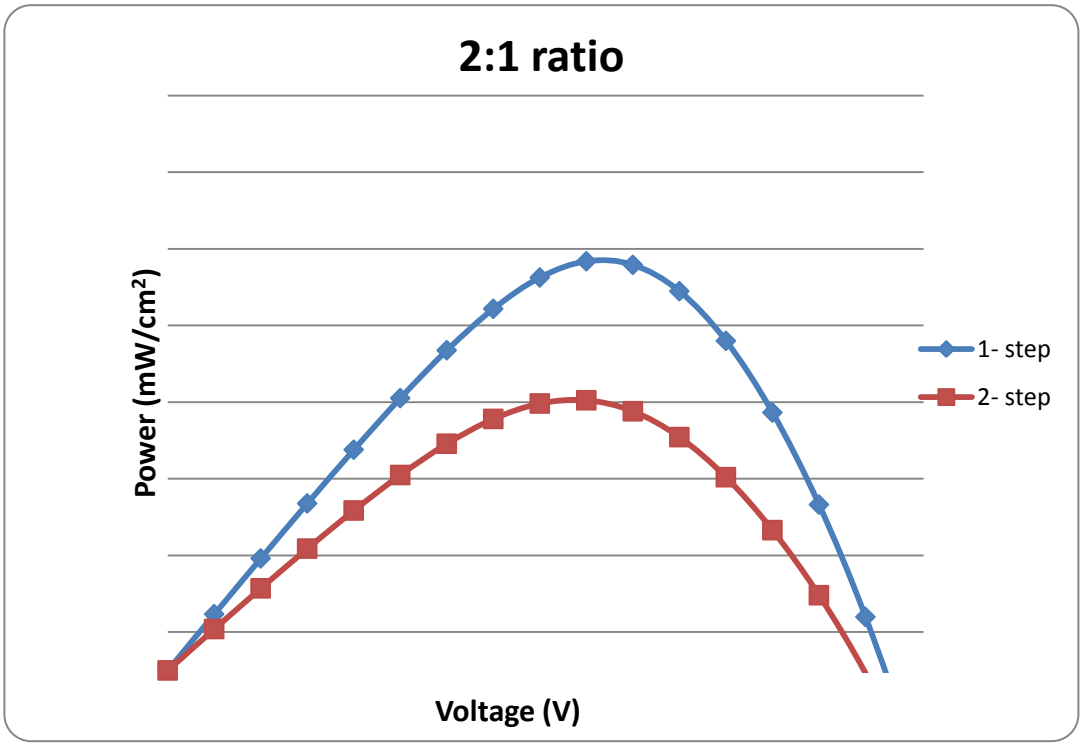

Figure 3.6: c)Spin coating effect on Power- Voltage curve for various mixing ratios

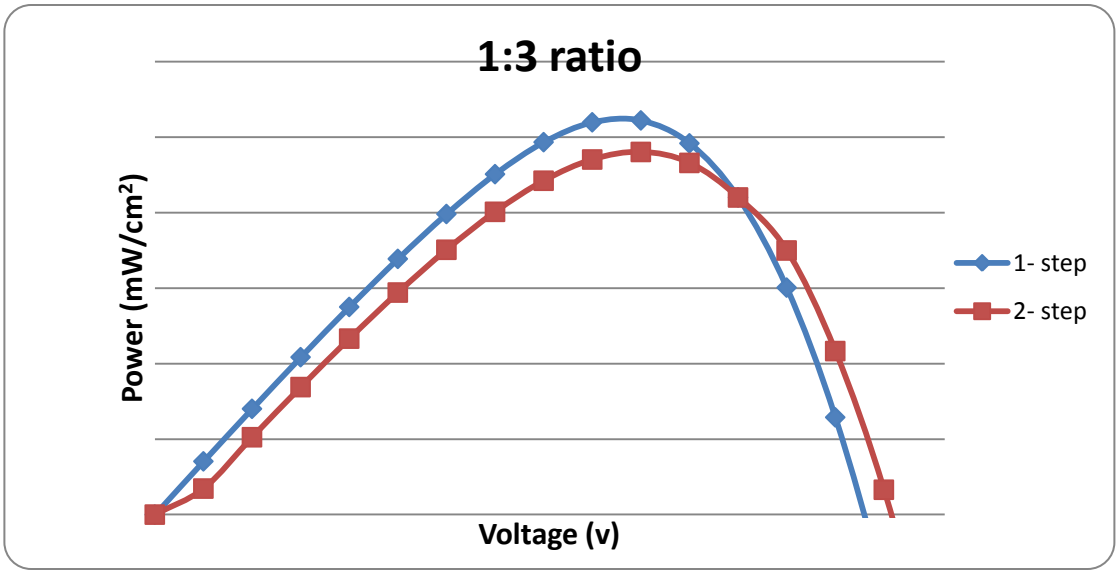

Figure 3.6d: Spin coating effect on Power- Voltage curve for various mixing ratios

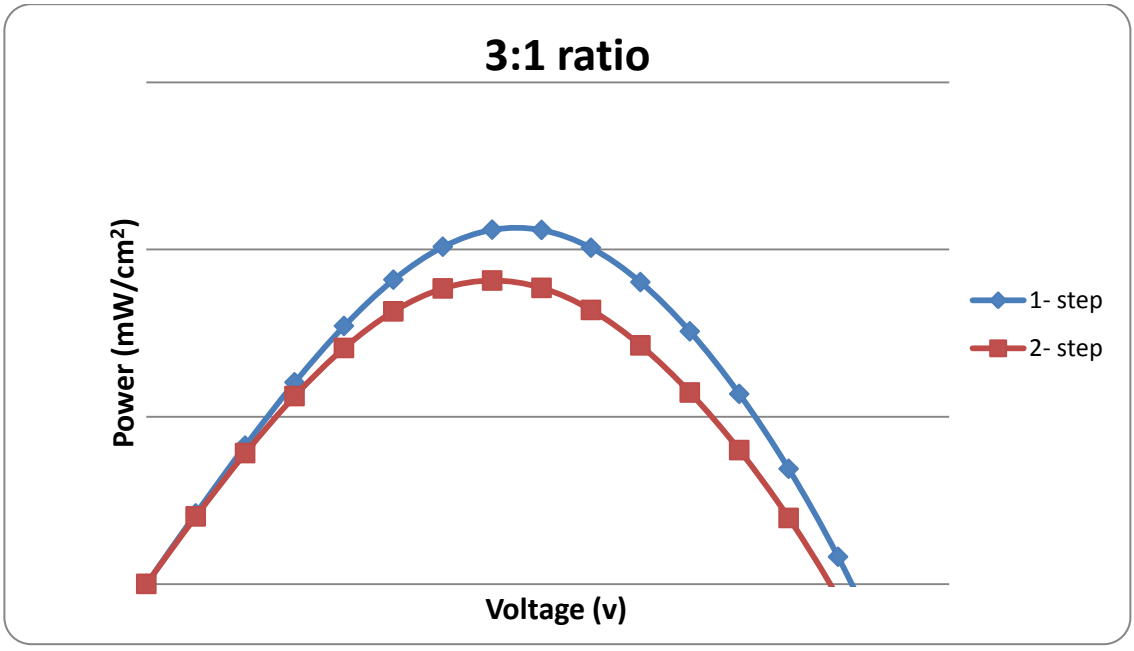

Figure 3.6: e)Spin coating effect on Power- Voltage curve for various mixing ratios.

Chapter Four

Conclusions and Recommendations

4.1 Summary of Conclusions

In this experiment we have built the cells and tested them. Different parameters effects on the efficiency we investigated.The conclusions are summarized in the following:

1. **The active layer ratio between the acceptor and the donor:** The best ratio was around 1:1 with 4.65% conversion efficiency. But from the overall point of view it seems there is a tendency to be less than 1:1 for the 1 step coating and the other way around for the 2-step coating. That could be a result of measurements errors or a result of the process of coating that could have affected the actual ratio due to the difference in viscosity.
2. **The blend depositing conditions**: The spin coating time and the annealing time. There is a general tendency to have better efficiency using the one step coating with an impact of around 20%. It is not clear what is the source for that variation but it seems the two steps coating has affected the actual blend ratio as pointed above.
3. **Annealing:** The AFM images show the impact but there was no IV testing of any cell without annealing.
4. **The active layer thickness:**The best value is around 100nm which is expected because it is comparable to the range of the polymersshort excitation diffusion length.
5. **Input power effect on the efficiency**: For an ideal fixed band structure in the photovoltaic material the output current is proportional to the incident radiation intensityand the voltage should not depend on the intensity, but it could do if the band structure changes as a result of the variation in the number of exitons created due to the radiation. This is besides the effect of temperature. In other words the efficiency should not suffer if the band structure is not dependent on the intensity of the incident light. From our measurement there it seems the effect of intensity on the band structure is not significant because we achieved efficiencies comparable to near optimum conditions. Still we cannot exclude the effect. Our measured efficiency was only 90% of the maximum achieved values. Certainly it will make better conclusionsif compare for different incident intensities.

6. **The temperature effect on the V_{sc} and I_{sc}**: according to **(Al Naser Q. et al, 2012)**: V_{oc} = (KT/q) ln(I_{ph}/I_s) -1 and I_{sc}= $I_s$exp (q.V_{oc}/KT-1) -I_{ph}Where I_{ph} photocurrent, I_s: saturation current, K: Boltzmann constant, T: temperature, and q: charge. For our case the impact was minimized because saturation current was very small and counting the temperature factor still the variation will not count over few percent of the photocurrent compared to the measured current.

4.2 Recommendations for Future Work.

Our research is concerned with synthesizing copolymers with promising properties like high absorption coefficient, solubility, small band gap; high mobility and percolating morphology.

Many solutions are suggested: one is by doping the n-type and p-type to bridge thebandwidth and change the alignment of the polymers, to increase the absorption coefficient.

Another solution is suggested by adding metallic nano-particles (gold) that could improve efficiency by blocking the excitons recombination because of its plasmon effect.**(KACST, 2013)**The proposed doping is shown in **figure 4.1**

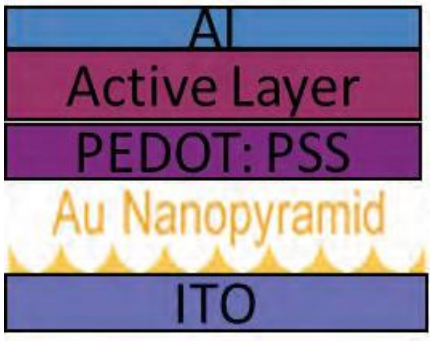

Figure 4.1: Gold Nanoparticle doped OPV (KACST, 2013).

Surface Plasmon Resonance (SPR) is the collective oscillation of electrons in a solid or liquid stimulated by incident light. The resonance condition is established when the frequency of light photons matches the natural frequency of surface electrons oscillating against the restoring force of positive nuclei. SPR in nanometer-sized structures is called localized surface plasmon resonance.

SPR is the basis of many standard tools for measuring adsorption of materials onto planar metal(typically gold and silver) surfaces or onto the surface of metal Nanoparticles. It is the principle behind many color-based biosensor applications and different lab-on-a-chip sensors.**Figure 4.2**shows the plasmonic effects.

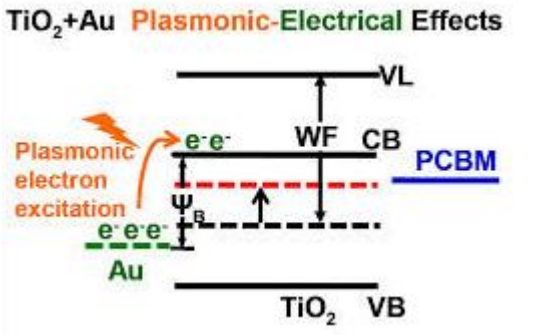

Figure 4.2: Gold Plasmonic- Electrical Effect on PCBM (Choy W. C. H., 2013)

The effect of inserting low density gold nanorods in the metallic back electrode of the polymer on performance was studied. Gold nanorods were introduced by spin-coating their aqueous solution directly on top of the p3HT: PCBM layer [Poly 3-HexylThiophene-2, 5-diyl): [6, 6]-Phenyl-C_{61}-Butyric-acid-Methyl-ester]. The resulting device showed a 5% increase in the short circuit current that leads to a 14% enhancement in the power conversion efficiency.

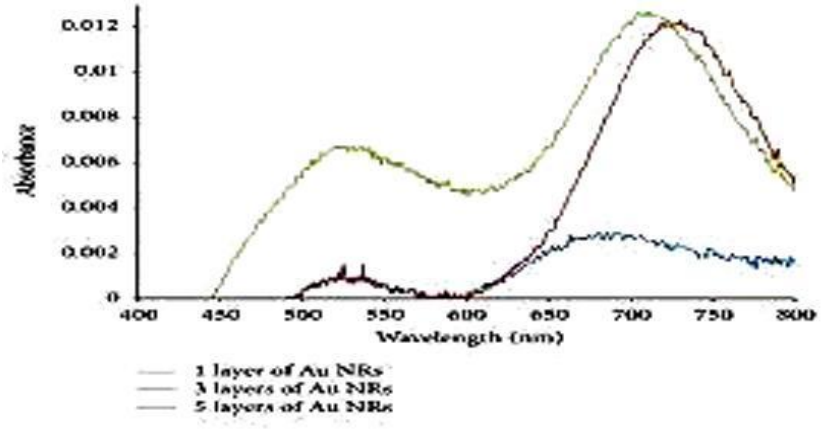

Figure 4.3: UV-Vis Spectra for 1, 3, and 5 layers of Au NRs spin-coated on top of ITO-coated glass. (Mahmoud A. Y., 2014).

Investigation on the photocurrent spectral response of devices with/without gold nanorods revealed that incorporating the rods helped enhance the devices photo generated current near the plasmonic absorption modes of the rods.

The enhancement in the devices efficiency is related to the increase in absorption due to the far-field and near-field effect of localized surface plasmon resonance induced by the presence of the rods in the interface between the photoactive layer and the metallic back electrode, as shown in **figure 4.3(Mahmoud A. Y., et al, 2014).**

Another method for adding metallic Nanoparticles with varying sizes is by spraying under an electric field (DC 0 V and 1 kV applied to the nozzle). The application of the electric field during the spraying results in a smaller particle size (35 nm vs. 70 nm) with more uniform distribution. **(Chaturvedi N., et al, 2014)**

The photovoltaic performances of plasmonic inverted organic solar cells (ITO/Au/ZnO/P3HT: PCBM/Ag) using spray-deposited Au and ZnO layers (both at 1 kV) showed improved efficiency. Fast exciton quenching in the P3HT: PCBM layer was achieved by using a spray-deposited Au layer in between ITO and ZnO layers. The absorption spectra and internal power conversion efficiency (IPCE) curve showed that the Au Nanoparticles provide significant plasmonic broadband light absorption enhancement. **(Chaturvedi N., et al, 2014)**

Other techniques are used for the metallic NPs such as E- beam which increase the CPE as a function of the silver Ag NPs thickness, at the thickness of 50Å increase the efficiency about 60% compared to the cells that are not containing Ag NPs, **(Kim H., Jeon T., 2012)**. The layer-bylayer technique increased the cell efficiency from 3.04% to 3.65%, **(Lee J. H, et al, 2009)**.

Bibliography

(Abd-El-Aziz A. et al, 2010) Macromolecules Containing Metal and Metal-like Elements, Photo physics and Photochemistry of Metal-containing Polymers, volume 10, 1st edition, John Wiley & sons Ltd, New Jersey, and USA.

(Adikaari A. A. T. et al, 2009) Hybrid Organic – Inorganic Solar Cells: Recent Developments & Outlook.

(Al-Hallaj S., Kiszynski K., 2011) Hybrid Hydrogen Systems: Stationary and Transportation Applications, Springer, England.

(Al-Ibrahim M., Ambacher O., 2005) Effect of solvent and annealing on the improved performance of solar cells based on poly(3-hexylthiophene):Fullerene, Appl. Phys. Lett. 86.

(Al-Naser Q. A. H. et al, 2012) The effect of temperature variations on solar cell efficiency, International Journal of Engineering, Business and Enterprise Application (IJEBEA), pp 108-109.

(Augustin T. J. et al,) Practical Handbook of photovoltaics: Fundamentals and Application,

(Benanti T., Venkataraman D., 2006) Organic solar cells: An Overview Focusing on active Layer Morphology, Springer, 87, PP. 73-81

(Bottari G., T. Torres, 2013) Organic Nanomaterials: Synthesis, characterization and Devise Application, Wiley.

(Brabec C. J., 2003) Organic Photovoltaics: Concepts and realization, Springer, Germany.

(Brutting W., Adachi C., 2012) Physics of Organic Semiconductors, 2nd edition, John Wiley & Sons Ltd., Germany.

(Burkhard G. F., 2011) Exciton Recombination in the Fullerene Phase of Bulk Heterojunction Organic Solar Cells, Stanford University, USA.

(Cantatore E., 2012) Applications of Organic And Printed Electronics: A Technology- Enabled Revolution, Springer, UK.

(Carson J., 2008) Solar Cell Research Progress, Nova Publishers, NY, USA.

(Castellano R., 2010) Solar Panel Processing, Old City Publishing, USA.

(Chandra B. P., Nath R., 1989) Electrical and Optical Behavior of solids, 1st edition, p.49

(Chaturvedi N, et al, 2014) Plasmonic effect of spray-deposited Au nanoparticles on the performance of inverted organic solar cells, Royal Society of Chemistry.

(Cho C., 2010) Smart Clothing: Technology & Applications, CRC Press, Taylor & Francis Group, UK.

(Choy W. C., 2012) Organic Solar Cells: Materials and Device Physics, Springer, New York, USA.

(Choy W. C. H., 2013) Using plasmonic-electrical effects for high-performance organic solar cells, The International Society for Optics and Photonics (SPIE)

(Choy W. C., Fung D. D. S., 2013) Organic Solar Cells: Materials and Device Physics, Green Energy and Technology, Springer, London, UK, p.6.

(Dusastre V., 2011) Materials for Sustainable Energy: A collection of Peer-Reviewed Research and Review Articles from Nature, World Scientific publishing group & Macmillan Publisher Ltd., UK.

(Dusek K. et al, 2010) Polymer Characterization: Rheology, Laser Interferometry, Electro optics, Springer, Germany.Effects of active layer thickness and thermal annealing on P3HT-PCBM photovoltaic cells,

(Eftekhari A., 2011) Nanostructured Conductive Polymers, John Wiley & Sons Ltd., UK.

(Facchtti A., 2013) Polymer donor- Polymer acceptor (all polymer) Solar Cells, Elsevier, Vol. 16, pp. 123-127.

(Fonash S., 2012) Solar Cell Device Physics, Academic Press, Elsevier, UK.

(Goetzberger A., Uoffmann V., 2005) Photovoltaic Solar Energy Generation, Springer, Germany.

(Gregg B. A. Hanna M. C., 2003) Comparing organic to inorganic photovoltaic cells: Theory, Experiment and Simulation, Journal of Applied Physics, Vol. 93, No. 6, pp. 3605-3613**.**

(Grimes C., Mor G. K., 2009) TiO_2 Nanotube Arrays: Synthesis, Deposition and Applications, Springer, NY, USA.

(Guo J., et al, 2010) Charge generation and Recombination Dynamics in Poly (3-hexylthiophene)/ Fullerene Blend Films with Different Regioregularities and Morphologies, JACS Articles**.**

(Hamakawa Y., 2004) Thin-Film Solar Cells: Next generation Photovoltaics and its Applications, Springer, Germany

(Hopp H., Sarcifitci N. S., 2006) Morphology of Polymer/ Fullerene Bulk Heterojunction Solar Cells, Journal of Materials Chemistry, No. 16, pp. 45-61**.**

(Hopp H., Sarciftci N. S., 2007) Polymer Solar Cells, Springer, Berlin, Germany**.**

(Hoppe H., Sariciftci N. S., 2004) Organic solar cells: an overview, vol. 19. No. 7, pp.1924-1940.

(Hüttner S., 2010) Donor-Acceptor Block Copolymersin Organic Electronics Spectroscopy, Charge Transport, Morphology andDevice Application, Germany.

(Hu W. et al, 2012) Organic Optoelectronics, John Wiley & sons Ltd., Germany.

(Hu Zhongjian, Gesquiere A. J., 2009) PCBM concentration dependent morphology of P3HT in composite P3HT/PCBM nanoparticles, Chemical Physics Letters, Elsevier, lett. 476, pp. 51-55.

(Iwan A. et al, 2013) Opto-electrical properties of triphenylamine – based polyazomethine and its blend with [6,6]- phenyl C_{61} butyric acid methyl ester, High Performance Polymers, 25, P. 832-842.

(Jha A. R., 2009) Solar Cell Technology & Applications, CRC Press, Taylor & Francis Group, UK.

(Joltarand S. A., Jobin M.,2012) Characterization of O3HT:PCBM:CdSe hybrid solar cells, Elsevier, No.137, pp 117-123. **November 2012.**

(KACST, 2013)King Abd Al-Aziz City for Science & Technology Annual report,, Saudi Arabia.

(Kasap S., Copper p., 2006) Springer handbook of electronics and photonic materials, Springer, USA.

(Kawazoe H. et al, 1997) P-type electrical conduction in transparent thin films of $CuAlO_2$.Nature 389, 939-942 .

(Kim Ch. H., Jeon T., 2012) Bulk heterojunction solar cells, Japanese Journal of Applied physics.

(Kim Ch. H. et al, 2005) Effect of thermal annealing on the performance of P3HT/PCBM polymer photovoltaic cells, Journal of the Korean Physics Society, Vol, 48, No. 3, pp. 441-445.

(Kingshim C. F., 1997) Semiconductor Optics, Springer, USA.

(Kingsley J. W. et al, 2009) Fabrication and Optimization of P3HT: PCBM Organic Photovoltaic Devices, Organic Photovoltaics X., Vol. 7416

(Kital A., 2011) Principles of Solar Cells, LEDs and Diodes. The Role of PN Junction, 1st edition, John Wiley &sons Ltd, UK

(Kosyachenko L. A., 2011) Hybrid solar cells-new aspects and solutions, 1st edition, InTech, Croatia.

(Kosyachenko L. A., 2011) Solar Cells- New Aspects and Solutions, INTECH, Croatia.

(Krebs F. C., 2010) Polymeric Solar Cells: Materials, Design, Manufacture, DEStech Pub.Inc, USA.

(Krebs F. C., 2012) Stability and Degradation of Organic and Polymer Cells, Wiley & Sons., UK.

(Krichartz T., 2009) Generalized Detailed Balance Theory of Solar Cells, FZJülich, Germany.

(Kymissis L., 2008) Organic Field Effect Transistors: Theory, Fabrication and Characterization, Springer, NY, USA.

(Langa F., Nierengarten J., 2007) Fullerenes: Principles and Applications, Royal Society of Chemistry, UK.

(Lee C.T., 2010) III-V compound based solar cells, college of electrical engineering and computer science, National Cheng Kung University

(Lee J. H., et al, 2009) High efficiency polymer solar cells with wet deposited plasmonic gold nanodots, Organic Electronics, Elsevier, pp. 416-420.

(Li J., 2008) Design, Deposition, Characterization and Modification of Transparent Conducting Anode Materials for Organic Light-emitting Diodes, ProQuest Information and Learning Company, USA.

(Luque A., Hegedus S., 2011) Handbook of photovoltaic Science and Engineering, 2nd edition, Hohn Wiley & sons Ltd, UK

(Mahmoud A Y., et al, 2014) Gold Nanorods Incorporated Cathode for Better Performance of Polymer Solar Cells, Ricardo Izquierdo, and Vo-Van Truong, Journal of Nanomaterials, Article ID 464160, 29 January.

(Marcus T. Ch., 2012) P3HT: PCBM Bilayer Planar Heterojunction Organic Photovoltaic Thin –film solar Cell Efficiency Optimization, University of Teknologi Malaysia, Malaysia.

(McEvoy A. et al, 2013) Solar Cells: Materials, Manufacture and Operation, 2nd edition, Elsevier, USA.

(McEvoy A., et al, 2012) Practical Handbook of Photovoltaics: Fundamentals and Applications, 2nd edition, Academic Press, Elsevier, USA.

(McGehee M. D., et al, 2005) Nano-StructuredPhotovoltaic Cells, GCEP Technical Report.

(McGehee M. D. et al, 2006) Ordered bulk heterojunctionphotovoltaic cells, GCEP Tech Report.

(Nam Ch. Y., 2011) Photovoltaic Materials and Devices: Organic Bulk Heterojunction Solar Cells, NSLS-II Beamline Development Proposals workshop, Soft X-ray Spectro-microscopy, Centre for functional Nanomaterials, Brookhaven National Laboratory.

(Nath R., 1989) Electrical and Optical Behavior of solids, 1st edition, Mittal Publications, India.

(Nayak P. K. et al, 2011) Assessing Possibilities and Limits for Solar Cells, Advanced Materials, Wiley- VCH Verlag GmbH, No. 23, pp. 2870-2876.

(Nayak P. K. et al, 2012) Photovoltaic efficiency limits and material disorder, Energy and Environmental Science, The Royal Society of Chemistry.

(Neville R. C., 1995) Solar Energy Conversion: The Solar Cell, 2nd edition, Elsevier, Netherlands.

(Ngo Trinh T. et al, 2012) Glass transition of PCBM, P3HT and their blends in quenched state, IOP science.

(Özgür, Ü. et al, 2005) A Review of ZnO materials and devices, Journal of Applied Physics 98.

Pani R. C., et al, 2013) Correlating Fullerene diffusion with the Polythiphene morphology: molecular dynamics simulation, Soft Matter, Issue 42, p. 10048.

(Poortmans J., Arkhipov V., 2006) Thin Film Solar Cells: Fabrication, Characterization and Applications, John Wiley & sons Ltd, UK.

(Reddy P. J., 2012) Solar Power Generation: Technology, New Concepts and Policy, 2nd edition, CRC Press and Taylor &Francis Group, UK.

(Reyes- Reyes M., et al, 2005) High efficiency photovoltaic devices based on annealed poly(3-hexylthiophene) and 1-(3-methoxycarbonyl)-propyl-1-phenel-(6,6)C_{61} blends, appl. phys. lett. 87.

(Salleo et al, 2008) Organic and hybrid materials for large area functional systems, Materials Research Society, San Francisco.

(Sariciftci N. S., Scharber M. C., 2013) Efficiency of bulk heterojunction organic solar cells, Progress in Polymer Science, El-Sevier, issue 38, pp. 1929-140.

(Sariciftci N., Sun S., 2005) Organic Photovoltaics: Mechanisms, Materials and Devices, CRC Press, UK.

(Sariciftci N. S. et al, 2007) Conjugated Polymer – Based Organic Solar Cells, American Chemical Society, Vol. 107, No. 4, p.1336

(Sattler K. D., 2010) Handbook of Nanophysics: Clusters and Fullerenes, CRC Press and Taylor & Francis Group, UK.

(Satyen K. D., 2004) Thin film solar cells: Next generation photovoltaics and it application, Springer p.39, UK.

(Savenije, T. J., 2012) Organic Solar Cells, solar cells, ch. 8, Faculty of Applied Sciences Delft University of Technology, Netherlands.

(**Srivani A., et al, 2013**)Investigation of Physical Properties in II-VI Ternary Semiconductors of Sulphides, Selenides&Tellurides, International Journal of Engineering & Science, p.26.

(Skotheim T. A., Reynolds J., 2006) Conjugated Polymers: Theory, Synthesis, Properties and Characterization, 3rd edition, CRC Press and Taylor & Francis Group, UK.

(So F., 2010) Organic Electronics: Materials, Processing, Device and Applications, CRC Press and Taylor & Francis Group, UK.

(Solanki C. S., 2011) Solar Photovoltaics Fundamental, Technologies and Applications, 2nd edition, PHI Learning Pvt. Ltd, New Delhi.

(Solanki C. S., 2013) Solar photovoltaic technology and systems. A manual for Technician, Trainers and Engineers, PHI learning Pvt. Ltd., New Delhi, p. 51.

(Solar Cells- Advances in Research and Application, 2013) Scholarly edition, Georgia, USA.

(Swarup A., Khare P. S., 2009) Engineering Physics: Fundamentals & Modern applications, Jones & Bartlett Learning, London, UK

(Thapa R. B., 2008) Hybrid Polymer: Inorganic- nanoparticle Composites Devices for Photo detection and Photovoltaics, ProQuest Information & Learning Company, USA.

(Thompson B. C., Frechert M. J., 2008) Polymer- Fullerene Composite Solar Cells, AngewandteChemie, No. 47, pp. 58-77.

(Thurm M., 2010) Organic Solar Cells: Advantages, Possibilities and limits of Bulk Heterojunction Solar Cells, Sustainability Marketing and Innovation, Germany.
(Torres T., Bottari G., 2013) Organic Nano-materials: Synthesis, Characterization and Device Applications, John Wiley & sons Ltd., USA.

(Verploegen E. et al, 2010) Effects of thermal annealing upon the Morphology of Polymer Fullerene-Blends, Advanced Functional Materials.

(WeihaoGe., 2009) An Overview on P3HT: PCBM, the most efficient organic cell material so far.

(Wohrle D.,Meissner D., 1991) Organic Solar Cells: Advanced Materials, No. 3, pp. 129-138.

(Wurfel U.,Glunz S., 2013) Organic Solar cells, Franhofer Institute for Solar Energy System ISE. **April 2013.**

(Wurfel U. et al, 2011) Quantum Efficiency in Complex Systems: From Molecular Aggregates to Organic Solar Cells, Part 2, volume 85, 1st edition, Academic Press, Elsevier, USA.

(Yan H. et al, 2012) Bridging mesoscopic blend structure and property to macroscopic device performance via in situ optoelectronic characterization, Journal of Materials Chemistry, 22, pp. 4349-4355.

(Yang X., 2012) Semi conducting Polymer Composites: Principles, Morphologies, Properties and Applications, John Wiley & sons Ltd., Germany.

(Zang L., 2011) Energy Efficiency and Renewable Energy through Nanotechnology, Springer, New York,USA.

Appendixes

Appendix A: Chronology of Solar Cells Development

"New World Record Achieved in Solar Cell Technology" (Press release). United States Department of Energy. December 5, 2006. Retrieved 2008-01-16

1. 1930s – Walter Schottky, Neville Mott and some others developed a theory of metal-semiconductor barrier layers.

2. 1950s – Bell Labs produce solar cells for space activities.

3. 1954 – Three researchers, Gerald Pearson, Daryl Chapin and Calvin Fuller, at Bell Laboratories discovered a silicon solar cell, which was the first material to directly convert enough sunlight into electricity to run electrical devices. The efficiency of the silicon cell, which Bell Labs produced, was 4% and later increased to 11%. The cells were made by hand and cost $1000 per watt.

4. 1954 – A cadmium sulphide p-n junction was produced with an efficiency of 6%

5. 1958 – The first PV-powered satellite, Vanguard I, was launched. The solar panel had an area of 100cm² and delivered an effect of approximately 0.1W. The satellite power system operated for 8 years, and is the world's oldest satellite still in orbit (2007).

6. 1958 – Ted Mandelkorn of U.S. Signal Corps Laboratories fabricates n-on-p (negative layer on positive layer) silicon photovoltaic cells,

7. 1960 – Hoffman Electronics achieved 14% efficient PV cells.

8. 1962 – The Telstar communications satellite, launched by Bell Labs, is initial powered (14W) by solar cells.

9. 1963 – A Japanese electronics manufacturer, Sharp Corporation, produces a viable photovoltaic module of silicon solar cells.

10. 1970 – First highly effective GaAsheterostructure solar cells are created by ZhoresAlferov (a Russian physicist) and his team in the USSR.

11. 1972 – The Institute of Energy Conversion is established at the University of Delaware to perform research and development on thin-film photovoltaic and solar thermal systems, becoming the world's first laboratory dedicated to photovoltaic research and development.

12. 1976 – David Carlson and Christopher Wronski of RCA Laboratories produced the first amorphous silicon photovoltaic cells, which could be less expensive to manufacture than crystalline silicon devices. The efficiency was of 1.1%.

13. 1980 – At the University of Delaware, the first thin-film solar cell exceeds 10% efficiency. It's made of copper sulfide (Cu_2S) and cadmium sulfide(CdS).

14. 1982 – Hans Tholstrup, an Australian, drives the first solar-powered car, the Quiet Achiever, 4,000km between Sydney and Perth in 20 days. That was 10 days faster than the first gasoline-powered car to do so. The maximum speed was 72 km/h, and the average speed was 24 km/h.

15. 1985 – The University of South Wales breaks the 20% efficiency barrier for silicon solar cells under one sun conditions.

16. 1991 – Efficient Photo electrochemical cells (PEC) are developed. Each cell consists of a semi conducting photo anode and a metal cathode immersed in an electrolyte. The Dye-sensitized solar cell (DSSC), also called Grätzel cells, is invented. It was a new class of low-class DSC.

17. 1992 – University of South Florida develops a 15.9% efficient thin-film photovoltaic cell made of cadmium telluride, breaking the 15% barrier for the first time for this technology.

18. 1994 – The National Renewable Energy Laboratory develops a solar cell, made from gallium indium phosphide and gallium arsenide that becomes the first one to exceed 30% conversion efficiency.

19. 1996 – Renewable Energy Corporation (REC), a Norwegian solar energy company established.

20. 1996 – EPFL, the Swiss Federal Institute of Technology in Lausanne, achieves 11% efficiency with the DSCs.

21. 1999 – Spectrolab, Inc. and the National Renewable Energy Laboratory develop a photovoltaic solar cell that converts 32.3 percent of the sunlight that hits it into electricity. The high conversion efficiency was achieved by combining three layers of photovoltaic materials into a single solar cell. The cell performed most efficiently when it received sunlight concentrated to 50 times normal. To use such cells in practical applications, the cell is mounted in a device that uses lenses or mirrors to concentrate sunlight onto the cell. Such "concentrator" systems are mounted on tracking systems that keep them pointed toward the sun.

22. 1999 – The National Renewable Energy Laboratory achieves a new efficiency record for thin-film photovoltaic solar cells. The new measurement is of 18.8 % efficiency.

23. 2001 – TerraSun LLC develops a method of using holographic films to concentrate sunlight onto a solar cell.

24. 2006 - New World Record Achieved in Solar Cell Technology - New Solar Cell Breaks the "40 Percent Efficient" Sunlight-to-Electricity Barrier.

25. 2008 - New record achieved in solar cell efficiency. Scientists at the U.S. Department of Energy's National Renewable Energy Laboratory (NREL) have set a world record in solar cell efficiency with a photovoltaic device that converts 40.8 percent of the light that hits it into electricity. However, it was only under the concentrated energy of 326 suns that this was achieved.

26. The inverted metamorphic triple-junction solar cell was designed, fabricated and independently measured at NREL.

Appendix B1: 1:1- 1 step (50 nm) B1, C11-1-50

Voltage (v)	Light (mA)	Dark (mA)	P= J*V (mW/cm^2)
-1	-0.0481	-1.21E-11	0.171799643
-0.96	-0.0481	-1.21E-11	0.164912914
-0.92	-0.0481	-1.21E-11	0.158026429
-0.88	-0.04809	-1.21E-11	0.15114
-0.84	-0.04808	-1.21E-11	0.1442541
-0.8	-0.04808	-1.21E-11	0.137368286
-0.76	-0.04807	-1.21E-11	0.130482771
-0.72	-0.04807	-1.21E-11	0.123597771
-0.68	-0.04806	-1.21E-11	0.1167135
-0.64	-0.04805	-1.21E-11	0.109829486
-0.6	-0.04804	-1.21E-11	0.1029465
-0.56	-0.04803	-1.21E-11	0.096064
-0.52	-0.04802	-1.21E-11	0.089182786
-0.48	-0.04801	-1.21E-11	0.082302514
-0.44	-0.048	-1.21E-11	0.0754237
-0.4	-0.04798	-1.21E-11	0.068546571
-0.36	-0.04797	-1.21E-11	0.061671343
-0.32	-0.04795	-1.21E-11	0.054798514
-0.28	-0.04793	-1.21E-11	0.0479286
-0.24	-0.04791	-1.21E-11	0.041062114
-0.2	-0.04788	-1.21E-11	0.034199929
-0.16	-0.04785	-1.21E-11	0.027342914
-0.12	-0.04782	-1.20E-11	0.020492486
-0.08	-0.04778	-1.15E-11	0.013650286
-0.04	-0.04773	-9.30E-12	0.006818457
0	-0.04767	9.78E-13	0
0.04	-0.04761	4.86E-11	-0.00680103
0.08	-0.04753	2.71E-10	-0.01357897
0.12	-0.04743	1.31E-09	-0.02032564
0.16	-0.0473	6.15E-09	-0.02702891
0.2	-0.04714	2.88E-08	-0.03367014
0.24	-0.04692	1.34E-07	-0.04021869
0.28	-0.04662	6.26E-07	-0.0466221
0.32	-0.04619	2.92E-06	-0.05278343
0.36	-0.04551	1.36E-05	-0.05851414
0.4	-0.0444	6.30E-05	-0.06343086
0.44	-0.04248	2.90E-04	-0.06675759
0.48	-0.03911	1.31E-03	-0.06703834
0.52	-0.03339	5.62E-03	-0.06200591

0.56	-0.02454	2.14E-02	-0.0490868
0.6	-0.0123	6.54E-02	-0.0263625
0.64	0.003127	1.54E-01	0.007146743
0.68	0.021484	2.92E-01	0.052175671
0.72	0.042761	4.75E-01	0.109957886
0.76	0.067193	7.01E-01	0.182380186
0.8	0.095088	9.69E-01	0.271679429
0.84	0.126692	1.28E+00	0.380076
0.88	0.162143	1.63E+00	0.509592286
0.92	0.20148	2.02E+00	0.662005714
0.96	0.244681	2.45E+00	0.838906286
1	0.29169	2.92E+00	1.04175

Appendix B2: 1:1 – 1 step (150 nm) B2, C11-1-150

Voltage (v)	Light (mA)	Dark (mA)	P= J*V (mW/cm^2)
-1	-0.08714	-1.21E-10	0.3112275
-0.96	-0.08713	-1.21E-10	0.298724229
-0.92	-0.08711	-1.21E-10	0.286220871
-0.88	-0.08709	-1.21E-10	0.273717714
-0.84	-0.08707	-1.21E-10	0.2612151
-0.8	-0.08705	-1.21E-10	0.248712857
-0.76	-0.08703	-1.21E-10	0.236210986
-0.72	-0.087	-1.21E-10	0.223710171
-0.68	-0.08697	-1.21E-10	0.211210186
-0.64	-0.08694	-1.21E-10	0.198711543
-0.6	-0.0869	-1.21E-10	0.186214286
-0.56	-0.08686	-1.21E-10	0.1737192
-0.52	-0.08681	-1.21E-10	0.161226557
-0.48	-0.08676	-1.21E-10	0.148736914
-0.44	-0.08671	-1.21E-10	0.136251343
-0.4	-0.08664	-1.21E-10	0.123770714
-0.36	-0.08656	-1.21E-10	0.111296571
-0.32	-0.08648	-1.21E-10	0.098830629
-0.28	-0.08638	-1.21E-10	0.0863753
-0.24	-0.08626	-1.21E-10	0.0739338
-0.2	-0.08611	-1.21E-10	0.061510571
-0.16	-0.08595	-1.21E-10	0.049111657
-0.12	-0.08574	-1.20E-10	0.036745629
-0.08	-0.08549	-1.15E-10	0.024424857
-0.04	-0.08517	-9.45E-11	0.012167286
0	-0.08477	3.16E-12	0

0.04	-0.08425	4.57E-10	-0.012035286
0.08	-0.08355	2.58E-09	-0.023872543
0.12	-0.08261	1.25E-08	-0.035404543
0.16	-0.08129	5.91E-08	-0.046454057
0.2	-0.07942	2.77E-07	-0.056728214
0.24	-0.07672	1.29E-06	-0.065760686
0.28	-0.07287	6.04E-06	-0.0728726
0.32	-0.06757	2.82E-05	-0.077222286
0.36	-0.06065	0.000130669	-0.077984229
0.4	-0.0522	0.000597044	-0.074571
0.44	-0.04247	0.00261709	-0.066734957
0.48	-0.03179	0.0103062	-0.054503314
0.52	-0.02047	0.0328077	-0.038010143
0.56	-0.00865	0.0793242	-0.01730096
0.6	0.003659	0.151499	0.007839879
0.64	0.016612	0.246336	0.037969371
0.68	0.030441	0.361151	0.073928871
0.72	0.045383	0.494548	0.116699143
0.76	0.061624	0.645893	0.167265143
0.8	0.079292	0.814832	0.226548571
0.84	0.098464	1.00107	0.2953932
0.88	0.119182	1.20432	0.374572
0.92	0.141463	1.42428	0.464807
0.96	0.165309	1.66064	0.566773714

Appendix B3 Cell 1 1:1 – 1 step cell (100 nm) B3, C11-1-100

Voltage (v)	Light (mA)	Dark (mA)	P =J*V (mW/cm^2)
-1	-1.270728	-2.90E-10	4.538314286
-0.96	-1.270512	-2.90E-10	4.356041143
-0.92	-1.270284	-2.90E-10	4.173790286
-0.88	-1.270032	-2.90E-10	3.991529143
-0.84	-1.269768	-2.90E-10	3.809304
-0.8	-1.269468	-2.90E-10	3.627051429
-0.76	-1.269156	-2.90E-10	3.444852
-0.72	-1.268808	-2.90E-10	3.262649143
-0.68	-1.268424	-2.90E-10	3.080458286
-0.64	-1.268016	-2.90E-10	2.898322286
-0.6	-1.26756	-2.90E-10	2.7162
-0.56	-1.267056	-2.90E-10	2.534112

-0.52	-1.266492	-2.90E-10	2.352056571
-0.48	-1.26588	-2.90E-10	2.17008
-0.44	-1.265196	-2.90E-10	1.988165143
-0.4	-1.264416	-2.90E-10	1.806308571
-0.36	-1.263552	-2.90E-10	1.624566857
-0.32	-1.262568	-2.90E-10	1.442934857
-0.28	-1.261452	-2.90E-10	1.261452
-0.24	-1.26018	-2.90E-10	1.080154286
-0.2	-1.258704	-2.90E-10	0.899074286
-0.16	-1.257	-2.89E-10	0.718285714
-0.12	-1.254984	-2.87E-10	0.537850286
-0.08	-1.252608	-2.76E-10	0.357888
-0.04	-1.249764	-2.26E-10	0.178537714
0	-1.24632	1.14E-11	0
0.04	-1.242072	1.11E-09	-0.177438857
0.08	-1.236756	6.27E-09	-0.353358857
0.12	-1.229964	3.04E-08	-0.527127429
0.16	-1.221036	1.43E-07	-0.697734857
0.2	-1.208964	6.70E-07	-0.863545714
0.24	-1.1919768	3.13E-06	-1.0216944
0.28	-1.1670828	1.46E-05	-1.1670828
0.32	-1.1290884	6.81E-05	-1.290386743
0.36	-1.0695672	3.15E-04	-1.375157829
0.4	-0.976764	1.44E-03	-1.395377143
0.44	-0.8385036	6.31E-03	-1.317648514
0.48	-0.6478476	2.51E-02	-1.110595886
0.52	-0.4061916	8.24E-02	-0.754355829
0.56	-0.1198956	2.09E-01	-0.2397912
0.6	0.2060352	4.17E-01	0.441504
0.64	0.5718852	7.05E-01	1.307166171
0.68	0.9829572	1.07E+00	2.387181771
0.72	1.446636	1.50E+00	3.719921143
0.76	1.969428	2.00E+00	5.345590286
0.8	2.555664	2.58E+00	7.301897143
0.84	3.20748	3.22E+00	9.62244
0.88	3.925464	3.94E+00	12.33717257
0.92	4.709244	4.72E+00	15.47323029
0.96	5.557992	5.56E+00	19.05597257

1	6.47064	6.48E+00	23.10942857

Appendix B4: 1:1 – 2 steps cell (100 nm) B4, C11-2-100

Voltage (v)	Light (mA)	Dark (mA)	P =J*V (mW/cm^2)
-1	-1.05894	-2.42E-10	3.781928571
-0.96	-1.05876	-2.42E-10	3.630034286
-0.92	-1.05857	-2.42E-10	3.478158571
-0.88	-1.05836	-2.42E-10	3.326274286
-0.84	-1.05814	-2.42E-10	3.17442
-0.8	-1.05789	-2.42E-10	3.022542857
-0.76	-1.05763	-2.42E-10	2.87071
-0.72	-1.05734	-2.42E-10	2.718874286
-0.68	-1.05702	-2.42E-10	2.567048571
-0.64	-1.05668	-2.42E-10	2.415268571
-0.6	-1.0563	-2.42E-10	2.2635
-0.56	-1.05588	-2.42E-10	2.11176
-0.52	-1.05541	-2.42E-10	1.960047143
-0.48	-1.0549	-2.42E-10	1.8084
-0.44	-1.05433	-2.42E-10	1.656804286
-0.4	-1.05368	-2.42E-10	1.505257143
-0.36	-1.05296	-2.42E-10	1.353805714
-0.32	-1.05214	-2.42E-10	1.202445714
-0.28	-1.05121	-2.42E-10	1.05121
-0.24	-1.05015	-2.42E-10	0.900128571
-0.2	-1.04892	-2.42E-10	0.749228571
-0.16	-1.0475	-2.41E-10	0.598571429
-0.12	-1.04582	-2.39E-10	0.448208571
-0.08	-1.04384	-2.30E-10	0.29824
-0.04	-1.04147	-1.88E-10	0.148781429
0	-1.0386	9.50E-12	0
0.04	-1.03506	9.28E-10	-0.147865714
0.08	-1.03063	5.23E-09	-0.294465714
0.12	-1.02497	2.53E-08	-0.439272857
0.16	-1.01753	1.19E-07	-0.581445714
0.2	-1.00747	5.58E-07	-0.719621429
0.24	-0.993314	2.61E-06	-0.851412
0.28	-0.972569	1.22E-05	-0.972569
0.32	-0.940907	5.67E-05	-1.075322286
0.36	-0.891306	0.000262613	-1.145964857
0.4	-0.81397	0.00119805	-1.162814286
0.44	-0.698753	0.00525423	-1.098040429

0.48	-0.539873	0.0209096	-0.925496571
0.52	-0.338493	0.0686777	-0.628629857
0.56	-0.099913	0.173987	-0.199826
0.6	0.171696	0.347791	0.36792
0.64	0.476571	0.587411	1.089305143
0.68	0.819131	0.888597	1.989318143
0.72	1.20553	1.24949	3.099934286
0.76	1.64119	1.66961	4.454658571
0.8	2.12972	2.1486	6.084914286
0.84	2.6729	2.68582	8.0187
0.88	3.27122	3.28032	10.28097714
0.92	3.92437	3.93097	12.89435857
0.96	4.63166	4.63656	15.87997714
1	5.3922	5.39592	19.25785714

Appendix B5: 1:2- 1 step cell B5, C12-1-100

Voltage (V)	Light (mA)	Dark (mA)	P= J*V (mW/cm^2)
-1	-0.890214	-7.25E-11	3.179335714
-0.96	-0.890154	-7.25E-11	3.051956571
-0.92	-0.890094	-7.25E-11	2.924594571
-0.88	-0.890028	-7.25E-11	2.797230857
-0.84	-0.889962	-7.25E-11	2.669886
-0.8	-0.889884	-7.25E-11	2.542525714
-0.76	-0.8898	-7.25E-11	2.415171429
-0.72	-0.889716	-7.25E-11	2.287841143
-0.68	-0.889614	-7.25E-11	2.160491143
-0.64	-0.889512	-7.25E-11	2.033170286
-0.6	-0.889392	-7.25E-11	1.90584
-0.56	-0.889266	-7.25E-11	1.778532
-0.52	-0.889128	-7.25E-11	1.651237714
-0.48	-0.888972	-7.25E-11	1.523952
-0.44	-0.888804	-7.25E-11	1.396692
-0.4	-0.888612	-7.25E-11	1.269445714
-0.36	-0.888396	-7.25E-11	1.142223429
-0.32	-0.888156	-7.25E-11	1.015035429
-0.28	-0.887886	-7.25E-11	0.887886
-0.24	-0.88758	-7.25E-11	0.760782857
-0.2	-0.887226	-7.25E-11	0.633732857
-0.16	-0.886824	-7.24E-11	0.506756571
-0.12	-0.88635	-7.18E-11	0.379864286

-0.08	-0.885798	-6.90E-11	0.253085143
-0.04	-0.88515	-5.62E-11	0.12645
0	-0.884364	3.84E-12	0
0.04	-0.883416	2.83E-10	-0.126202286
0.08	-0.882246	1.59E-09	-0.252070286
0.12	-0.88077	7.68E-09	-0.377472857
0.16	-0.878874	3.61E-08	-0.502213714
0.2	-0.876372	1.69E-07	-0.62598
0.24	-0.87297	7.90E-07	-0.74826
0.28	-0.86817	3.68E-06	-0.86817
0.32	-0.861084	1.72E-05	-0.984096
0.36	-0.850044	7.99E-05	-1.092913714
0.4	-0.83163	3.70E-04	-1.188042857
0.44	-0.79845	1.70E-03	-1.254707143
0.48	-0.734556	7.62E-03	-1.259238857
0.52	-0.609738	3.20E-02	-1.132370571
0.56	-0.3825744	1.16E-01	-0.7651488
0.6	-0.02108142	3.28E-01	-0.045174471
0.64	0.4806648	7.12E-01	1.0986624
0.68	1.110426	1.26E+00	2.696748857
0.72	1.85283	1.96E+00	4.76442
0.76	2.696502	2.77E+00	7.319076857
0.8	3.634818	3.69E+00	10.38519429
0.84	4.664586	4.70E+00	13.993758
0.88	5.78463	5.81E+00	18.18026571
0.92	6.99468	7.01E+00	22.98252
0.96	8.29488	8.31E+00	28.43958857
1	9.68526	9.70E+00	34.59021429

Appendix B6: 1:2- 2 steps cell B6, C12-2-100

Voltage (v)	Light (mA)	Dark (mA)	P= J*V (mW/cm^2)
-1	-0.740865	-1.21E-10	2.645946429
-0.96	-0.740775	-1.21E-10	2.5398
-0.92	-0.74067	-1.21E-10	2.43363
-0.88	-0.740565	-1.21E-10	2.32749
-0.84	-0.74045	-1.21E-10	2.22135
-0.8	-0.740325	-1.21E-10	2.115214286
-0.76	-0.740185	-1.21E-10	2.009073571
-0.72	-0.74004	-1.21E-10	1.90296
-0.68	-0.73988	-1.21E-10	1.796851429
-0.64	-0.739705	-1.21E-10	1.690754286

-0.6	-0.739515	-1.21E-10	1.584675
-0.56	-0.739305	-1.21E-10	1.47861
-0.52	-0.73907	-1.21E-10	1.372558571
-0.48	-0.738815	-1.21E-10	1.26654
-0.44	-0.738535	-1.21E-10	1.160555
-0.4	-0.73822	-1.21E-10	1.0546
-0.36	-0.73787	-1.21E-10	0.94869
-0.32	-0.737475	-1.21E-10	0.842828571
-0.28	-0.73703	-1.21E-10	0.73703
-0.24	-0.736525	-1.21E-10	0.631307143
-0.2	-0.73595	-1.21E-10	0.525678571
-0.16	-0.73529	-1.21E-10	0.420165714
-0.12	-0.73452	-1.20E-10	0.314794286
-0.08	-0.733625	-1.15E-10	0.209607143
-0.04	-0.732565	-9.37E-11	0.104652143
0	-0.7313	6.39E-12	0
0.04	-0.72977	4.71E-10	-0.104252857
0.08	-0.72789	2.65E-09	-0.207968571
0.12	-0.72554	1.28E-08	-0.310945714
0.16	-0.722535	6.02E-08	-0.412877143
0.2	-0.718605	2.82E-07	-0.513289286
0.24	-0.71332	1.31E-06	-0.611417143
0.28	-0.70598	6.13E-06	-0.70598
0.32	-0.69537	2.85E-05	-0.794708571
0.36	-0.67932	1.32E-04	-0.873411429
0.4	-0.653675	6.09E-04	-0.933821429
0.44	-0.610235	2.75E-03	-0.958940714
0.48	-0.533545	1.19E-02	-0.914648571
0.52	-0.399087	4.63E-02	-0.741161571
0.56	-0.1794875	1.48E-01	-0.358975
0.6	0.142247	3.65E-01	0.304815
0.64	0.56741	7.15E-01	1.296937143
0.68	1.088315	1.19E+00	2.643050714
0.72	1.696275	1.76E+00	4.36185
0.76	2.38518	2.43E+00	6.47406
0.8	3.151845	3.18E+00	9.005271429
0.84	3.99512	4.02E+00	11.98536
0.88	4.914875	4.93E+00	15.44675
0.92	5.9113	5.92E+00	19.42284286
0.96	6.98455	6.99E+00	23.94702857

1	8.13455	8.14E+00	29.05196429

Appendix B7: 2:1- 1 step cell B7, C21-1-100

Voltage (V)	Light (mA)	Dark (mA)	P= J*V (mW/cm^2)
-1	-1.046132	-4.84E-11	3.736185714
-0.96	-1.046008	-4.84E-11	3.586313143
-0.92	-1.045872	-4.84E-11	3.436436571
-0.88	-1.045728	-4.84E-11	3.286573714
-0.84	-1.045568	-4.84E-11	3.136704
-0.8	-1.045396	-4.84E-11	2.986845714
-0.76	-1.045212	-4.84E-11	2.837004
-0.72	-1.045008	-4.84E-11	2.687163429
-0.68	-1.044788	-4.84E-11	2.537342286
-0.64	-1.044544	-4.84E-11	2.387529143
-0.6	-1.044276	-4.84E-11	2.237734286
-0.56	-1.04398	-4.84E-11	2.08796
-0.52	-1.043652	-4.84E-11	1.938210857
-0.48	-1.043284	-4.84E-11	1.788486857
-0.44	-1.042876	-4.84E-11	1.638805143
-0.4	-1.042416	-4.84E-11	1.489165714
-0.36	-1.041896	-4.84E-11	1.339580571
-0.32	-1.041304	-4.84E-11	1.190061714
-0.28	-1.040628	-4.84E-11	1.040628
-0.24	-1.039844	-4.83E-11	0.891294857
-0.2	-1.038928	-4.83E-11	0.742091429
-0.16	-1.037848	-4.82E-11	0.593056
-0.12	-1.036556	-4.79E-11	0.444238286
-0.08	-1.034984	-4.60E-11	0.295709714
-0.04	-1.033032	-3.75E-11	0.147576
0	-1.030552	2.56E-12	0
0.04	-1.027312	1.89E-10	-0.146758857
0.08	-1.022936	1.06E-09	-0.292267429
0.12	-1.016824	5.12E-09	-0.435781714
0.16	-1.007976	2.41E-08	-0.575986286
0.2	-0.994764	1.12E-07	-0.710545714
0.24	-0.974608	5.24E-07	-0.835378286
0.28	-0.943692	2.44E-06	-0.943692
0.32	-0.897184	1.13E-05	-1.025353143
0.36	-0.83038	5.19E-05	-1.067631429
0.4	-0.740804	2.35E-04	-1.058291429
0.44	-0.62972	1.03E-03	-0.98956

0.48	-0.501668	4.28E-03	-0.860002286
0.52	-0.3623624	1.56E-02	-0.672958743
0.56	-0.2163324	4.62E-02	-0.4326648
0.6	-0.065142	1.08E-01	-0.13959
0.64	0.0933496	2.04E-01	0.213370514
0.68	0.264202	3.35E-01	0.641633429
0.72	0.4534	5.00E-01	1.165885714
0.76	0.666052	6.97E-01	1.807855429
0.8	0.905724	9.27E-01	2.587782857
0.84	1.174624	1.19E+00	3.523872
0.88	1.47404	1.49E+00	4.632697143
0.92	1.804688	1.81E+00	5.929689143
0.96	2.16694	2.17E+00	7.429508571

Appendix B8: 2:1- 2 steps cell B8, C21-2-100

Voltage (v)	Light (mA)	Dark (mA)	P= J*V (mW/cm^2)
-1	-0.782718	-7.25E-11	2.795421429
-0.96	-0.782532	-7.25E-11	2.682966857
-0.92	-0.782331	-7.25E-11	2.570516143
-0.88	-0.782115	-7.25E-11	2.458075714
-0.84	-0.781881	-7.25E-11	2.345643
-0.8	-0.781629	-7.25E-11	2.233225714
-0.76	-0.781353	-7.25E-11	2.120815286
-0.72	-0.781053	-7.25E-11	2.008422
-0.68	-0.780726	-7.25E-11	1.896048857
-0.64	-0.780366	-7.25E-11	1.783693714
-0.6	-0.77997	-7.25E-11	1.671364286
-0.56	-0.779535	-7.25E-11	1.55907
-0.52	-0.779052	-7.25E-11	1.446810857
-0.48	-0.778515	-7.25E-11	1.334597143
-0.44	-0.777915	-7.25E-11	1.222437857
-0.4	-0.777243	-7.25E-11	1.110347143
-0.36	-0.776481	-7.25E-11	0.998332714
-0.32	-0.77562	-7.25E-11	0.886422857
-0.28	-0.774633	-7.25E-11	0.774633
-0.24	-0.773499	-7.25E-11	0.662999143
-0.2	-0.772179	-7.25E-11	0.551556429
-0.16	-0.770625	-7.24E-11	0.440357143
-0.12	-0.768777	-7.18E-11	0.329475857
-0.08	-0.766542	-6.90E-11	0.219012
-0.04	-0.763788	-5.62E-11	0.109112571

0	-0.76032	3.83E-12	0
0.04	-0.755841	2.83E-10	-0.107977286
0.08	-0.749895	1.59E-09	-0.214255714
0.12	-0.741756	7.67E-09	-0.317895429
0.16	-0.730311	3.60E-08	-0.417320571
0.2	-0.713889	1.68E-07	-0.509920714
0.24	-0.69015	7.81E-07	-0.591557143
0.28	-0.65625	3.62E-06	-0.65625
0.32	-0.609468	1.66E-05	-0.696534857
0.36	-0.54831	7.53E-05	-0.70497
0.4	-0.473391	3.32E-04	-0.676272857
0.44	-0.387405	1.39E-03	-0.608779286
0.48	-0.294138	5.29E-03	-0.504236571
0.52	-0.197079	1.70E-02	-0.366003857
0.56	-0.0981204	4.42E-02	-0.1962408
0.6	0.00343992	9.30E-02	0.007371257
0.64	0.1110483	1.66E-01	0.253824686
0.68	0.2297478	2.63E-01	0.557958943
0.72	0.364398	3.85E-01	0.937023429
0.76	0.518577	5.32E-01	1.407566143
0.8	0.694491	7.04E-01	1.98426
0.84	0.893367	9.00E-01	2.680101
0.88	1.11585	1.12E+00	3.506957143
0.92	1.362261	1.37E+00	4.476000429
0.96	1.632729	1.64E+00	5.597928
1	1.927281	1.93E+00	6.883146429

Appendix B9: 1:3 - 1 step cell B9, C13-1-100

Voltage (v)	Light (mA)	Dark (mA)	P= J*v (mW/cm^2)
-1	-0.254749	1.21E-11	0.909817857
-0.96	-0.254695	-1.21E-11	0.87324
-0.92	-0.254637	-1.21E-11	0.836664429
-0.88	-0.254574	-1.21E-11	0.800089714
-0.84	-0.254506	-1.21E-11	0.763518
-0.8	-0.254432	-1.21E-11	0.726948571
-0.76	-0.254351	-1.21E-11	0.690381286
-0.72	-0.254263	-1.21E-11	0.653819143
-0.68	-0.254167	-1.21E-11	0.617262714
-0.64	-0.254061	-1.21E-11	0.580710857
-0.6	-0.253944	-1.21E-11	0.544165714
-0.56	-0.253815	-1.21E-11	0.50763

-0.52	-0.253672	-1.21E-11	0.471105143
-0.48	-0.253512	-1.21E-11	0.434592
-0.44	-0.253333	-1.21E-11	0.398094714
-0.4	-0.253132	-1.21E-11	0.361617143
-0.36	-0.252904	-1.21E-11	0.325162286
-0.32	-0.252644	-1.21E-11	0.288736
-0.28	-0.252347	-1.21E-11	0.252347
-0.24	-0.252005	-1.21E-11	0.216004286
-0.2	-0.251606	-1.21E-11	0.179718571
-0.16	-0.251139	-1.20E-11	0.143508
-0.12	-0.250585	-1.18E-11	0.107393571
-0.08	-0.249923	-1.09E-11	0.071406571
-0.04	-0.24912	-6.39E-12	0.035588571
0	-0.248135	1.54E-11	0
0.04	-0.246908	1.20E-10	-0.035272571
0.08	-0.245354	6.27E-10	-0.070101143
0.12	-0.24335	3.07E-09	-0.104292857
0.16	-0.240716	1.48E-08	-0.137552
0.2	-0.23718	7.14E-08	-0.169414286
0.24	-0.23233	3.44E-07	-0.19914
0.28	-0.225541	1.65E-06	-0.225541
0.32	-0.215895	7.90E-06	-0.246737143
0.36	-0.202139	3.76E-05	-0.259893
0.4	-0.182791	1.76E-04	-0.26113
0.44	-0.156511	8.03E-04	-0.245945857
0.48	-0.122563	3.38E-03	-0.210108
0.52	-0.080977	1.20E-02	-0.150385857
0.56	-0.032224	3.24E-02	-0.064448
0.6	0.0232648	6.77E-02	0.049853143
0.64	0.0853712	1.17E-01	0.195134171
0.68	0.154264	1.77E-01	0.374641143
0.72	0.230231	2.47E-01	0.592022571
0.76	0.313529	3.27E-01	0.851007286
0.8	0.404325	4.15E-01	1.155214286
0.84	0.502702	5.11E-01	1.508106
0.88	0.608684	6.16E-01	1.913006857
0.92	0.722261	7.28E-01	2.373143286
0.96	0.84341	8.48E-01	2.891691429

Appendix B10: 1:3 – 2 steps cell B10, C13-2-100

Voltage (v)	Light (mA)	Dark (mA)	P= J*V (mW/cm^2)

-1	-0.2537	-2.42E-11	0.906053571
-0.96	-0.25359	-2.42E-11	0.869448
-0.92	-0.25348	-2.42E-11	0.832846429
-0.88	-0.25335	-2.42E-11	0.796249143
-0.84	-0.25322	-2.42E-11	0.759654
-0.8	-0.25307	-2.42E-11	0.723065714
-0.76	-0.25292	-2.42E-11	0.686486286
-0.72	-0.25274	-2.42E-11	0.649913143
-0.68	-0.25256	-2.42E-11	0.613350286
-0.64	-0.25235	-2.42E-11	0.5768
-0.6	-0.25212	-2.42E-11	0.540263571
-0.56	-0.25187	-2.42E-11	0.503744
-0.52	-0.2516	-2.42E-11	0.467247857
-0.46	-0.25129	-2.42E-11	0.412828643
-0.42	-0.25094	-2.42E-11	0.376413
-0.38	-0.25056	-2.42E-11	0.340040286
-0.34,	-0.25012	-2.42E-11	0.303717143
-0.3	-0.24963	-2.42E-11	0.267456429
-0.26	-0.24906	-2.42E-11	0.231271857
-0.22	-0.24842	-2.42E-11	0.195183214
-0.18	-0.24767	-2.42E-11	0.159215143
-0.14	-0.2468	-2.41E-11	0.1233985
-0.1	-0.24577	-2.37E-11	0.087776071
-0.06	-0.24456	-2.18E-11	0.052405714
-0.02	-0.24311	-1.28E-11	0.017364714
0.02	-0.24134	3.08E-11	-0.017238857
0.06	-0.23919	2.41E-10	-0.051253929
0.1	-0.2365	1.25E-09	-0.084465714
0.14	-0.23313	6.12E-09	-0.116566
0.18	-0.22883	2.96E-08	-0.147105643
0.22	-0.22327	1.42E-07	-0.175428786
0.26	-0.21601	6.82E-07	-0.200576071
0.3	-0.20642	3.26E-06	-0.221162143
0.34	-0.19373	1.55E-05	-0.235238714
0.38	-0.17701	7.28E-05	-0.240225143
0.42	-0.15532	3.34E-04	-0.232974
0.46	-0.12787	1.45E-03	-0.210072143
0.52	-0.09421	5.58E-03	-0.174957343
0.56	-0.05416	1.73E-02	-0.1083282
0.6	-0.00768	4.14E-02	-0.016465693

0.64	0.045375	7.90E-02	0.1037136
0.68	0.105292	1.29E-01	0.255709143
0.72	0.172399	1.90E-01	0.443311714
0.76	0.246975	2.60E-01	0.670360714
0.8	0.329191	3.39E-01	0.940545714
0.84	0.419122	4.27E-01	1.257366
0.88	0.51678	5.23E-01	1.624165714
0.92	0.622137	6.28E-01	2.044164429
0.96	0.735152	7.40E-01	2.520521143
1	0.855783	8.60E-01	3.056367857

Appendix B11: 3:1 - 1 step cell B11, C31-1-100

Voltage (v)	Light (mA)	Dark (mA)	P= J*V (mW/cm^2)
-1	-0.15499	-1.21E-11	0.553535714
-0.96	-0.15497	-1.21E-11	0.531318857
-0.92	-0.15494	-1.21E-11	0.509101714
-0.88	-0.15492	-1.21E-11	0.486885143
-0.84	-0.15489	-1.21E-11	0.46467
-0.8	-0.15486	-1.21E-11	0.442454286
-0.76	-0.15483	-1.21E-11	0.420239286
-0.72	-0.15479	-1.21E-11	0.398023714
-0.68	-0.15475	-1.21E-11	0.375809286
-0.64	-0.1547	-1.21E-11	0.353597714
-0.6	-0.15465	-1.21E-11	0.331386429
-0.56	-0.15459	-1.21E-11	0.309178
-0.52	-0.15452	-1.21E-11	0.286969429
-0.48	-0.15445	-1.21E-11	0.264766286
-0.44	-0.15436	-1.21E-11	0.242564143
-0.4	-0.15426	-1.21E-11	0.220367143
-0.36	-0.15414	-1.21E-11	0.198174857
-0.32	-0.15399	-1.21E-11	0.175989714
-0.28	-0.15381	-1.21E-11	0.153813
-0.24	-0.15359	-1.21E-11	0.131649429
-0.2	-0.15331	-1.21E-11	0.109505714
-0.16	-0.15294	-1.20E-11	0.087393143
-0.12	-0.15244	-1.18E-11	0.065333143
-0.08	-0.15177	-1.09E-11	0.043361714
-0.04	-0.15082	-6.38E-12	0.021545286
0	-0.14947	1.54E-11	0
0.04	-0.14751	1.20E-10	-0.021073143

0.08	-0.14469	6.23E-10	-0.041339143
0.12	-0.14064	3.04E-09	-0.060272143
0.16	-0.13497	1.46E-08	-0.077123429
0.2	-0.12735	7.00E-08	-0.090961429
0.24	-0.11763	3.33E-07	-0.100822286
0.28	-0.10592	1.57E-06	-0.105924
0.32	-0.09261	7.32E-06	-0.105835429
0.36	-0.07818	3.33E-05	-0.100516114
0.4	-0.06317	1.45E-04	-0.090249571
0.44	-0.04805	5.77E-04	-0.0755139
0.48	-0.03314	1.97E-03	-0.056808857
0.52	-0.01853	5.36E-03	-0.034416386
0.56	-0.00405	1.16E-02	-0.0080997
0.6	0.01079	2.10E-02	0.023121643
0.64	0.02664	3.34E-02	0.060890971
0.68	0.044116	4.88E-02	0.107137886
0.72	0.06367	6.70E-02	0.163723114
0.76	0.085587	8.80E-02	0.232308386
0.8	0.110034	1.12E-01	0.314382857
0.84	0.137105	1.38E-01	0.411315
0.88	0.166858	1.68E-01	0.524410857
0.92	0.199328	2.00E-01	0.654934857
0.96	0.234534	2.35E-01	0.804116571

Appendix B12: 3:1 - 2 steps cell B12, C31-2-100

Voltage (v)	Light (mA)	Dark (mA)	P= J*V (mW/cm^2)
-1	-0.15458	-2.42E-11	0.552067857
-0.96	-0.15454	-2.42E-11	0.529837714
-0.92	-0.15449	-2.42E-11	0.507603429
-0.88	-0.15444	-2.42E-11	0.485373429
-0.84	-0.15438	-2.42E-11	0.463143
-0.8	-0.15432	-2.42E-11	0.440914286
-0.76	-0.15425	-2.42E-11	0.418686714
-0.72	-0.15418	-2.42E-11	0.396457714
-0.68	-0.1541	-2.42E-11	0.374235571
-0.64	-0.15401	-2.42E-11	0.352013714
-0.6	-0.1539	-2.42E-11	0.329794286
-0.56	-0.15379	-2.42E-11	0.30758
-0.52	-0.15366	-2.42E-11	0.285368571
-0.48	-0.15351	-2.42E-11	0.263165143
-0.44	-0.15334	-2.42E-11	0.240967571

-0.4	-0.15315	-2.42E-11	0.218778571
-0.36	-0.15291	-2.42E-11	0.196599857
-0.32	-0.15263	-2.42E-11	0.174436571
-0.28	-0.15229	-2.42E-11	0.152291
-0.24	-0.15187	-2.42E-11	0.130173429
-0.2	-0.15134	-2.41E-11	0.108096429
-0.16	-0.15064	-2.40E-11	0.086082286
-0.12	-0.14973	-2.36E-11	0.064170429
-0.08	-0.1485	-2.18E-11	0.042429143
-0.04	-0.14682	-1.27E-11	0.020974571
0	-0.1445	3.06E-11	0
0.04	-0.14129	2.39E-10	-0.020184857
0.08	-0.13691	1.24E-09	-0.039115714
0.12	-0.13103	6.02E-09	-0.056157429
0.16	-0.12345	2.88E-08	-0.070544
0.2	-0.11409	1.37E-07	-0.081491429
0.24	-0.10307	6.42E-07	-0.088346571
0.28	-0.09072	2.97E-06	-0.0907151
0.32	-0.07744	1.34E-05	-0.088507429
0.36	-0.06371	5.83E-05	-0.081913886
0.4	-0.04993	2.36E-04	-0.071326857
0.44	-0.03642	8.50E-04	-0.057224986
0.48	-0.02333	2.57E-03	-0.040002686
0.52	-0.01061	6.31E-03	-0.019709486
0.56	0.002125	1.27E-02	0.00424924
0.6	0.015513	2.21E-02	0.033241071
0.64	0.030257	3.44E-02	0.069159086
0.68	0.046934	4.97E-02	0.1139816
0.72	0.065917	6.78E-02	0.1695006
0.76	0.087421	8.88E-02	0.237284214
0.8	0.11156	1.13E-01	0.318742857
0.84	0.1384	1.39E-01	0.4152
0.88	0.167973	1.69E-01	0.527915143
0.92	0.2003	2.01E-01	0.658128571
0.96	0.235392	2.36E-01	0.807058286

تصنيع واختبار خلايا P3HT: PCBM العضوية الكهروضوئية (الفوتوفولتية)

P3HT: PCBM Organic Photovoltaic Devices Fabrication and Testing

اعداد: آلاء عزمي أبوعرقوب

إشراف: الدكتور سلمان سلمان

الملخّص

الطاقة المتجددة احد أهم مجالات البحث الحديثة وذلك بسبب أهمية الطاقة في جميع المجالات الحياتية وتأثيرها على البيئة. وتعد الخلايا الكهروضوئية القائمة على استخدام المبلمرات من أحد أهم حقول البحث الواعدة في الحصول على طاقة نظيفة بتكلفة وكتلة أقل من أنواع الخلايا الأخرى, وهذه الخصائص تعتمد كثيرا على الطبقة الفعالة المستخدمة في هذه الخلايا.

في هذه الدراسة قمت باستخدام أحد أهم مشتقات مبلمرات فيولرين كطبقة فعالة، المركب المانح P3HT (بولي 3 هكسل ثايوفينين) والمستقبل يتكون من (PCBMحمض فينيل كربون 61 ميثل استر). وهذا المزيج الذي سجل أكبر فعالية من المبلمرات الأخرى التي تم تجربتها في هذه الخلايا حيث بلغت قيمتها حوالي 5%.

وتمت هذه التجربة في مختبر أبحاث النانو في جامعة القدس لتغليف الطبقة الفعالة ولإجراء الفحوص والاختبار بالاشتراك مع مختبر الفيزياء في جامعة بيت لحم باستخدام المبخر لتركيب وصلات الذهب والألومنيوم. وقد تم بناء 12 خلية باستخدام P3HT: PCBM كطبقة فعالة مذابة في ثنائي كلوروبنزين، بنسب متفاوتة من مكونات المادة الفعالة وبأسماك مختلفة بالإضافة إلى طريقتين لتغليف الطبقة الفاعلة بسرعة واحدة أو سرعتين باستخدام التغليف المغزلي Spin coating.

وقد تم فحص الخلايا من خلال دراسة العلاقة بين الجهد والتيار تحت إضاءة بنسبة 30% من المعيارية لكن ذلك لم ينقص الكفاءة بشكل كبير. وتم الحصول على أفضل كفاءة تحويل للطاقة بقيمة 4.5% عند استخدام خلايا بسمك الطبقة الفاعلة حوالي 100 نانومتر والنسبة الأفضل بين مكونات الطبقة الفاعلة هي 1:1. ولم يظهر تأثير كبير لطريقة تصنيع الطبقة الفعالة بسرعة واحدة أو سرعتين.

وللحصول على فعالية أكبر نوصي بإجراء تجارب لاحقة تركز البحث على مركبات المادة الفعالة بحيث تحقق التالي

1. معامل امتصاص عالي.
2. ذائبية أعلى في المذيبات العضوية.
3. طاقة الفجوة اقل بين مستويات الطاقة في المدى.
4. أو من خلال إضافة الشوائب أو دقائق متناهية الصغر من معادن جيدة التوصيل مثل الذهب.